Yuriy Zabulonov
Igor Peer
Mark Zheleznyak   *Editors*

Liquid Radioactive Waste Treatment: Ukrainian Context

LWRT 2022

Springer

Lecture Notes in Civil Engineering 469

Lecture Notes in Civil Engineering (LNCE) publishes the latest developments in Civil Engineering—quickly, informally and in top quality. Though original research reported in proceedings and post-proceedings represents the core of LNCE, edited volumes of exceptionally high quality and interest may also be considered for publication. Volumes published in LNCE embrace all aspects and subfields of, as well as new challenges in, Civil Engineering. Topics in the series include:

- Construction and Structural Mechanics
- Building Materials
- Concrete, Steel and Timber Structures
- Geotechnical Engineering
- Earthquake Engineering
- Coastal Engineering
- Ocean and Offshore Engineering; Ships and Floating Structures
- Hydraulics, Hydrology and Water Resources Engineering
- Environmental Engineering and Sustainability
- Structural Health and Monitoring
- Surveying and Geographical Information Systems
- Indoor Environments
- Transportation and Traffic
- Risk Analysis
- Safety and Security

To submit a proposal or request further information, please contact the appropriate Springer Editor:

- Pierpaolo Riva at pierpaolo.riva@springer.com (Europe and Americas);
- Swati Meherishi at swati.meherishi@springer.com (Asia—except China, Australia, and New Zealand);
- Wayne Hu at wayne.hu@springer.com (China).

All books in the series now indexed by Scopus and EI Compendex database!

Yuriy Zabulonov · Igor Peer · Mark Zheleznyak
Editors

Liquid Radioactive Waste Treatment: Ukrainian Context

LWRT 2022

Springer

Editors
Yuriy Zabulonov
Institute of Environmental Geochemistry
National Academy of Sciences of Ukraine
Kyiv, Ukraine

Igor Peer
Alpha Atom LLC
Kyiv, Ukraine

Mark Zheleznyak
Institute of Environmental Radioactivity
Fukushima University
Fukushima, Japan

Preface

The International Conference "Liquid Radioactive Waste Treatment: Ukrainian Context" (LWRT 2022), held in Kyiv, has been a landmark event, assembling a myriad of experts, researchers, industry professionals, and policymakers. This conference has served as a pivotal platform for addressing the multifaceted challenges and opportunities in the field of liquid radioactive waste treatment and management.

The proceedings encapsulate a wide array of innovative research and discussions that echo the conference's commitment to ecological safety and sustainable practices in the face of significant environmental challenges. The collected papers reflect the conference's comprehensive approach, covering vital aspects such as the challenges of managing radioactive waste during postwar reconstruction, the role of innovative environmental engineering in waste treatment, and the critical importance of safety measures and best practices in this domain.

The contributions in these proceedings offer insights into the development of effective strategies, cutting-edge technologies, and robust policies tailored to the unique challenges faced by Ukraine. They also highlight the importance of integrating sustainable practices into waste treatment processes, emphasizing the need for a balanced approach that considers environmental, economic, and social sustainability.

LWRT 2022 has not only fostered a deeper understanding of the current state of liquid radioactive waste treatment in Ukraine but also contributed significantly to the global discourse on radioactive waste management. The discussions and findings presented here are intended to spur further research, collaboration, and innovation in this crucial field, ultimately contributing to a safer and more sustainable future.

Contents

Comparative Legal Analysis of Safe Handling of Liquid Radioactive Waste in Ukraine and Most EU Countries

Volodymyr Bozhko$^{(\boxtimes)}$ ⓘ and Oleksiy Kushch ⓘ

Poltava Law Institute of Yaroslav Mudryi National Law University, Poltava, Ukraine
volodya_bozhko@ukr.net

Abstract. The article is devoted to the study of legislation aimed at regulating relations on the safe management of liquid radioactive waste in the EU, individual EU Member States, and Ukraine. This problem is relevant for the entire global community, as such waste can emit harmful ionizing radiation, which can not only lead to radiation sickness but also cause radiation pollution of the environment. Ukrainian legislation also deserves special attention, as in 1986, the Chornobyl Nuclear Power Plant accident occurred in Ukraine, which resulted in a large release of radioactive materials. Therefore, the approaches to the safe management of liquid radioactive waste implemented in Ukraine deserve special attention.

The article focuses on a comparative analysis of Council Directive 2011/70/Euroatom with the national legislation of all EU Member States and Ukrainian legislation.

The author draws a reasonable conclusion that all European Community States seek to protect their populations from the hazards that may arise because of ionizing radiation. A comparative analysis of the results of the implementation of this Directive has shown that the EU Member States face the greatest problems with the development of a national radioactive waste management program containing key performance indicators; timely informing the European Commission of new national programs and any significant changes to them; and the establishment of a regulatory body in the field of radioactive waste management safety that would be sufficiently independent of public authorities. Several proposals were made to bring Ukrainian legislation in line with Council Directive 2011/70/Euratom.

Keywords: Radioactive waste · Safe radioactive waste management · Council Directive 2011/70/Euratom · European Union · Environmental law · Ukrainian legislation on safe radioactive waste management

1 Introduction

The relevance of studying the problems of radioactive waste treatment is since for a long time they have been potentially dangerous not only for the environment but also for the lives and health of current and many future generations. After all, their ability to emit harmful ionizing radiation can lead to radiation sickness and cause radiation contamination of the environment over a vast area.

Among the variety of possible types of radioactive waste, the problems of processing liquid waste deserve special attention. After all, they may include materials with a high level of radioactivity, such as uranium, plutonium, and other radioactive isotopes. Such waste can have a high concentration of radioactive substances and take up a significant amount of space. This complicates their storage, transportation, further processing, and disposal. In addition, liquid radioactive waste can enter water bodies because of discharges from nuclear power plants, medical facilities, industrial facilities, and other sources of radioactivity. This can contaminate aquatic ecosystems around the world.

According to the 2020 annual report of the State Register of Radioactive Waste and the State Cadastre of Radioactive Waste Storage Facilities and Temporary Radioactive Waste Storage Sites, 789 m^3 of liquid radioactive waste with the activity of 1.06 × 10–13 Bq has been accumulated in Ukraine, while approximately 20.000 m^3 of liquid radioactive waste is stored in Chornobyl NPP storage facilities. A significant part of it is stored in conditions that do not meet the established norms, rules, and standards of radiation safety [1].

As noted in the Concept of the National Target Environmental Programme for Radioactive Waste Management approved by the Cabinet of Ministers of Ukraine on 4 November 2022 [1], liquid radioactive waste storage facilities located at nuclear power plant sites are 20 to 80 percent full. To further dispose of radioactive waste at these sites, it is necessary to process and condition it. The solution to this issue is complicated by the lack of conditioning technologies for certain types of liquid radioactive waste, appropriate transport packaging sets, and containers in Ukraine.

Therefore, new research is needed on effective methods for processing liquid radioactive waste, the implementation of which can not only reduce its volume and concentration but also reduce the risks of its spread and ensure its safe storage. Experts in various fields of knowledge have been fruitfully working on their search for decades. However, the aforementioned problems are in one way or another caused by important legal aspects not only of the relevant state policy but also of the regulation of various social relations related to radioactive waste management. Therefore, as Nick Kimberly Sexton, Head of the Nuclear Law Division of the Organisation for Economic Cooperation and Development at the Nuclear Energy Agency, rightly points out, an effective solution to the above problems is impossible without the use of legal instruments [2]. In his opinion, it is "lawyers who can synthesize information from different perspectives to pave the way forward". In our opinion, the role of lawyers in solving the existing problems with radioactive waste management is not so much to synthesize the available information from different fields of knowledge as to use legal instruments to force the best practices of radioactive waste management to be applied to as many countries as possible, sometimes even against their will. This will help to improve the overall safety of radioactive waste management.

In 1986, the Chornobyl nuclear power plant disaster occurred in the territory of Ukraine. Since then, Ukraine has been striving not only to introduce the most advanced technologies to neutralize its consequences but also to implement the most advanced norms in its legislation that would prevent similar tragedies in the future. Therefore, the relevance of this study is also due to the search for an answer to the question of whether

the requirements of Ukrainian legislation comply with the secondary legislation of the EU and vice versa.

Therefore, the purpose of the article is to study the current EU legislation aimed at ensuring safe radioactive waste management; analyze the state of its implementation by EU member states; assess the extent to which Ukrainian legislation and law enforcement practice of radioactive waste management comply with the EU experience; and formulate proposals aimed at improving the efficiency of radioactive waste management in Ukraine and the EU.

2 Development of EU Legislation on Radioactive Waste Management

Humans have always been exposed to ionizing radiation from radioactive materials. Initially, however, such radiation came exclusively from cosmic bodies and from natural radioactive materials in the environment. Later, it was supplemented by radiation caused by intensive human use of the properties of natural materials that emit ionizing radiation[1]. Over time, the volume of such materials grew rapidly, and their ionizing radiation could harm many people and the environment over a vast territory. Therefore, it was only in the twentieth century that humanity began to introduce certain restrictions to prevent possible negative consequences from the use of not only radioactive materials but also their waste.

On 29 September 1997, the Joint Convention on the Safety of Spent Fuel Management and on the Safety of Radioactive Waste Management was signed in Vienna. This Joint Convention was the first legal instrument to address the safety of not only spent fuel management but also radioactive waste management. Currently, 63 states have acceded to it. According to Ute Blohm-Hieber, the Joint Convention binds the Parties to two types of obligations: first, to take appropriate measures to ensure the safety of spent fuel and radioactive waste management; and second, to periodically report and undergo peer review [3]. However, the first type of obligation is referred to as "de moyens" obligations, which means that they are exclusive of a coercive nature (the Joint Convention does not provide for instruments that would force a Party to change its behavioral practices, except for the pressure that other Parties may exert), the second type of obligations is legally binding on the Parties to the Convention.

Subsequently, the International Atomic Energy Agency developed several international standards aimed at safe radioactive waste management. On 8 September 2003, the Board of Governors of the International Atomic Energy Agency approved the IAEA Code of Conduct for the Safety and Security of Radioactive Sources. However, none of these rules are legally binding on the states that are members of the IAEA, however,

---

[1] In our opinion, the first mention of people using the properties of ionizing radiation can be found in the Old Testament, in the book of Leviticus, which describes the rules for the high priests to handle the Ark of the Covenant, which resemble instructions for handling radioactive substances. It was forbidden to touch the Ark or enter the Sanctuary. Only the high priest could do this once a year. On that day, he had to be tied with a rope and a bell tied to him so that if he made a mistake and died inside, his body could be dragged out.

they are binding on the IAEA itself when it provides technical assistance to countries that have requested it.

The EU also did not stand aside from the process of generating rules of conduct aimed at safe radioactive waste management. After all, all EU member states without exception have radioactive waste. They generate it mainly in the process of electricity generation at nuclear power plants, as well as in the use of radioisotope materials in medicine, industry, agriculture, education, and research. Therefore, in 2005, the European Atomic Energy Community even joined the Joint Convention[2].

In 2003, the European Commission initiated the development of a Council Directive aimed at managing spent nuclear fuel and radioactive waste. The Commission even held consultations with national governments, regulators, radioactive waste producers, individual EU institutions, non-governmental organizations, etc.

In accordance with Commission Decision 2007/530/Euratom of 17 July 2007, the European High Level Group on Nuclear Safety and Waste Management (ENSREG) was established [4]. The conclusions and recommendations of this European Group were reflected in the Council Resolution of 16 December 2008 on Spent Fuel and Radioactive Waste Management and in the Council Conclusions of 10 November 2009 on the Report of the European Nuclear Safety Regulators.

On 10 May 2007, the European Parliament adopted the resolution "Evaluation of Euroatom - 50 years of European Nuclear Energy Policy", which, among other things, called on the member states to agree on standards for radioactive waste management and invited the European Commission to prepare a relevant draft legislative proposal on radioactive waste management.

On 25 June, the Council of the European Union adopted Directive 2009/71/Euratom [5] aimed at establishing the limits of the Community's powers on nuclear safety of nuclear installations, authorizing the EU authorities to form secondary legislation on spent fuel and radioactive waste management.

On 03.11.2010, the European Commission submitted a proposal for a Council Directive on the management of spent fuel and radioactive waste SEC(2010) 1290 s(2010) 1289 [6], on 23 June 2011, the European Parliament adopted a Legislative Resolution on the proposal for a Council Directive on the management of spent fuel and radioactive waste [7]. Shortly thereafter, on 19 July 2011, the Council of the European Union adopted Council Directive 2011/70/Euratom establishing a Community framework for the responsible and safe management of spent fuel and radioactive waste [8]. This Council Directive entered into force on 22 August 2011 and had to be implemented by the Member States by 23 August 2013.

---

[2] For this purpose, on 24 January 2005, the European Council adopted a Decision approving the accession of the European Atomic Energy Community to the Joint Convention on the Safety of Spent Fuel Management and on the Safety of Radioactive Waste Management (2005/84/Euratom), and on 14 June 2005, the European Commission adopted a Decision approving this accession (2005/510/Euratom).

3 Overview of Ukrainian Legislation on Radioactive Waste Management

In Ukraine, after the Chornobyl NPP disaster, an extensive system of legislation in the field of radioactive waste management was formed. The basis of this system is the Constitution of Ukraine, as well as the Laws of Ukraine "On Radioactive Waste Management" [9], "On Nuclear Energy Use and Radiation Safety" [10], and "On Environmental Protection" [11]. On 20 April 2000, the Verkhovna Rada of Ukraine ratified the Joint Convention on the Safety of Spent Fuel Management and on the Safety of Radioactive Waste Management [12].

Presidential Decree № 1072/2000 of 14 September 2000 approved the Programme of Ukraine's Integration into the European Union [13]. This program envisaged the introduction of European and international standards for: "Comprehensive Radioactive Waste Management Programme" [14]; improvement of the existing system of indicators for hazardous waste accounting (in accordance with Council Directives (EC) 75/442/EEC of 15 July 1975 on waste, 91/689/EEC of 12 December 1991 on hazardous waste and Council Decision (EC) 94/904/EC of 22 December 1994 on the definition of a list of hazardous wastes); protection of radioactive waste and other sources of ionising radiation; implementation of the Chornobyl radioactive waste disposal project, which included the creation of a spent nuclear fuel disposal and storage system and a plant for processing solid and liquid radioactive waste.

On 18 March 2004, the Verkhovna Rada of Ukraine adopted the Law of Ukraine "On the National Programme of Adaptation of Ukrainian Legislation to the Legislation of the European Union" [15]. This Law approved the National Programme for the Adaptation of Ukrainian Legislation to the Legislation of the European Union and instructed the Cabinet of Ministers of Ukraine to bring its regulations into compliance with this Law. The National Programme envisaged bringing Ukrainian legislation in line with several EU secondary legislation acts, in particular, Council Regulation (Euratom) № 1493/93 of 8 June 1993 on the carriage of radioactive substances between Member States [16] and a proposal for a Council Directive on the control of highly radioactive substances (COM (2003) 18 Proposal for a Council Directive on the control of high-level sealed radioactive sources) [17].

On 21 March 2014, the political part of the Association Agreement was signed, and on 27 June 2014 - the economic part of the Association Agreement between Ukraine, on the one hand, and the European Union, the European Atomic Energy Community, and their Member States, on the other hand [18]. According to this Agreement, cooperation between the Parties shall extend to the civil nuclear sector through the implementation of separate agreements between the Parties in this area (Article 342(1)), to the entire range of activities in the field of civil nuclear energy. The Parties shall promote civilian scientific research in the field of nuclear safety (Article 342(1)), as well as in the field of radioactive waste management (Article 342(3)(d)).

On 1 January 2020, the "Basic Principles (Strategy) of the State Environmental Policy of Ukraine for the Period up to 2030", approved by the Law of Ukraine of 28 February 2019, came into force [19]. This Law of Ukraine instructed the Cabinet of Ministers of Ukraine to develop and approve the National Environmental Action Plan within six months and prepare a report on the implementation of the Law of Ukraine

"On the Basic Principles (Strategy) of the State Environmental Policy of Ukraine for the Period up to 2020" and submit it to the Verkhovna Rada of Ukraine of 21 December 2010 [19].

In pursuance of these requirements, the Cabinet of Ministers of Ukraine approved the National Environmental Protection Action Plan for the period up to 2025 by Resolution № 443-r dated 21 April 2021 [20]. In pursuance of paragraph 168 of the above-mentioned National Plan, the Concept of the National Target Environmental Programme for Radioactive Waste Management was approved by the Cabinet of Ministers of Ukraine by Resolution № 992-r dated 4 November 2022 [21]. The purpose of this National Target Environmental Programme is to implement the state policy in the field of radioactive waste management to minimize the impact of radiation on the safety of human life, ensure the effective functioning of the radioactive waste management system, and lay the foundation for safe and cost-effective radioactive waste management.

The National Targeted Environmental Programme states that national legislation on radioactive waste management should be brought in line with the basic principles declared by the IAEA, taking into account Council Directives 2011/70/Euratom of 19 July 2011 establishing a framework for the responsible and safe management of spent fuel and radioactive waste and 2013/59/Euratom of 5 December 2013 establishing basic safety standards for protection against threats arising from exposure to ionizing radiation.

4   Analysis of the Main Innovations of Council Directive 2011/70/Euratom and Their Implementation by EU Member States

Council Directive 2011/70/Euratom introduced several key innovations related to the management and disposal of radioactive waste to avoid placing an undue burden on future generations. The Directive aims to create a common framework for the safe and responsible management of these materials within the European Union. Here are the main innovations introduced by Directive 2011/70/Euratom: to formulate a national policy on radioactive waste management based on a number of principles set out in part three of Article 4 of the Directive; to assign to the state the ultimate responsibility for damage caused by radioactive waste management (part two of Article 4); to develop a national radioactive waste management programme (Article 11) that meets the requirements specified in Article 12 of the Directive; inform the European Commission about national programmes and any subsequent significant changes made to them (Article 13 of the Directive); introduce a licensing system for radioactive waste management (Article 5(c)(1) and Article 7 of the Directive); to establish control, management and regulatory inspection systems for radioactive waste management (Article 5(d)(1) and Article 6 of the Directive); establish and facilitate the functioning of the competent regulatory authority in the field of radioactive waste management safety (Article 6 of the Directive); establish national requirements for public information and participation in radioactive waste management (Article 10 of the Directive); to introduce a national mechanism for financing radioactive waste management to ensure that sufficient funds are available (Article 9 of the Directive); to report to the European Commission on the

implementation of this Directive (first by 23 August 2015) and then every 3 years (Article 14 of the Directive).

4.1 Analysis of the Practice of Developing National Radioactive Waste Management Programs by EU Member States

According to Article 11 of Council Directive 2011/70/Euratom, Member States shall establish a national radioactive waste management program that meets the requirements set out in Article 12 of the Directive.

At the time of writing, all EU Member States have developed and approved national radioactive waste management programs. This conclusion is based on the analysis of the content of their national programs, which are available on the 'Energy' portal [22]. The same conclusion was reached by the European Commission in its Report to the Council and the European Parliament on the progress of the implementation of Council Directive 2011/70/Euratom of 17.12.2019 [23].

National programs, in accordance with Article 4 of Council Directive 2011/70/Euratom, should be based on the following principles: generation of radioactive waste should be minimized; interdependencies between all stages of radioactive waste generation and management should be duly taken into account; radioactive waste management should be based on passive safety functions; measures should be implemented in stages; costs of radioactive waste management should be borne by persons whose activities led to its generation, etc.

According to the national legislation of most of the EU Member States, these programs were approved by national authorities. In particular, the National Radioactive Waste Management Programme of Belgium [24] was developed by the National Programme Committee. In 2015. The Directorate General for Energy of the Federal Civil Service agreed to its text with the Federal Agency for Nuclear Control (FANC) and only after that it was approved by the Federal Council of Ministers on 30 June 2016. Since then, its text has not been updated. However, active work is underway to update the national program.

Instead, in Austria, the draft National Radioactive Waste Management Programme was developed by the Austrian Federal Government, which subsequently underwent a strategic environmental assessment in accordance with § 8a para. 4–7 of the Austrian Radioactive Waste Act 2002 [25], underwent a strategic environmental assessment to ensure that the Programme would not have a negative impact on the environment. This also allowed representatives of the public (including residents of neighboring countries) to contribute to the development of the program. Only then was the National Programme approved by the Austrian Government Council of Ministers on 5 September 2018 and subsequently updated in 2020, in accordance with the requirements of the Radiation Protection Act [25].

The Croatian National Programme for the Implementation of the Strategy for the Disposal of Radioactive Waste, Spent Sources, and Spent Nuclear Fuel (Programme for the period up to 2025 with a view to 2060) was adopted in July 2018 [26]. For many years, the Republic of Croatia has been successfully using compensation instruments for local communities where energy facilities, including hydroelectric and thermal power

plants, are located. This payment is aimed at supporting the development of local communities, part of whose territory is occupied by energy facilities. Such funds can be used exclusively for socio-economic development and environmental protection. Local communities will also receive financial assistance in implementing their sustainable development programs.

In some EU Member States, national plans were developed and adopted long before the entry into force of Council Directive 2011/70/Euratom. Spain has had a national program for spent fuel and radioactive waste management (GRWP) since 1987. It contains strategies and technical solutions to be implemented in Spain in the short, medium, and long term to ensure safe radioactive waste management. The GRWP approval procedure begins with a proposal for its update, which ENRESA submits to the Ministry of Information Technology and Environmental Development (MITERD) every four years. The Plan may be approved by the Government (Council of Ministers) upon a proposal by MITERD, following a report by the Council for Nuclear Safety (CSN) and after consultation on land use and environmental planning with the Autonomous Communities. In addition, Royal Decree 102/2014 requires public participation in the preparation of the Plan in accordance with the conditions stipulated by environmental regulations. The draft Plan will also be subject to a strategic environmental assessment, which is currently regulated by Law № 21/2013 of 9 December 2013 on environmental assessment. In March 2020, ENRESA submitted the GRWP proposal to MITERD, which started updating it.

In Italy, on 8 November 1987, after the Chornobyl accident, a referendum was held, most participants voted in favor of abandoning the further use of nuclear energy for electricity generation, except for a few research reactors. Following this, the then Ministers of Industry and Environment announced the holding of a "National Roundtable on Nuclear Waste Management" to determine a further action plan in this area. In July 2009, Law № 99/2009 renewed the authorization for the use of nuclear energy for electricity generation. However, on 12–13 June 2011, a few months after the Fukushima Daiichi accident, another national referendum was held to repeal the above law. In March 2014, Legislative Decree № 45/2014 was issued to implement Council Directive 2011/70/Euratom.

At the time of writing, Italy has a National Spent Fuel and Radioactive Waste Management Policy Implementation Programme [27], which was published in the form of a Decree by the President of the Council of Ministers on 30 October 2019 following public consultations related to its Strategic Environmental Assessment.

In Sweden, the concept of radiation protection originated in the late 1800s, when radium and X-ray machines were used for medical diagnosis and treatment of tumors. Several times between the late 1950s and early 1960s, radioactive waste from Sweden was dumped into the sea, both in Swedish territorial waters and in the Atlantic. Since the early 1970s, Sweden has acceded to several international conventions banning dumping into the sea. This prohibition was implemented in Chapter 15 of the Swedish Environmental Code, which prohibits the dumping of waste in Swedish territorial waters, in the Swedish economic zone, and from Swedish ships and aircraft in international waters.

In 2010, the Riksdag repealed the Nuclear Phase-out Act and allowed the construction of new nuclear reactors if they replace existing reactors only at sites with existing

reactors. The Riksdag also decided that licensees should bear greater responsibility for compensation for damages in connection with an accident, and the state was prohibited from subsidizing new investments in nuclear energy.

The program "Safe and Responsible Management of Spent Nuclear Fuel and Radioactive Waste in Sweden", adopted on 20 August 2015, is in force in Sweden. The Swedish Security Management (SSM) has been mandated by the Swedish government to maintain an up-to-date national plan for the management of non-reusable nuclear materials, nuclear, and other radioactive waste.

In accordance with Article 12(1)(a) of Council Directive 2011/70/Euratom, national programs should contain information on how the Member States intend to implement their national policies referred to in Article 4 of that Directive for the responsible and safe management of radioactive waste. In Ukraine, the Law "On the National Target Environmental Programme for Radioactive Waste Management" of 17 September 2008 is still in force [28], approved the "National Target Environmental Programme for Radioactive Waste Management". It declares the following goal: to implement the state policy in the field of radioactive waste management aimed at protecting the environment, life, and health of the population from ionizing radiation. In addition, the Cabinet of Ministers of Ukraine approved the Concept of the National Target Environmental Programme for Radioactive Waste Management by its Resolution № 992-r dated 4 November 2022 [21]. According to this Concept, the purpose of the National Target Environmental Programme for Radioactive Waste Management is to minimize the impact of the radiation factor on the safety of the population, create an integrated radioactive waste management system, and lay the foundation for safe and cost-effective radioactive waste management.

In accordance with paragraph 2 of the Order of the Cabinet of Ministers of Ukraine of 4 November 2022, the State Agency of Ukraine on Exclusion Zone Management, together with other interested central executive authorities, was instructed to develop and submit to the Cabinet of Ministers of Ukraine within twelve months (i.e. by November 2023) a draft National Target Environmental Programme for Radioactive Waste Management.

Therefore, the Concept of the National Targeted Environmental Programme for Radioactive Waste Management more correctly and fully outlines the general objectives of the national policy on radioactive waste management and is more in line with the requirements of Article 12(1)(a) of Council Directive 2011/70/Euratom than the objectives set out in the National Targeted Environmental Programme for Radioactive Waste Management.

It should be noted that more than two-thirds of the EU Member States in the texts of their national programs informed about their radioactive waste register using the classification scheme in accordance with the IAEA GSG-1 standard or provided such information in the form of a matrix that allows it to be brought in line with the IAEA standards. Therefore, we propose that the State Agency of Ukraine on Exclusion Zone Management, when developing the draft National Target Environmental Programme for Radioactive Waste Management, should include information on available radioactive waste using the classification scheme in accordance with the IAEA GSG-1 standard.

4.2 Analysis of the Practice of Informing the European Commission About the Adoption of National Programs by EU Member States

In accordance with Article 13 of Council Directive 2011/70/Euratom, Member States are required to inform the European Commission of the adoption of national programs and of any subsequent significant amendments to them.

Pursuant to Article 15(1) of that Directive, Member States had to adopt the acts necessary to implement Council Directive 2011/70/Euratom by 23 August 2013 and had to inform the Commission immediately. At the time of writing, all Member States have complied with this provision. However, not all of them were able to do so in time. In November 2013, the European Commission sent letters to thirteen Member States formally notifying them that they had failed to inform it of the national measures taken to implement the Directive. Out of the four cases of lack of information initiated in 2016, three (against Austria, Germany, and France) were closed within one year, and the last one was closed in January 2018.

In addition, the European Commission has appealed to the EU Court of Justice against individual Member States for failing to inform it of their national programs. In particular, the judgment of the Court of Justice of the European Union dated 11 July 2019 in Case C-434/18 states that "by failing to notify the European Commission of its national program for the implementation of the policy on spent fuel and radioactive waste management, the Italian Republic failed to fulfill its obligations under Article 15(4) and Article 13(1) of Council Directive 2011/70/Euratom" [29]. Case C-391/18 states that "the Republic of Croatia has failed to comply with its obligations… And has not informed the Commission of its national program for spent fuel and radioactive waste management" [30]. Case C-487/18 alleged that "by failing to inform the Commission of its national program for spent fuel and radioactive waste management, the Republic of Austria breached its obligations under Article 15(4) in conjunction with Article 13(1) of Council Directive 2011/70/Euratom" [31].

As noted in the Report of the European Commission to the Council and the European Parliament on the progress of the implementation of Council Directive 2011/70/Euratom of 17.12.2019, some Member States have had problems with the proper implementation of the requirements of this Directive in their national legislation. Therefore, back in 2018, the European Commission concluded that more than half of the Member States had incorrectly transposed the provisions of the Directive, and therefore it initiated infringement proceedings against 15 Member States: Austria, the Czech Republic, Denmark, Estonia, Croatia, Hungary, Ireland, Italy, Latvia, Malta, the Netherlands, Poland, Portugal, Romania, and the United Kingdom[3].

Given that Article 13 of Council Directive 2011/70/Euratom requires Member States to inform the European Commission not only of the adoption of national radioactive waste management programs but also of any subsequent significant changes made to them, it would be advisable to clarify what changes are considered significant so that other Member States are not forced to defend themselves in the Court of Justice of the EU against the European Commission.

---

[3] The cases against the Czech Republic and Ireland were closed in July 2019.

4.3 Analysis of the Practice of Forming and Ensuring the Functioning of a Competent Regulatory Authority by EU Member States

In accordance with Article 6 of Council Directive 2011/70/Euratom, Member States shall establish and promote the functioning of a competent regulatory authority for the safety of radioactive waste management.

An analysis of national programs and reports on the implementation of the above Directive by EU Member States showed that all of them have established one or more competent regulatory authorities. However, the European Commission cooperated with individual Member States to further explain to them how to ensure the functional independence of the competent regulatory authority provided for in Article 6(1) of this Directive.

To implement the National Radioactive Waste Management Programme, the Austrian government established the Austrian Radioactive Waste Management Council (Entsorgungsbeirat). This Council develops recommendations and draft acts of the Austrian Federal Government aimed at regulating relations in the final disposal of radioactive waste in accordance with Articles 141 and 142 of the Radiation Protection Act. The Council includes representatives from the Ministry, federal states, experts, and civil society.

In Belgium, according to the Law of 15 April 1994 [32], ONDRAF/NIRAS was established to control the proper management of radioactive waste. ONDRAF/NIRAS is a state organization with a legal personality. Its legal status is set out in Article 179 of the Law of 8 August 1980 and the Royal Decree of 30 March 1981 [33].

The competent regulatory authority in Belgium for radioactive waste management is the Federal Agency for Nuclear Control (FANC), which was established in accordance with Article 2 of the Act of 15 April 1994 on the protection of the public and the environment against dangers arising from ionizing radiation. The FANC is a state organization responsible for the protection of the population and the environment against hazards related to ionizing radiation. FANC is subordinated to the Minister of the Interior, who reports annually to the Parliament on its activities.

The Swedish Radiation Safety Authority (SSI) was established in 1965 to oversee radiation-related activities. On 1 July 2008, the Swedish Radiation Safety Authority (SSM) was established. It is the administrative body responsible for the areas related to the protection of human health and the environment from harmful effects of ionizing and non-ionizing radiation, safety, and physical protection of nuclear and other radiation activities, as well as nuclear non-proliferation. As of 1 January 2015, the SSM employed 321 people, and in 2020, 305 people. The SSM inspects and assesses the condition of nuclear facilities to confirm their compliance with the rules and conditions of the license. During the license term, the SSM may impose conditions related to licensed activities to ensure nuclear safety (in accordance with Section 8 of the Nuclear Activities Act) or radiation protection (in accordance with Section 20–22 of Chapter 6 of the Radiation Protection Act).

In 1992, the Swedish National Nuclear Waste Board was established by the Ministry of the Environment and Energy as an independent scientific advisory body. Its task is to conduct research on issues related to nuclear waste and decommissioning of nuclear facilities, as well as to advise the government and other state authorities in this area.

In Ukraine, in accordance with the Resolution of the Cabinet of Ministers of Ukraine № 564 of 2 October 2014 [34], the State Agency of Ukraine on Exclusion Zone Management is the central executive body responsible for state management of radioactive waste at the stage of its long-term storage and disposal.

Therefore, Ukraine also has a competent regulatory body in the field of radioactive waste management safety, but it is directly subordinated to the Cabinet of Ministers of Ukraine.

4.4   Analysis of the Practice of Formulating National Requirements of the EU Member States for Public Participation in Radioactive Waste Management

According to Article 10 of Council Directive 2011/70/Euratom, Member States must establish national requirements for public information and participation in radioactive waste management.

When members of the public are asked to identify what type of waste they would never allow to be placed near their homes, radioactive waste is the first thing they mention, despite the numerous safety safeguards for its management. Therefore, it is not only necessary to strengthen safeguards against radioactive waste but also to establish mechanisms that allow decisions on the disposal of such waste to be made after the draft decisions have been agreed with the public to promote overall harmony within the country. That is why Article 10 of Council Directive 2011/70/Euratom requires that national legislation should include a requirement for public information and participation in decision-making on radioactive waste management.

The analysis of national reports on the implementation of Council Directive 2011/70/Euratom and national radioactive waste management programs showed that all Member States provide for public involvement in the decision-making process beyond public consultations, for example, participation in working groups and other advisory bodies. Most of the Member States also inform the public through specially created websites, periodic published reports, mass media, etc. and consult with the public through other mechanisms of public information.

The national legislation of all EU member states contains a requirement to provide the public with access to information on radioactive waste management. Bulgarian legislation guarantees public access to information at the earliest stage of implementation of any project related to radioactive waste management. Such access is provided during mandatory public discussions provided for by the Laws on Environmental Protection and Water Resources; Access to Public Information; and Safe Use of Nuclear Energy. Decisions on the siting of radioactive waste facilities are discussed not only with the public but also with local governments and the competent authority that makes the final decision. Such a decision should include measures to prevent negative environmental impacts that are mandatory for the investor/operator during the design, construction, operation, and final closure of the facility.

In Germany, the legislation requires that the public at the national and regional levels can actively participate in the procedure for selecting a site for the disposal of high-level radioactive waste. The BASE is the organizer and coordinator of public engagement. Even "informal meetings" can be used, such as online consultations, conferences on radioactive waste management, or workshops for young people.

At the national level, in December 2016, the National Council of Civil Society was formed in Germany. It consists of 18 members, 12 of whom are prominent public figures appointed by the Bundestag and Bundesrat. The remaining six members are citizens selected from a random sample through a system of qualified selection (including two representatives of the younger generation), who are appointed by the Federal Minister for the Environment. The main task of the National Council is to support the site selection process as an independent body. To this end, the council can seek scientific advice and hire external experts or prepare its own scientific opinions.

Sweden has introduced special tools to involve the public in radioactive waste management. Firstly, local councils have a veto right over undesirable nuclear activities in or near their municipalities. According to Chapter 17, Section 6 of the Environmental Code, the Government can only authorize the use of nuclear facilities if the municipal council of the municipality where the facility is to be located has given permission for its location. However, if the location of a particular facility for the temporary storage or disposal of nuclear material is in the national interest and the decision should be made as soon as possible, the Government may override the municipal veto. In such a case, municipal authorities are empowered to supervise the intended use of the territory, buildings, or structures that may cause damage to the environment because of exposure to ionizing or non-ionizing radiation.

Second, by government decision, five Swedish municipalities with nuclear power plants (Osthammar, Oskarshamn, Kävlinge, Varberg, and Nyköping) have had local nuclear safety boards since the early 1980s to inform the public about their activities. They are composed of members appointed by the government upon nomination by the respective municipality. In accordance with the Nuclear Activities Law and Regulation 2007:1054, the licensee is obliged to provide the local safety council with information on safety and radiation protection activities at each facility. The local council monitors and analyses the information and communicates it to the public and local authorities regarding radiation protection at the facility. It has the right to conduct investigations to assess the measures taken or planned for nuclear or radiation safety at each nuclear facility. The Swedish Radiation Safety Authority regularly participates in meetings of local safety councils.

Thirdly, according to the Act (2006:647) and regulation (2017:1179) on financing the management of nuclear residual products, municipalities that may host a nuclear waste repository receive financial compensation for activities aimed at informing the residents of their municipalities about the safety of radioactive waste management. Currently, the municipalities of Osthammar and Oskarshamn have been receiving such compensation since the mid-1990s. The decision to reimburse the municipalities is made by the Swedish Public Debt Authority. Since 2004, non-profit non-governmental organizations have also been able to apply for reimbursement of costs incurred in consultations related to the disposal of spent nuclear fuel and radioactive waste.

In Ukraine, in accordance with Article 22 of the Law of Ukraine "On Radioactive Waste Management" [9], the decision to construct a radioactive waste storage facility or a facility intended for radioactive waste management, as well as to start design and exploration works at the planned site of a specialized radioactive waste management company, is made by the Verkhovna Rada of Ukraine and the Cabinet of Ministers of

Ukraine. In addition, according to Article 8 of the Law of Ukraine "On Radioactive Waste Management", local state executive authorities and local self-government bodies: organize public hearings on the defense of projects for the siting, construction, and decommissioning of facilities intended for radioactive waste management and closure of disposal facilities; approve the siting of facilities intended for radioactive waste management on their territory based on the interests of citizens living in the area. In accordance with Article 13(3) of the Law of Ukraine "On Information" [35], information on the state of the environment cannot be classified as restricted information.

Therefore, in accordance with the national legislation of Ukraine, the public and local governments have access to information on radioactive waste management. However, Ukraine has been implementing the decentralization reform for almost ten years, which redistributed powers between state authorities and local governments in favor of the latter. Moreover, on 11 February 2021, the European Parliament approved the Report on Ukraine's implementation of the Association Agreement with the European Union. It notes the effectiveness of the decentralization reform, which the EU considers to be one of the most successful in Ukraine, and calls for its completion through a broad, open dialogue between central and local governments [36].

On 15 June 2023, the European Parliament adopted a resolution on Ukraine's sustainable recovery and integration into the Euro-Atlantic community [37], calling on the Ukrainian government to continue to strengthen local governance and to build the success of decentralization reform into the overall architecture of Ukraine's repair, recovery, and reconstruction processes by giving local authorities a prominent role in decision-making (paragraph 15).

Under these conditions, we consider the existing procedure for deciding on conducting design and survey work for the location of facilities intended for radioactive waste management, as well as approving a decision on the selection of a site for the construction of a storage facility or a facility intended for radioactive waste management, to be incorrect. In accordance with Articles 22–23 of the Law of Ukraine "On Radioactive Waste Management", such a decision is made by the State Agency of Ukraine on Exclusion Zone Management, which has the status of a public authority. In our opinion, it is advisable to borrow the experience of Sweden and give the local council the right to veto any decision that may result in the placement of radioactive materials on its territory or the construction of a site for radioactive waste storage. In addition, we propose to introduce a special fee (for example, in the form of rent) for the placement of such hazardous facilities on the territory of the municipality, the proceeds of which should go to the local budget of the municipality.

4.5 Analysis of the Practice of Developing Key Performance Indicators for National Radioactive Waste Management Programs by EU Member States

In accordance with Articles 5 and 11 of Council Directive 2011/70/Euratom, Member States must establish a national legislative framework for the safe management of radioactive waste. States should adopt national programs for the implementation of national waste management policies. To monitor the progress of the implementation of national programs, Member States had to reflect key performance indicators in

them (according to Article 12(1)(g)). However, the Directive is silent on how these key performance indicators should be formulated and assessed.

Our research has confirmed that Member States do not often include such indicators in their national programs. The Report of the European Commission to the Council and the European Parliament on the implementation of Council Directive 2011/70/Euratom of 17.12.2019 states that one of the main challenges in implementing the above Directive is the identification of key performance indicators for monitoring program implementation. The Commission states that more than a third of Member States have not defined key performance indicators and therefore calls on them to comply with the requirements of the Directive [23]. After all, KPIs are used to measure progress definitively, objectively, and quantitatively towards achieving the objectives set. Well-developed KPIs contribute to the effectiveness of the national program, to the safety of radioactive waste management, and responsible use of financial resources.

According to the authors of the research "Study on key performance indicators for monitoring the implementation of national programs on safe and long-term management of spent fuel and radioactive waste" [38], about half of the participating states did not reflect any information on the use of performance indicators in their national radioactive waste management programs. Such information is absent in the French, Italian, and Spanish national programs. The national programs of the Republic of Cyprus and Germany reflect these indicators in a very laconic and uninformative manner.

The Belgian National Programme for the Management of Spent Fuel and Radioactive Waste Kingdom of Belgium (October 2015) includes the following key performance indicators: whether a national policy is in place; whether general and specific radiation protection regulations exist; whether operational management is in place; whether a funding mechanism is in place; and whether R&D is in place. The key performance indicators are shown in Table 7 of the national program [39].

In the Croatian National Programme, the performance indicators include adherence to deadlines (assesses the actual duration of a particular stage compared to the planned duration); legal framework (assesses the number of legal acts amended in accordance with the requirements of the national program compared to the total number of acts to be amended); safety indicators (assessing the fulfillment of acceptance criteria in terms of their impact on the population and the environment); assessment of research and development (assesses the amount of survey work in relation to the amount of work required, implementation of training programs in accordance with human resource needs, participation in international projects); effective financial management (assessing the ratio of available funds to the required funds, actual expenses to planned expenses).

Many states that have developed their national radioactive waste management programs have included as performance indicators those indicators that mostly do not meet the criteria of key performance indicators. As rightly noted in the Croatian National Programme, performance indicators should allow for tracking the achievement of important milestones in accordance with the set goals and measuring progress towards the overall goal of whether individual stages of the national radioactive waste management program have been successfully implemented. Therefore, it would be advisable for the European Commission to provide its recommendations on the formulation, assessment, and use of

key performance indicators so that all Member States can use them in the preparation of their next national programs.

The key performance indicators formulated in Ukraine in the section "Expected Results of the Programme Implementation, Determination of its Effectiveness" of the Concept of the National Target Environmental Programme for Radioactive Waste Management are also not free from the above-mentioned shortcomings. Instead, Annex 3 "Expected Results of the National Target Environmental Programme for Radioactive Waste Management" contains correct indicators that, on the one hand, allow monitoring the achievement of important milestones in accordance with the set goals, and, on the other hand, allow measuring progress in achieving the overall goal.

5   Conclusions

The comparative legal analysis of the safe management of liquid radioactive waste in Ukraine and the EU Member States has shown that they not only declare common values but also really strive to ensure high safety standards to protect the public from the hazards that may arise from ionizing radiation. After all, it is the ethical duty of every European state to avoid any undue burden on future generations in terms of spent fuel and radioactive waste management.

The adoption of Council Directive 2011/70/Euratom was not only a significant step towards the implementation of safety standards to protect human life and health from ionizing radiation but also necessitated the development of national programs for the safe management of radioactive waste by all EU member states. Until now, less than a third of these countries had such programs. Therefore, all EU member states and Ukraine are now making efforts to implement the provisions of Council Directive 2011/70/Euratom into their national legislation.

The comparative analysis of the results of the implementation of Council Directive 2011/70/Euratom into the national legislation of the EU Member States showed that most problems arise in the following areas: development of a national radioactive waste management program that would meet the requirements specified in Article 12 of the Council Directive, in particular, containing key performance indicators that would facilitate monitoring of progress in the implementation of this program; informing the European Commission about the national programs and any subsequent significant changes made to them; establishing a competent regulatory body in the field of radioactive waste safety that is sufficiently independent of state authorities.

Certain countries that have more experience in safe radioactive waste management can be a good guides for other countries. This is also emphasized by the European Commission, which encourages Member States to share their experience and facilitate the exchange of best practices and knowledge.

In the wake of the Chornobyl disaster, Ukraine is striving to implement not only the most advanced technologies to neutralize its consequences, but also to implement the most advanced requirements in its national legislation to prevent a similar tragedy in the future. Therefore, Ukrainian national legislation on radioactive waste management generally meets the requirements of Council Directive 2011/70/Euratom. However, several more important steps need to be taken to ensure that our country fully fulfills its

obligations to implement this Directive. Instead of the current National Target Environmental Programme for Radioactive Waste Management approved by the Law of Ukraine of 17 September 2008, a new one should be adopted based on the above Directive and the Concept of the National Target Environmental Programme for Radioactive Waste Management approved by the Cabinet of Ministers of Ukraine on 4 November 2022. In addition, the Law of Ukraine "On Radioactive Waste Management" of 30 June 1995 should be amended to provide village, settlement, and town councils with the right to veto any decision that may result in the placement of radioactive materials on their territory or the construction of a radioactive waste storage facility. Moreover, a special fee (e.g., in the form of rent) should be introduced for the placement of such hazardous facilities on the territory of a municipality, the proceeds of which should go to its local budget.

References

1. Concept of the National Targeted Environmental Program for Radioactive Waste Management: Order of the Cabinet of Ministers of Ukraine № 992-r of 4 November 2022. https://zakon.rada.gov.ua/laws/show/992-2022-%D1%80#Text. Accessed 24 June 2023
2. Nick, K.S.: The future of nuclear energy and the role of nuclear law. Nucl. Law Bull. **108/109**, 7 (2022)
3. Ute, B.H.: The Radioactive Waste Directive: a necessary step in the management of spent fuel and radioactive waste in the European Union. Nucl. Law Bull. **88**, 21 (2021). https://www.oecd-nea.org/upload/docs/application/pdf/2020-11/nlb88.pdf#page=23. Accessed 24 June 2023
4. Commission Decision of 17 July 2007 on establishing the European High Level Group on Nuclear Safety and Waste Management. OJ L **195/44** (2007). https://eur-lex.europa.eu/LexUriServ/LexUriServ.do?uri=OJ:L:2007:195:0044:0046:EN:PDF. Accessed 24 June 2023
5. Council Directive 2009/71/Euratom of 25 June 2009 establishing a Community framework for the nuclear safety of nuclear installations. OJ L **172**, 18–22 (2009). https://eur-lex.europa.eu/legal-content/EN/TXT/?uri=celex%3A32009L0071. Accessed 24 June 2023
6. Proposal for a Council Directive on the management of spent fuel and radioactive waste. https://eur-lex.europa.eu/legal-content/en/TXT/?uri=CELEX%3A52010PC0618. Accessed 24 June 2023
7. Spent fuel and radioactive waste. European Parliament legislative resolution of 23 June 2011 on the proposal for a Council directive on the management of spent fuel and radioactive waste (COM(2010)0618 – C7 – 0387/2010 – 2010/0306(NLE)). https://eur-lex.europa.eu/legal-content/EN/ALL/?uri=CELEX:52011AP0295. Accessed 24 June 2023
8. Council Directive 2011/70/Euratom of 19 July 2011 establishing a Community framework for the responsible and safe management of spent fuel and radioactive waste. OJ L **199**, 48–56 (2011). https://eur-lex.europa.eu/legal-content/EN/TXT/?uri=CELEX%3A32011L0070&qid=1685717887981. Accessed 24 June 2023
9. On radioactive waste management: Law of Ukraine № 255/95-VR of 30 June 1995. https://zakon.rada.gov.ua/laws/show/255/95-%D0%B2%D1%80#Text. Accessed 24 June 2023
10. On the use of nuclear energy and radiation safety: Law of Ukraine of 8 February 1995 № 39/95-VR. https://zakon.rada.gov.ua/laws/show/39/95-%D0%B2%D1%80#Text. Accessed 24 June 2023
11. On environmental protection: Law of Ukraine of 25 June 1991 № 1264-XII. https://zakon.rada.gov.ua/laws/show/1264-12#Text. Accessed 24 June 2023

12. On Ratification of the Joint Convention on the Safety of Spent Fuel Management and on the Safety of Radioactive Waste Management: Law of Ukraine of 20 April 2000 № 1688-III. https://zakon.rada.gov.ua/laws/show/1688-14#Text. Accessed 24 June 2023
13. On the Programme of Ukraine's Integration into the European Union: Decree of the President of Ukraine of 14 September 2000 № 1072/2000. https://zakon.rada.gov.ua/laws/show/1072/2000#Text. Accessed 24 June 2023
14. On the Integrated Radioactive Waste Management Programme: Resolution of the Cabinet of Ministers of Ukraine of 5 April 1999. № 542. https://zakon.rada.gov.ua/laws/show/542-99-%D0%BF#Text. Accessed 24 June 2023
15. On the National Programme of Adaptation of Ukrainian Legislation to the Legislation of the European Union: Law of Ukraine of 18 March 2004 № 1629-IV. https://zakon.rada.gov.ua/laws/show/1629-15#Text. Accessed 24 June 2023
16. Council Regulation (Euratom) № 1493/93 of 8 June 1993 on shipments of radioactive substances between Member States OJ L **148**, 93 (1993). Accessed 24 June 2023
17. On the National Programme for the Adaptation of Ukrainian Legislation to the Legislation of the European Union, approved by the Law of Ukraine № 1629-IV of 18 March 2004. https://zakon.rada.gov.ua/laws/show/1629%D0%B2-15#Text. Accessed 24 June 2023
18. The Association Agreement between Ukraine, on the one hand, and the European Union, the European Atomic Energy Community, and their Member States, on the other hand. https://zakon.rada.gov.ua/laws/show/984_011#Text. Accessed 24 June 2023
19. On the Basic Principles (Strategy) of the State Environmental Policy of Ukraine for the period up to 2030: Law of Ukraine of 28 February 2019 № 2697-VIII. https://zakon.rada.gov.ua/laws/show/2697-19#n8. Accessed 24 June 2023
20. On approval of the National Environmental Action Plan for the period up to 2025: Order of the Cabinet of Ministers of Ukraine of 21 April 2021. № 443-r. https://zakon.rada.gov.ua/laws/show/443-2021-%D1%80#Text. Accessed 24 June 2023
21. On Approval of the Concept of the National Target Environmental Programme for Radioactive Waste Management: Order of the Cabinet of Ministers of Ukraine of 4 November 2022 № 992-r. https://zakon.rada.gov.ua/laws/show/992-2022-%D1%80#Text. Accessed 24 June 2023
22. Radioactive waste and spent fuel. https://energy.ec.europa.eu/topics/nuclear-energy/radioactive-waste-and-spent-fuel_en. Accessed 24 June 2023
23. Report from the Commission to the Council and the European Parliament on the progress of implementation of Council Directive 2011/70/EURATOM and an inventory of radioactive waste and spent fuel present in the Community's territory and the future prospects. Second report. Brussels, 17.12.2019, COM (2019) 632 final. https://eur-lex.europa.eu/legal-content/EN/TXT/?uri=CELEX%3A52019DC0632&qid=1685717887981. Accessed 24 June 2023
24. National Programme for the Management of Spent Fuel and Radioactive Waste Kingdom of Belgium. First edition (2015). https://economie.fgov.be/sites/default/files/Files/Energy/National-programme-courtesy-translation.pdf. Accessed 24 June 2023
25. The General Radiation Protection Ordinance 2020. Federal Law Gazette I № 133/2015, and the General Radiation Protection Ordinance. Federal Law Gazette II № 22/2015
26. Nacionalni program provedbe Strategije zbrinjavanja radioaktivnog otpada, iskorištenih izvora i istrošenog nuklearnog goriva (Program za razdoblje do 2025. godine s pogledom do 2060. godine). https://circabc.europa.eu/ui/group/d84073d4-cd8f-4c86-b010-e5e4ba2ed899/library/afd620d9-aca5-478f-9833-81911d6ea5b9/details. Accessed 24 June 2023
27. Programma Nazionale per la gestione del combustibile esaurito e dei rifiuti radioattivi. https://www.mase.gov.it/sites/default/files/archivio/allegati/rifiuti_radioattivi/programma_conformepdfa.pdf. Accessed 24 June 2023

28. On the National Target Environmental Programme for Radioactive Waste Management: Law of Ukraine of 17 September 2008 № 516-VI. https://zakon.rada.gov.ua/laws/show/516-17#Text. Accessed 24 June 2023

29. Judgment of the Court of 11 July 2019 – European Commission v Italian Republic. Case C-434/18. OJ 9.9.2019, C 305/25. https://eur-lex.europa.eu/legal-content/EN/TXT/?uri=CELEX%3A62018CA0434&qid=1685717887981. Accessed 24 June 2023

30. Judgment of the Court of 17 December2018 – European Commission v Republic of Croatia. Case C-391/18. OJ C **280**, 33 (2019). By an order of the President of the Ninth Chamber of the Court of Justice of the European Union dated 8 April 2019, this Case was removed from the general register of court decisions. https://eur-lex.europa.eu/legal-content/EN/TXT/?uri=CELEX%3A62018CB0391&qid=1685717887981. Accessed 24 June 2023

31. Judgment of the Court of 17 December2018 – European Commission v Republic of Austria. Case C-487/18. OJ C **328** (2018). https://eur-lex.europa.eu/legal-content/EN/TXT/?uri=uriserv%3AOJ.C_.2018.328.01.0029.02.ENG&toc=OJ%3AC%3A2018%3A328%3ATOC. By an order of the President of the Ninth Chamber of the Court of Justice of the European Union dated 17 December 2018, this case was removed from the general register of court decisions. https://eur-lex.europa.eu/legal-content/EN/TXT/?uri=CELEX%3A62018CB0487&qid=1685717887981. Accessed 24 June 2023

32. Belgian Official Journal, 1994b; Kingdom of Belgium (2014)

33. Belgian Official Journal, 1980; Belgian Official Journal (1981)

34. On Approval of the Regulation on the State Agency of Ukraine on Exclusion Zone Management: Resolution of the Cabinet of Ministers of Ukraine of 22 October 2014. № 564. https://zakon.rada.gov.ua/laws/show/564-2014-%D0%BF#Text. Accessed 24 June 2023

35. On information: Law of Ukraine of 2 October 1992 № 2657-XII. https://zakon.rada.gov.ua/laws/show/2657-12#Text. Accessed 24 June 2023

36. European Parliament Resolution of 11 February 2021 on the implementation of the EU Association Agreement with Ukraine. https://www.europarl.europa.eu/doceo/document/TA-9-2021-0050_EN.html. Accessed 24 June 2023

37. European Parliament Resolution of 15 June 2023 on the sustainable reconstruction and integration of Ukraine into the Euro-Atlantic community. https://www.europarl.europa.eu/doceo/document/TA-9-2023-0247_EN.html. Accessed 24 June 2023

38. Study on key performance indicators for monitoring the implementation of national programs on safe and long-term management of spent fuel and radioactive waste. Final report. ENER/2020/NUCL/SI2.827547. Luxembourg: Publications Office of the European Union, p. 9 (2022). https://op.europa.eu/en/publication-detail/-/publication/41631ae8-0708-11ed-acce-01aa75ed71a1/language-en/format-PDF/source-261756268. Accessed 24 June 2023

39. National Spent Fuel and Radioactive Waste Management Programme of the Kingdom of Belgium. Document drafted by the National Programme Committee pursuant to the Law of 3 June 2014 transposing European Directive 2011/70/Euratom of 19 July 2011, p. 66. https://economie.fgov.be/sites/default/files/Files/Energy/National-programme-courtesy-translation.pdf. Accessed 24 June 2023

Liquid Radionuclide Waste Treatment at Fukushima Daiichi NPP Site: A Brief Review of Environmental Impacts

Maksym Gusyev[1]([✉]) [ID], Naoaki Shibasaki[1,2] [ID], and Mark Zheleznyak[1] [ID]

[1] Institute of Environmental Radioactivity, Fukushima University, 1 Kanayagawa, Fukushima 960-1296, Japan
maksymgusyev@gmail.com, r891@ipc.fukushima-u.ac.jp
[2] Symbiotic Systems Science, Fukushima University, 1 Kanayagawa, Fukushima 960-1296, Japan

Abstract. The Fukushima Daiichi Nuclear Power Plant (NPP) suffered a severe accident in March 2011, resulting in large amounts of radioactive water accumulated at the NPP site. This water has been treated by a combination of various technologies with Advanced Liquid Processing System (ALPS) to remove multiple radionuclides except for tritium, which is difficult to separate from the water molecule, and stored in above ground water tanks at the NPP site. The limited storage capacity prompted the Government of Japan to approve the ALPS treated water discharge into the ocean after dilution of tritium below 1,500 Bq/L. This article reviews the main challenges, technologies, and environmental impacts of the liquid waste at the Fukushima Daiichi NPP site, covering the following topics: 1) Measures to reduce groundwater flows from the NPP site to the marine environment; 2) Modeling of the groundwater fluxes from the NPP site to the marine environment; 3) Technologies of the liquid waste treatment and storage at the NPP site; 4) Technologies of the tritiated water releases to the marine environment from the NPP site; and 5) Modeling of the dispersion of radionuclides released from the NPP site to marine environment.

Keywords: Fukushima – Daiichi Nuclear Power Plant · Advanced Liquid Processing System · Multi-nuclide removal system · tritium · cesium-137 · radionuclides · groundwater · coastal zone radioactivity · modeling

1 Introduction

The Fukushima Daiichi Nuclear Power Plant (NPP) suffered a severe accident in March 2011 with a meltdown of reactor cores and hydrogen explosions due to the earthquake and tsunami related loss of all electrical power resulting in the release of large amounts of radioactive materials into the environment [1–7]. Following the NPP accident, the liquid waste has been generated by the water cooling of damaged nuclear reactors and melted fuel debris that was mixed with contaminated ocean water and groundwater in the flooded basement of the damaged reactor buildings.

To prevent radioactivity movement from the NPP site to the marine environment, groundwater flow reduction measures have been implemented at the NPP site while transferring the high-level radioactive liquid waste to the Centralized Waste Treatment Facility [8]. The contaminated water was treated by a combination of various technologies with Advanced Liquid Processing System (ALPS) removing most of the radionuclides except for tritium in tritiated water, which is difficult to separate by the conventional treatment methods [9, 10]. As the result, the ALPS treated water has been stored at the NPP site in about 1,000 above ground water tanks, which accumulated 1.17 million cubic meters (m^3) by October 2019 [11]. From 2023, the ALPS treated water, which meets regulatory standards for radionuclide discharge into the environment except for tritium, is discharged from the NPP site to the Pacific Ocean after further dilution of tritium below 1,500 Bq/L [12]. This article reviews the main challenges, technologies, and environmental impacts of the liquid waste at the NPP site covering these five topics:

1) Measures to reduce groundwater flows from the Fukushima Daiichi NPP site to the marine environment; 2) Modeling of the groundwater fluxes from Fukushima Daiichi NPP site to the marine environment; 3) Technologies of the liquid waste treatment at the Fukushima Daiichi NPP site; 4) Technologies of the tritiated water releases to the marine environment from the Fukushima Daiichi NPP site; and 5) Modeling of the dispersion of radionuclides released from the Fukushima Daiichi NPP site to marine environment.

2 Measures to Reduce Groundwater Flows from the Fukushima Daiichi NPP Site to the Marine Environment

One of the main challenges in the aftermath of the accident has been the uncontrolled groundwater inflow into the damaged reactor buildings of the Fukushima Daiichi NPP site increasing liquid waste volume and leading to radionuclide-contaminated water discharge to the marine environment [13–15]. Multilayered implementation of removal, containment, and leakage prevention of contaminated water at the NPP site was the highest priority for reducing liquid waste volume and preventing groundwater flow through damaged reactors of the NPP site. These measures have been implemented at the NPP site reducing the average annual groundwater inflow from about 500 m^3/day in 2014 to 150 m^3/day in 2021 (Fig. 1) [16–19]: 1) waterproof pavement to prevent rainfall infiltration and groundwater recharge; 2) 12 groundwater bypass pumping wells installed at the 35 m elevation area to lower groundwater levels and flow rates, 3) sea-side metal sheet wall to prevent coastal groundwater discharge; and 4) land-side frozen wall surrounding damaged reactor and turbine buildings to prevent groundwater inflow.

The waterproof pavement of the NPP site land surface was the first of four measures started implementation in 2013 for preventing rainfall infiltration and groundwater recharge and was followed by the groundwater bypass wells operation starting in 2014. For the groundwater bypass, 12 pumping wells were installed at the 35 m elevation area with well screens near the bottom of the upper permeable layer (Fig. 1) and were designed to lower groundwater levels and flow rates by the combined pumping rate of 200–300 m^3/day [19, 20].
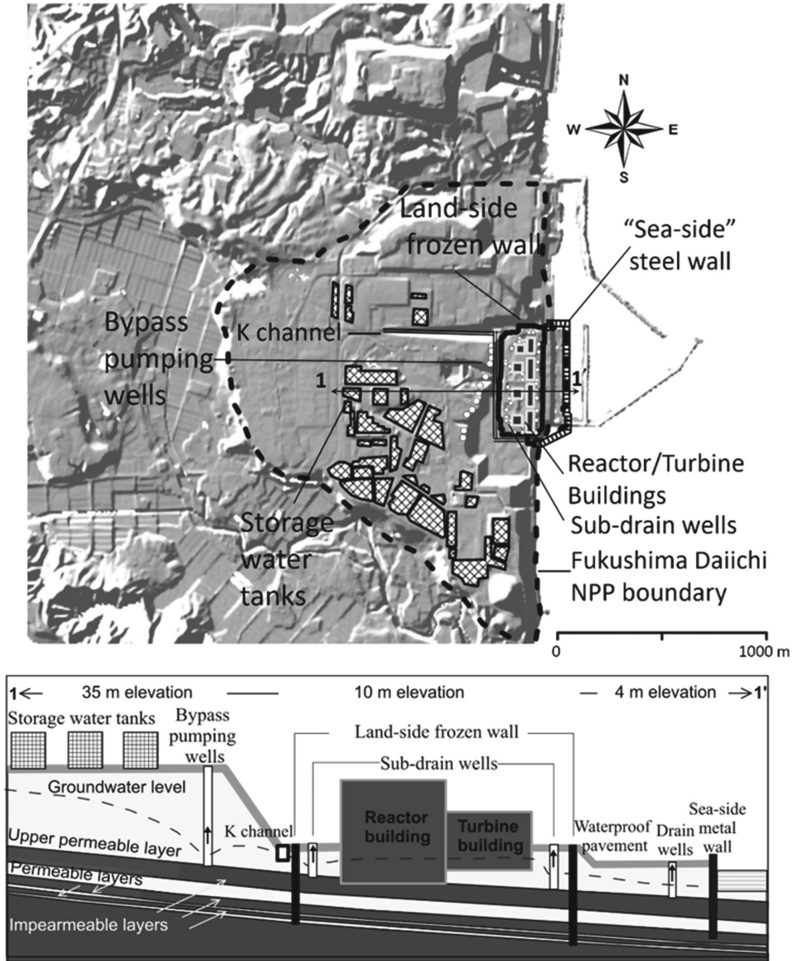
Fig. 1. Location (top) and cross-sectional view (bottom) of implemented measures to reduce groundwater flow at the Fukushima Daiichi NPP site (modified from [16]).

In 2015, the sub-drain and groundwater drain wells started pumping followed by the completion of the sea-side metal wall (Fig. 1) and the average annual groundwater inflow was about 500 m^3/day [16]. The land-side frozen wall became operational by freezing east side on April 2016 (Stage 1 Phase 1) and west side on June 2016 (Stage 1 Phase 2) having the average annual groundwater inflow of about 400 m^3/day. Three phases of partial closure in Stage 2 became operational between December 2016 and August 2017 and the average annual groundwater inflow decreased to about 300 m^3/day. The additional construction of unfrozen portions was completed in September 2018 and the average annual groundwater inflow was the lowest at about 150 m^3/day after that [16]. Groundwater levels of the upper permeable layer are shown in Fig. 2.
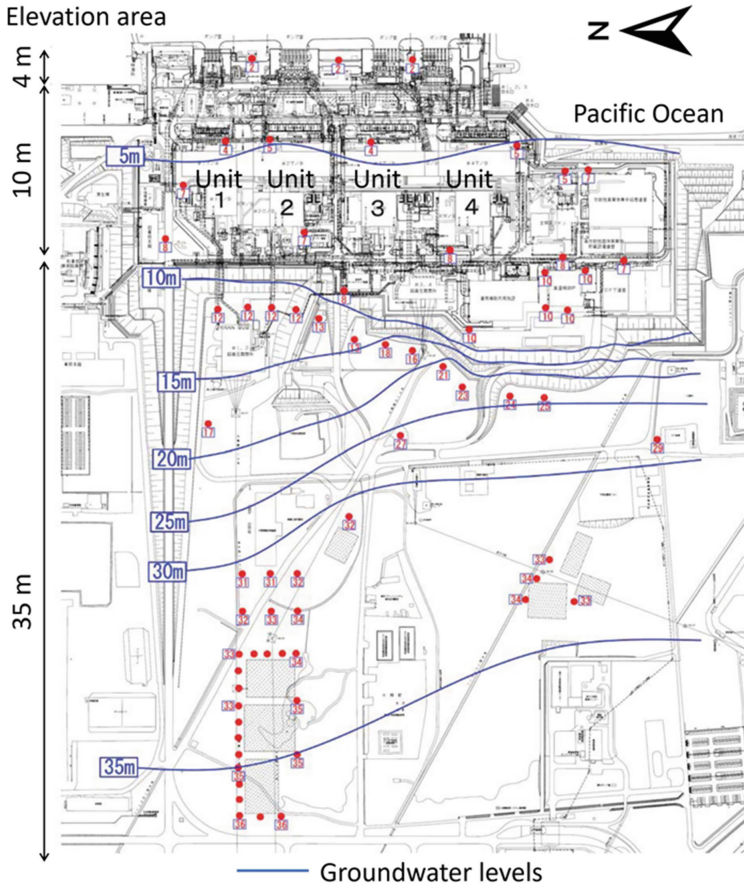
Fig. 2. Groundwater level contours at the upper permeable layer (unconfined aquifer) from 35 m to 10 m at the 35 m elevation area and from 10 m to 5 m at the 10 m elevation area near four units of the Fukushima Daiichi NPP site (modified from [21]).

Comparing the timing of implemented measures with the generated amount of contaminated water, the groundwater inflow reduction due to the groundwater pumping of 12 bypass wells was lesser than the operation of the sub-drain pumping wells. As the result, the combined efforts of implemented measures reduced the contaminated water generation at the NPP site [16] while the issue of additional contaminated water volume still remains to be addressed in future groundwater flow and pathways investigations: rainfall infiltration via damaged reactor buildings and cracked pavement, preferential groundwater flow through the land-side frozen wall, and vertical inflow from the medium permeable layer to upper permeable layer near reactor buildings within enclosed land-side and sea-side walls.

3   Modeling of the Groundwater Fluxes from the Fukushima Daiichi NPP Site to the Marine Environment

For the Fukushima Daiichi NPP site, groundwater flow models were used to evaluate implemented measures in steady-state [21–24] while the transient groundwater flow model represented implemented measures from 2011 to 2022 [16]. The groundwater flow model developed by TEPCO [21] had 110 m thickness and 1.5 km by 2.0 km domain, which covers the half of the NPP site (Fig. 3). The groundwater flow model developed by CCCWT [22, 23] had the same thickness of 110 m and covered the entire NPP site with the model domain of 5.3 km by 3.7 km (Fig. 4). The JAEA [24] developed the groundwater flow model with the largest domain of 6 km by 4 km and thickness of
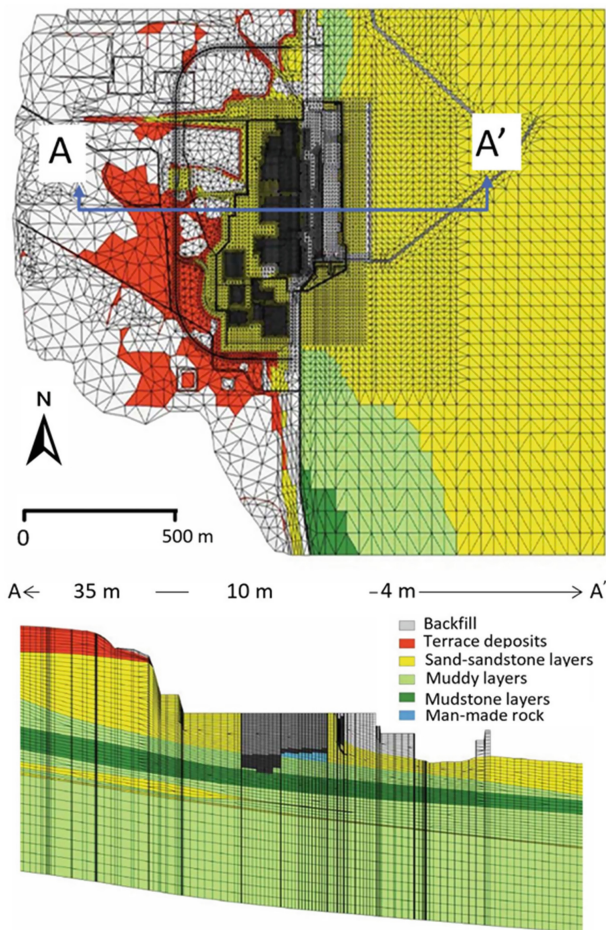
Fig. 3. Groundwater flow model domain (top) and cross-sectional view (bottom) of the Fukushima Daiichi NPP site by TEPCO (modified from [21]).
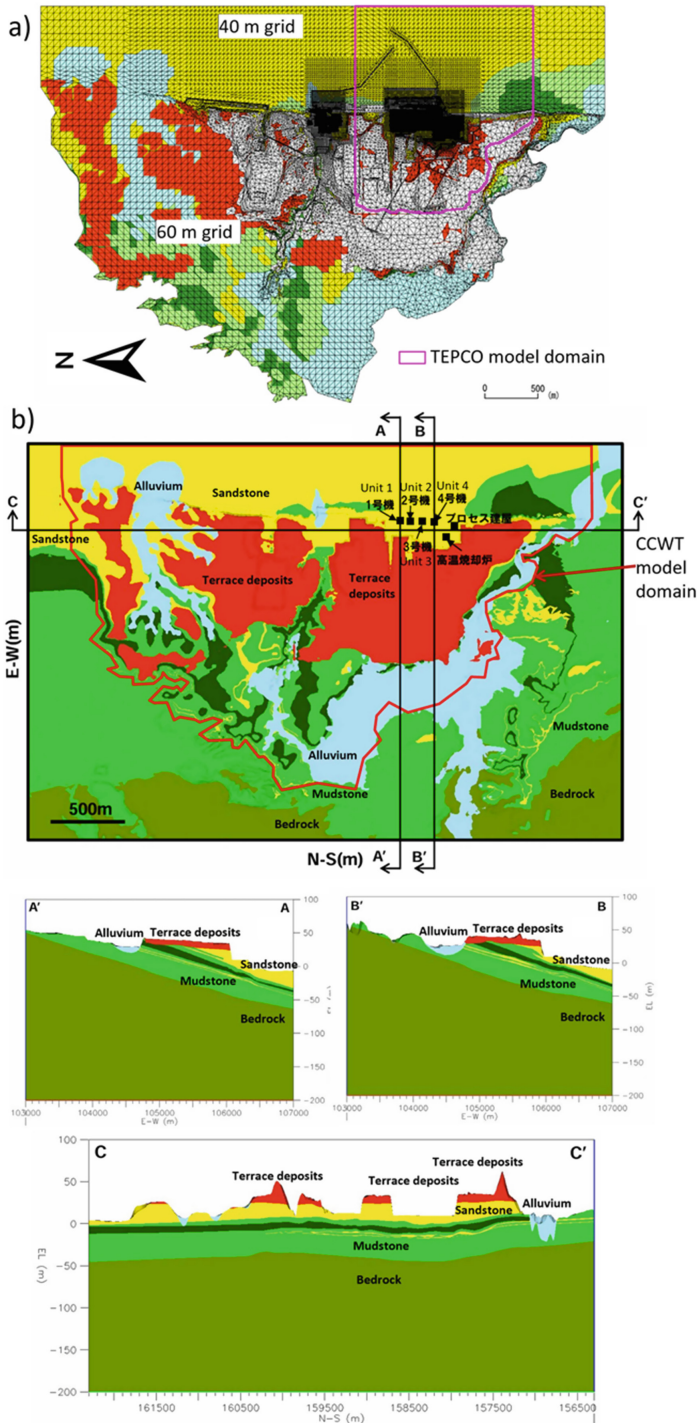
Fig. 4. Spatial extent of the CCCWT model (a) and of the JAEA model with cross-sections A'-A, B'-B, and C-C' (b) for the Fukushima Daiichi NPP site (modified from [22–24]).

260 m (Fig. 4). The domain of the transient groundwater model was similar to the JAEA model covering the entire Fukushima Daiichi NPP site [16].

Figure 5 demonstrates simulated groundwater levels and flow directions by the CCCWT groundwater model in the top (Fig. 5a) and medium (Fig. 5b) aquifers [23]. The groundwater flow models were calibrated to groundwater levels measured at the NPP site boreholes and simulated well pumping scenarios with groundwater discharge of 400 m^3/day through the reactors and turbine buildings [21–24]. Using the finite-difference MODFLOW code with operation dates of implemented measures, eight transient groundwater flow models were set up to simulate the effectiveness of waterproof pavement, sea-side metal wall, bypass pumping wells, sub-drain wells, groundwater drain wells, and
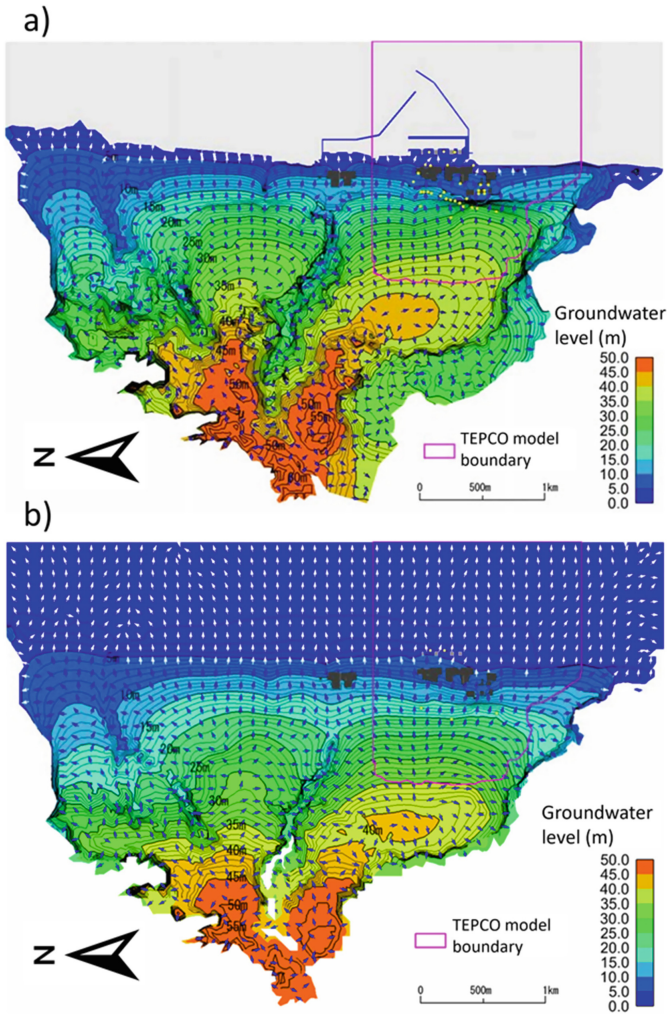
Fig. 5. Simulated groundwater levels and flow directions indicated by arrows in the top (a) and medium (b) aquifers for the Fukushima Daiichi NPP site (modified from [22, 23]).

landside frozen wall [16]. The groundwater flow model was also set up to obtain groundwater travel times using water particle tracking with simulated groundwater velocities by releasing particles at the 35 m elevation area [16].

Groundwater flow model results with implemented measures indicated that groundwater pathway has a limited contamination impact from the 35 m elevation area of the NPP site to the marine environment [16]. From the particle tracking results, groundwater travel times were longer with implemented countermeasures for the unconfined aquifer of above 50 years and for medium deep aquifer of above 100 years. Since tritium radionuclide with a half-life of 12.32 years is a part of the water molecule, tritiated water moves as groundwater and is not slowed down by chemical and aquifer matrix reactions compared to other radionuclides such as ^{137}Cs. In future studies, these simulated groundwater velocities can be used to estimate travel times of infiltrated radionuclide concentrations similar to the tritiated water [26, 27].

4   Technologies of the Liquid Waste Treatment and Storage at the Fukushima Daiichi NPP Site

Since one of the major challenges in the aftermath of the accident is the management of the liquid waste generated by the cooling and decontamination of the damaged reactors. The liquid waste includes contaminated water, spent fuel pool water, and secondary waste from water treatment processes. The technologies of the liquid waste treatment and storage at the Fukushima Daiichi NPP site involve several steps (Fig. 6) [9]:

– Filtration and desalination to remove suspended solids, salts, and some radionuclides from the contaminated water.
– Advanced liquid processing system (ALPS) to remove 62 remaining radionuclides, except for tritium, from the filtered and desalinated water.
– Storage tanks for the ALPS treated water, which still contains tritium and some residual radionuclides.
– Solidification and vitrification to immobilize the secondary waste, such as sludge, spent adsorbents, and evaporator concentrates, in a stable matrix suitable for disposal.
– Interim storage facilities to store the solidified and vitrified waste until final disposal.
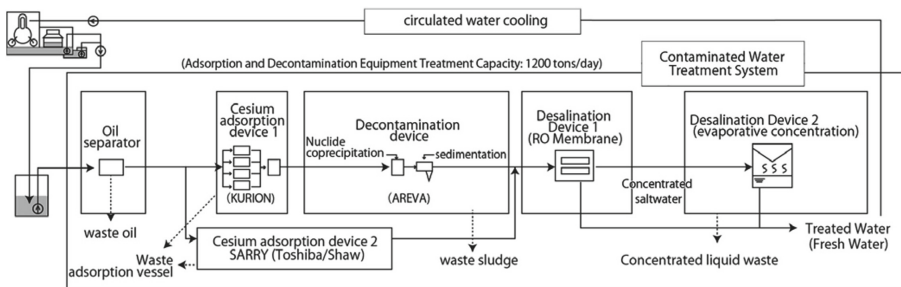

Fig. 6. Contaminated water treatment system supporting circulating water cooling [9].

The ALPS was developed by Toshiba and Energy Solutions for the liquid waste of Fukushima Daiichi NPP site and the system has been in operation since 2013 treating the contaminated water [9]. To date, the experience gained from the operation of ALPS has been invaluable for Japan advancing the treatment technologies of the liquid radioactive waste internationally.

5 Technologies of the Tritiated Water Releases to the Marine Environment from the Fukushima Daiichi NPP Site

Tritium has been released from the Fukushima Daiichi NPP site to the marine environment before the scheduled release of the ALPS treated water [27–30]. Tritium concentrations exceed the regulatory limit for discharge due to tritiated water, which is inseparable from normal water molecule by conventional treatment methods. For the health hazard, tritium radionuclide emits low-energy beta radiation that can be easily shielded by water or skin and can have an impact through ingestion and/or inhalation. As a result, the Government of Japan decided to release tritiated water of the ALPS treated water into the marine environment after dilution of tritium below 1,500 Bq/L [12].

The technology of water dilution for the ALPS treated water releases is based on the principle of dispersion and dilution of the radionuclides in the ocean, which reduces their environmental impact and human exposure (Fig. 7). The dilution process involves mixing the tritiated and ocean waters in a controlled manner using pumps, valves, pipes, and monitoring systems. The diluted water is then discharged through an outlet that is located about 1 km away from the shore and near the ocean bottom insuring adequate dispersion. The ALPS treated water discharge rate and timing are adjusted according to the ocean currents and weather conditions to avoid accumulation or recirculation of the
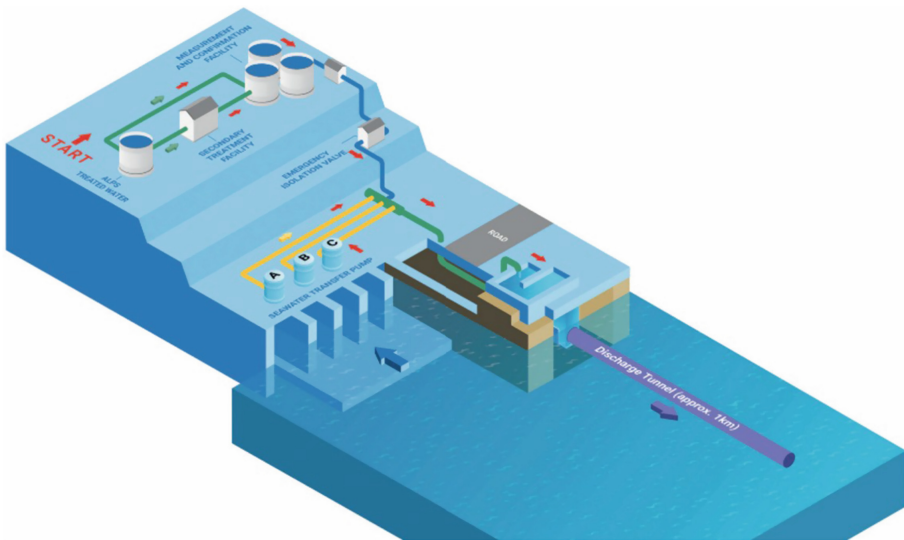

Fig. 7. Schematic diagram of water dilution technology for the ALPS treated water releases [10].

radionuclides near the coast of the Fukushima Daiichi NPP site. The whole process is supervised by independent experts and IAEA regulators, who verify that the radiation levels in the seawater, marine life, and seafood are within acceptable limits.

6 Dispersion of Radionuclides Released from the Fukushima Daiichi NPP Site to Marine Environment

After the accidental release of radionuclides from the reactor units of the Fukushima Daiichi NPP into the atmosphere, the long-term process of direct discharge of radioactive water into coastal waters began. This occurred during the emergency cooling process and continued through surface runoff from the contaminated site, increased flow of contaminated groundwater and leakage of contaminated water from the basements of reactor buildings into the marine environment [31].

The largest contributor to the marine contamination was ^{137}Cs with activity measured by TEPCO in seawater samples from the northern canal of the undamaged reactor unit 5 and 6 at the NPP site reached 68 MBq/m^3 on 6 April 2011. Based on the processing of the monitoring data, the direct ^{137}Cs fluxes to the coastal waters were also estimated to be about 100 GBq/day until June 2011 and 10 GBq/day in July–August 2011 [32]. The consensus assessment of ^{137}Cs fluxes to the ocean via the various pathways until 2020 [31, 32] includes 15–21 PBq as total atmospheric release, 3–6 PBq as atmospheric deposition on land, 12–15 PBq as atmospheric deposition on the North Pacific Ocean, and 3–6 PBq as direct discharge to the ocean. The total inventory in the North Pacific is 15–18 PBq with 0.06–0.13 PBq in marine sediments.

To address scarce monitoring data, atmospheric modelling and modelling of radionuclide dispersion in the ocean based on 3-D oceanographic models were the primary tools used for assessments of inventory of marine contamination since the first years after the Fukushima Daiichi NPP accident [33–35]. The oceanographic 3-D models used in the post-accident studies were the OGCM of Tokyo University [33], ROMS [34–36], FVCOM [37], HYCOM [38] and the regional 3-D oceanographic and radionuclide transport model THREETOX of the JRODOS decision support system [39]. The description of ^{137}Cs interaction with bottom and suspended sediments was performed in the JAEA models SEA-GEARN and STEAMER [33, 36], based on the approach of Perianes [5], modified in the JAEA modelling systems [40, 41]. The models successfully predicted the dispersion in the North Pacific of radioactivity deposited on the ocean surface and released directly into the ocean from the NPP site [33–39, 42, 43]. The measured data of Fukushima-derived radionuclides in water, sediment and marine biota of the North Pacific provide an opportunity to compare the efficiency of different modelling approaches for modelling radionuclide dynamics in water, sediment and marine biota within the intercomparison studies of the IAEA MODARIA programme [43]. As a result of this comprehensive project, it was concluded that there is a general trend towards describing sediment processes in a dynamic manner using kinetic transfer coefficients rather than an equilibrium approach based on partition coefficients. For coastal areas, recent developments in numerical modelling include approaches based on comprehensive modelling of the redistribution exchange in the "water-sediments-suspended sediments" system. Examples of such studies are the modelling of ^{137}Cs dynamics in

the coastal areas of the NPP site [44] based on the 3-D model ROMS and the modelling of the nearshore zone [45], where a significant input to the water dynamics is provided by the wind wave generated currents described by 2-D model COASTOX [46, 47]. The transport models developed and validated for the Fukushima Daiichi NPP accident were used to assess the consequences of radionuclide releases from the ALPS system to the ocean.

According to the Radiological Environmental Impact Assessment (REIA) refined by TEPCO [25] after the review of the first version of the REIA by the IAEA [10], ALPS treated water releases were planned from three groups of tanks – K4, J1-C, and J1-G with the following water parameters:

– K4: Concentration of tritium at 90,000 Bq/L. Sum of the ratios of the activity concentration of 30 nuclides other than tritium to the regulatory concentration: 0.28;
– J1-C: Concentration at 820,000 Bq/L. Sum of the ratios: 0.23;
– J1-G: Concentration at 270,000 Bq/L. Sum of the ratios: 0.12.

All scenarios assume that the amount of tritium in the discharged treated water is less than 22 TBq per year and that the tritium concentration in the treated water after dilution is less than 1,500 Bq/L. When ALPS treated water is discharged, the water is treated with ALPS and other equipment so that the sum of the ratios of radionuclides other than tritium is less than one, and then diluted with seawater 100 times or more before discharge until the tritium concentration is 1/40 (1,500 Bq/L) of the regulatory limit for tritium (less than 60,000 Bq/L). As a result, the concentrations of radionuclides other than tritium will be well below the regulatory concentration limit of each.

The JAEA model, based on the nested ROMS oceanographic model and tested for ^{137}Cs modelling, was used in the TEPCO REIA study [25, 35, 36, 44]. The computational grid with a horizontal resolution of 185 m by 147 m was used in the vicinity of the Fukushima Daiichi NPP site, and a larger grid of 1 km by 1 km was chosen in the outer area of 500 km (east-west) by 300 km (north-south) with 30 vertical layers.

The assessment based on the meteorological and ocean data for 2019 showed that the area with higher tritium concentrations than the current surrounding area (0.1–1 Bq/L) will be limited to the area 2 to 3 km from the Fukushima Daiichi NPP site. The REIA emphasizes that tritium concentrations in this area are much lower than the WHO drinking water quality guideline for tritium of 10,000 Bq/L [10].

The results of the dose assessment by modelled radionuclide concentrations after ALPS treated water releases for the population groups in coastal areas with the large assumption of marine food for releases from three groups of tanks [10]: K4 - 0.00002 mSv/year, J1-C - 0.000005 mSv/year, and J1-G - 0.000005 mSv/year. These doses are 4–5 orders of magnitude lower than the dose limit for the general public (1 mSv/year) and the regional dose from natural radiation (2.1 mSv/year).

The results of REIA have been reviewed and endorsed by the IAEA [10]. In addition to the results of the JAEA team presented in REIA, the consequences of the ALPS treated water releases have been modelled in several international modelling studies. In [48], the POSEIDON-R model, which has been widely validated against marine Fukushima radionuclide data [43], was used to simulate the consequences of the scenario of 10-year and 40-year releases of ALPS treated water. External and internal doses via the marine food chain were calculated not only for tritium but also for other nuclides present in

very small quantities in the ALPS treated water. It has been shown that, although the public is mainly concerned about the tritium releases, the input of tritium is only 1% of the input into the additional dose via marine pathways due to the release of the ALPS treated water. The predicted maximum annual dose corresponding to the third year after the start of the release is 0.00034 mSv for the 10-year release and 0.00014 mSv for the 40-year release, of which the ^{129}I input is 82% and the ^{14}C input is 16%.

The other 8 radionuclides contribute only 2% of the total dose, half of which is from tritium [49]. The main conclusions of this modelling study are: the activity concentrations in marine products in the future will not exceed food safety limits in Japan, no adverse effects on marine biota are expected. The spatio-temporal transport of tritium released from the Fukushima Daiichi NPP site was modelled for the Pacific Ocean scale in [49] using a 3-D global oceanographic model, POM, with the advection-dispersion radionuclide transport equation from [34]. Assuming a total tritium release of 1.2 PBq into the ocean with four release duration scenarios, it was simulated that the majority of the tritium would be mixed with radioactive water from the Fukushima Daiichi NPP site and rapidly diluted in the coastal waters of Japan, and then transported eastward along the Kuroshio extension. It would reach the Pacific coast of North America within 4–5 years (Fig. 8) [49]. The southward plume of contaminated water would be blocked at the sea surface by the strong Kuroshio current. The radioactive tritiated water would enter the Pacific mode water through vertical mixing such as winter cooling and buoyancy loss. This fraction of the tritium would be transported through the Luzon Strait to the China Seas. The transboundary effects of the releases on tritium concentrations are practically below the monitoring capabilities for the assumed volume of releases.
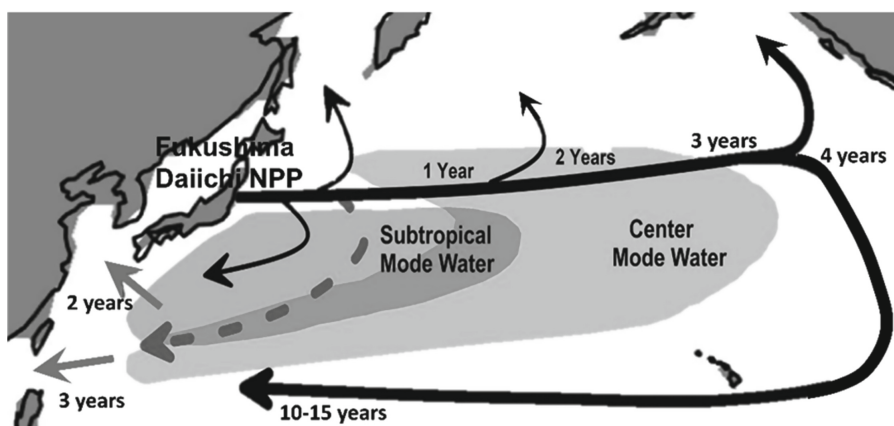
Fig. 8. A schematic view of tritium spreading fluxes from the Fukushima Daiichi NPP site release in the North Pacific Ocean and of the averaged time to reach the located region after the water discharge from the NPP site (modified from [50]).

For the long-term ALPS treated water release plans, the annual tritium discharges of 22 TBq is much smaller compared to tritium inventory in oceans [51, 52]. In 2016, the total tritium inventory of 1,900,000 TBq was estimated combining natural and artificial

tritium in the North Pacific Ocean [51]. The recent publication [52] adds to the non-significance of the ALPS treated water to a human health indicating that all tritium contributes only 0.04% of the total radioactivity of 8 billion TBq in the Pacific Ocean, where most of the radioactivity is due to naturally occurring potassium-40 (91%) and rubidium-87 (8.6%), which are not considered to be a health hazard.

An important aspect of the ALPS treated water release is the transparency of the monitoring data for radionuclide concentrations in the above ground storage tanks [53] and in the marine environment [54]. The environmental monitoring data during the first releases in 2023 confirmed the modelling assessment of no increase in concentrations above low levels in the coastal zones of the Fukushima Daiichi NPP site.

7   Concluding Remarks

The 2011 disaster at the Fukushima Daiichi NPP resulted in the accumulation of radionuclide-contaminated liquid waste, including water used for reactor cooling and rain and groundwater that seeped into the damaged buildings. Several countermeasures have been implemented at the NPP site to prevent the increase of liquid waste volume and the groundwater flow models were a valuable tool for selecting optimal options to reduce groundwater fluxes of radionuclides from the NPP site to the ocean. The contaminated water has been stored at the NPP site posing a significant challenge to the plant's operators, as it needed to be treated before it could be released into the environment. The Advanced Liquid Processing System (ALPS) was developed by Toshiba and Energy Solutions to remove radioactive contaminants from the water that has been used for cooling the reactors and fuel debris at the Fukushima Daiichi NPP. The system has been in operation since 2013 treating the contaminated water at the plant and the experience gained from the operation of ALPS has been invaluable in advancing the treatment of liquid radioactive waste. The system has removed more than 60 radioactive contaminants from the water below regulatory levels, but it cannot remove the tritium radionuclide, which is a part of the water molecule. The advanced modeling tools were developed to assess the consequences of direct releases of ^{137}Cs and ^{134}Cs from the NPP site to coastal waters. The modeling predicted low environmental impact of tritiated water releases to the ocean through the ALPS system and tritium monitoring data obtained in 2023 during the first ALPS treated water releases from the NPP site to the ocean confirmed the conclusions of the modeling results.

References

1. The Tokyo Electric Power Company, Inc. (TEPCO): Fukushima Nuclear Accident Analysis Report (Interim Report) (2011). https://www4.tepco.co.jp/en/press/corp-com/release/11120205-e.html
2. TEPCO: Spillage of liquid containing radioactive substances into the sea from the vicinity of the intake of Unit 2 of the Fukushima Daiichi Nuclear Power Plant (2011). https://www.tepco.co.jp/cc/press/11040202-j.html. (in Japanese)
3. Schwantes, J.M., Orton, C.R., Clark, R.A.: Analysis of a nuclear accident: fission and activation product releases from the Fukushima Daiichi nuclear facility as remote indicators of source identification, extent of release, and state of damaged spent nuclear fuel. Environ. Sci. Technol. **46**, 8621–8627 (2012)

4. Matsumoto, T., et al.: Tritium in Japanese precipitation following the March 2011 Fukushima Daiichi Nuclear Plant accident. Sci. Total. Environ. **445–446**, 365–370 (2013)
5. Steinhauser, G.: Fukushima's forgotten radionuclides: a review of the understudied radioactive emissions. Environ. Sci. Technol. **48**, 4649–4663 (2014)
6. Chino, M., et al.: Detailed source term estimation of the atmospheric release for the Fukushima Daiichi Nuclear Power Station accident by coupling simulations of an atmospheric dispersion model with an improved deposition scheme and oceanic dispersion model. Atmos. Chem. Phys. **15**, 1029–1070 (2015). https://doi.org/10.5194/acp-15-1029-2015
7. Takahata, N., Tomonaga, Y., Kumamoto, Y., Yamada, M., Sano, Y.: Direct tritium emissions to the ocean from the Fukushima Daiichi nuclear accident. Geochem. J. **52**, 211–217 (2018)
8. TEPCO: Transfer of high-level radioactive liquid waste to the Centralized Waste Disposal Facility (2011)
9. Yamagishi, I., Mimura, H., Idemitsu, K.: Difficulties in treatment of contaminated water in fukushima-1 nuclear power plant and disposal of its secondary waste –proposal of countermeasures with focus on disposal. J. Atomic Energy Soc. Jpn. **54**(3), 213–223 (2012). https://www.aesj.net/document/fukushima_vol1/1-213_223.pdf
10. IAEA: Comprehensive Report on the Safety Review of ALPS-Treated Water at the Fukushima Daiichi Nuclear Power Station, Ministry of Foreign Affairs (2023). https://www.mofa.go.jp/dns/inec/page6e_000369.html
11. Ministry of Economy, Trade and Industry (METI): The Subcommittee on Handling of the ALPS Treated Water Report. METI, p. 57 (2020). https://www.meti.go.jp/english/earthquake/nuclear/decommissioning/pdf/20200210_alps.pdf
12. METI: Change to the Definition of ALPS Treated Water at TEPCO's Fukushima Daiichi Nuclear Power Station on April 13th 2021. Website of the METI of Japan. Accessed 25 Oct (2023). https://www.meti.go.jp/english/press/2021/0413_004.html
13. Shibasaki, N: Contaminated water issues at Fukushima Daiichi Nuclear Power Station—its geological background and challenges. Earth Sci. **69**(5), 267–282 (2015). https://doi.org/10.15080/agcjchikyukagaku.69.5_267. (in Japanese)
14. Xu, S., et al.: 129I and 137Cs in groundwater in the vicinity of Fukushima Daiichi nuclear power plant. Geochem. J. **50**(3), 287–291 (2016)
15. Tanji, T., et al.: Analysis of groundwater flows under the Fukushima Daiichi Nuclear Power Plant reactors using contaminated water from 42 subdrain pits. ACS ES&T Water **3**(1), 139–146 (2022)
16. Shibasaki, N.: Geological and hydrogeological issues of Fukushima Daiichi Nuclear Power Station: current conditions and challenges of 10 years after the nuclear accident. Monograph **61**, 228 (2021). ISSN 0912–5760. (in Japanese)
17. Marui, A., Gallardo, A.H.: Managing groundwater radioactive contamination at the Daiichi nuclear plant. Int. J. Environ. Res. Public Health **12**(7), 8498–8503 (2015)
18. Gallardo, A.H., Marui, A.: The aftermath of the Fukushima nuclear accident: measures to contain groundwater contamination. Sci. Total. Environ. **547**, 261–268 (2016)
19. TEPCO: Groundwater bypass operation status and effectiveness analysis. Material **4** (2014). https://www.pref.fukushima.lg.jp/uploaded/attachment/77811.pdf. Accessed 30 Sept 2020. (in Japanese)
20. Suenaga, K.: Queries with effect of the groundwater bypass as countermeasures for contaminated water in Fukushima Daiichi Nuclear Power Plant. Earth Sci. **69**(5), 283–288 (2015). https://doi.org/10.15080/agcjchikyukagaku.69.5_283. (in Japanese)
21. TEPCO: Geology, groundwater and analysis around the Fukushima Daiichi Nuclear Power Plant. Document 3, Contaminated water treatment committee. Material 3, Contaminated water treatment committee, 5th meeting at Ministry of Economy, Trade and Industry (2013). https://www.meti.go.jp/earthquake/nuclear/pdf/130823/130823_01g.pdf. (in Japanese)

22. Committee on contaminated water treatment (CCCWT): Interim report of Sub-group 1: Understanding and visualizing the behaviour of groundwater and rainwater. Materials 2–1, 9th meeting at Ministry of Economy, Trade and Industry (2013). https://www.meti.go.jp/arthquake/nuclear/pdf/131115/131115_01d.pdf. (in Japanese)

23. CCCWT: Preventive and multilayered contaminated water treatment measures at the TEPCO's Fukushima Daiichi NPP - through comprehensive risk management. Materials 1–2, 11th meeting at Ministry of Economy, Trade and Industry (2013). https://www.meti.go.jp/earthquake/nuclear/pdf/131210/131210_01d.pdf. (in Japanese)

24. Japan Atomic Energy Agency (JAEA): Groundwater flow analysis for the Fukushima Daiichi nuclear power plant. Materials 1–3, Committee on contaminated water treatment, 11th meeting at Ministry of Economy, Trade and Industry (2013). https://www.meti.go.jp/earthquake/nuclear/pdf/131210/131210_01e.pdf. (in Japanese)

25. TEPCO. Radiological Environmental Impact Assessment Regarding the Discharge of ALPS Treated Water into the Sea. Construction stage, p. 34 (2022). https://www.tepco.co.jp/en/hd/decommission/information/committee/pdf/2022/technical_22112103-e.pdf. Accessed 02 Feb 2023

26. Gusyev, M.A., Abrams, D., Toews, M., Morgenstern, U., Stewart, M.K.: A comparison of particle-tracking and solute transport methods for simulation of tritium concentrations and groundwater transit times in river water. Hydrol. Earth Syst. Sci. **18**, 3109–3119 (2014)

27. Shozugawa, K., et al.: Landside tritium leakage over through years from Fukushima Daiichi nuclear plant and relationship between countermeasures and contaminated water. Sci. Rep. **10**(1), 19925 (2020)

28. Sato, H., Onda Y., Gusyev, M.: Factors contributing to the 137Cs variation in the drainage channel K at the Fukushima Daiichi Nuclear Power Plant by mixing model using 3H concentration. In: AGU Fall Meeting Abstracts, H32M-1082 (2022)

29. Machida, M., et al.: Tritium inventory and its temporal variation in Fukushima front sea area—comparison between coastal and offshore tritium inventories and 1F treated water and operational target values for discharge per year. J. Atomic Energy Soc. Jpn. **22**(1), 12–24 (2023). https://doi.org/10.3327/taesj.J22.001.(inJapanese)

30. Machida, M., et al.: Estimation of Temporal variation of discharged tritium from port of Fukushima Dai-ichi nuclear power plant: analysis of the temporal variation and comparison with released tritium from Japan and major nuclear facilities worldwide. J. Atomic Energy Soc. Jpn. **22**(1), 33–49 (2022). https://doi.org/10.3327/taesj.J20.036.(inJapanese)

31. Buesseler, K., et al.: Fukushima Daiichi–derived radionuclides in the ocean: transport, fate, and impacts. Ann. Rev. Mar. Sci. **9**, 173–203 (2017)

32. Aoyama, M., Tsumune, D., Inomata, Y., Tateda, Y.: Mass balance and latest fluxes of radiocesium derived from the Fukushima accident in the western North Pacific Ocean and coastal regions of Japan. J. Environ. Radioact. **217**, 106206 (2020)

33. Kawamura, H., et al.: Preliminary numerical experiments on oceanic dispersion of 131I and 137Cs discharged into the ocean because of the Fukushima Daiichi nuclear power plant disaster. J. Nucl. Sci. Technol. **48**(11), 1349–1356 (2011)

34. Tsumune, D., Tsubono, T., Aoyama, M., Hirose, K.: Distribution of oceanic 137Cs from the Fukushima Daiichi Nuclear Power Plant simulated numerically by a regional ocean model. J. Environ. Radioact. **111**, 100–108 (2012)

35. Kamidaira, Y., Uchiyama, Y., Kawamura, H., Kobayashi, T., Furuno, A.: Submesoscale mixing on initial dilution of radionuclides released from the Fukushima Daiichi Nuclear Power Plant. J. Geophys. Res. Oceans **123**(4), 2808–2828 (2018)

36. Kamidaira, Y., Kawamura, H., Kobayashi, T., Uchiyama, Y.: Development of regional downscaling capability in STEAMER ocean prediction system based on multi-nested ROMS model. J. Nucl. Sci. Technol. **56**(8), 752–763 (2019)

37. Lai, Z., et al.: Initial spread of 137 Cs from the Fukushima Dai-ichi Nuclear Power Plant over the Japan continental shelf: a study using a high-resolution, global-coastal nested ocean model. Biogeosciences **10**(8), 5439–5449 (2013)

38. Kawamura, H., et al.: Oceanic dispersion of Fukushima-derived Cs-137 simulated by multiple oceanic general circulation models. J. Environ. Radioact. **180**, 36–58 (2017)

39. Maderich, V., Brovchenko, I., Dvorzhak, A., Ievdin, I., Koshebutsky, V., Periáñez, R.: Integration of 3D model THREETOX in JRODOS, implementation studies and modelling of Fukushima scenarios. Radioprotection **51**(HS2), S133–S135 (2016)

40. Perianez, R.: A three dimensional σ-coordinate model to simulate the dispersion of radionuclides in the marine environment: application to the Irish Sea. Ecol. Model. **114**, 59 (1998)

41. Kobayashi, T., Otosaka, S., Togawa, O., Hayashi, K.: Development of a non-conservative radionuclides dispersion model in the ocean and its application to surface cesium-137 dispersion in the Irish Sea. J. Nucl. Sci. Technol. **44**(2), 238–247 (2007)

42. Kobayashi, T., Chino, M., Togawa, O.: Numerical simulations of short-term migration processes of dissolved cesium-137 due to a hypothetical accident of a nuclear submarine in the Japan Sea. J. Nucl. Sci. Technol. **43**(5), 569–575 (2006)

43. Aoyama, M., et al.: Radiocaesium derived from the TEPCO Fukushima accident in the North Pacific Ocean: Surface transport processes until 2017. J. Environ. Radioact. **189**, 93–102 (2018)

44. Periáñez, R., et al.: Fukushima 137Cs releases dispersion modelling over the Pacific Ocean: comparisons of models with water, sediment and biota data. J. Environ. Radioact. **198**, 50–63 (2019)

45. Kamidaira, Y., Uchiyama, Y., Kawamura, H., Kobayashi, T., Otosaka, S.: A modeling study on the oceanic dispersion and sedimentation of radionuclides off the coast of Fukushima. J. Environ. Radioact. **238**, 106724 (2021)

46. Zheleznyak, M., et al.: Modelling of Cs-137 transport in the nearshore zone of Fukushima-Daiichi NPP under the combined action of waves, currents and fluxes of sediments. In: EGU General Assembly Conference Abstracts, p. 19294 (2018)

47. Kivva, S.L., Zheleznyak, M.J.: Two-dimensional modeling of rainfall runoff and sediment transport in small catchment areas. Int. J. Fluid Mech. Res. **32**(6), 703–717 (2005)

48. Zheleznyak, M., Kivva, S., Pylypenko, O., Sorokin, M.: Modeling of behavior of Fukushima-derived radionuclides in freshwater systems. In: Nanba, K., Konoplev, A., Wada, T. (eds.) Behavior of Radionuclides in the Environment III, pp. 199–252. Springer, Singapore (2022)

49. Bezhenar, R., Takata, H., de With, G., Maderich, V.: Planned release of contaminated water from the Fukushima storage tanks into the ocean: simulation scenarios of radiological impact for aquatic biota and human from seafood consumption. Mar. Pollut. Bull. **173**, 112969 (2021)

50. Zhao, C., et al.: Transport and dispersion of tritium from the radioactive water of the Fukushima Daiichi nuclear plant. Mar. Pollut. Bull. **169**, 112515 (2021)

51. Oms, P.-E., et al.: Inventory and distribution of tritium in the oceans in 2016. Sci. Total Environ. **656**, 1289–1303 (2019)

52. Smith, J., Marks, N., Irwin, T.: The risks of radioactive waste water release. Science **382**(6666), 31–33 (2023)

53. JAEA, Japanese Atomic Energy Agency, Homepage Analysis of ALPS treated water as third-party. https://fukushima.jaea.go.jp/okuma/alps/index_e.html. Accessed 02 Nov 2023

54. ME, Ministry of the Environment of Japan, Homepage ALPS Treated Water Marine Monitoring Information. https://shorisui-monitoring.env.go.jp/en/map/01/. Accessed 02 Nov 2023

Geopolymer-Based Mineral Mixtures for Fire and Heating Protection of Concrete and Steel Products of Nuclear Power Plants

Sergii Guzii[1,1](✉) , Yurii Zabulonov[1] , Oleksandr Pugach[1] ,
Olena Prysiazhna[2] , Tetiana Kurska[3] , and Natalia Grygorenko[4]

[1] State Institution "The Institute of Environmental Geochemistry of National Academy of Sciences of Ukraine", [Pleaseinsert\PrerenderUnicode{Đš}intopreamble]yiv 03142, Ukraine
sguziy2@gmail.com
[2] V. Bakul Institute for Superhard Materials National Science Academy Ukraine, Kyiv 07074, Ukraine
[3] Odesa Polytechnic State University, Odesa 6504, Ukraine
[4] National University of Civil Defence of Ukraine, Kharkiv 61023, Ukraine

Abstract. The The article presents the results of the use of fireproof coatings and fire-insulating mixtures based on geopolymer to protect concrete and metal structures and products of nuclear power plants from fire and self-heating temperature from the heat release of radionuclides during their decay. According to the results of fire tests, it was determined that the treatment of the concrete surface with a fireproof geopolymer coating with thicknesses from 6 to 18 mm prevents critical heating of the surface of coated products (265.5–334 °C) to a critical temperature - 380 °C. It was determined that the temperature of concrete at the depth of reinforcement embedding (25 mm) warms up from 101.8 to 122.6 °C, which is 4.08–4.91 times less than the critical temperature of metal heating. It has been shown that 6 mm of coating is sufficient for fire protection of external concrete surfaces. And for interior concrete surfaces - 18 mm. The specified thickness of the geopolymer fire protection coating provides protection against the permissible thermal load (250 °C) on concrete from the heat release of radionuclides during their decay. The developed composition of the geopolymer coating provides a fire resistance class of concrete structures and products not lower than R180. The fire protection effectiveness of mineral mixtures on a geopolymer basis for the protection of metal structures and products has been determined. It is shown that at a thickness of 25 mm, the fireproof coating provides a fire resistance class of R90-R120 and group III of fire protection efficiency. Based on the calculation data in accordance with Eurocode 3, it is established that the coating thickness of 30 mm provides a fire resistance class of R120 and group II of fire protection efficiency. Below.

Keywords: Coating · Container · Concrete · Geopolymer binder · Fire protection · Fire test · Mineral mixture · Nuclear power plants · Steel structures · Temperature

1   Introduction

In today's reality, namely, military operations, there is a certain threat of fire at nuclear power plants as a result of rocket and artillery fire, fire failure of control equipment, etc. A fire can negatively affect the concrete and metal structures of plants and radioactive waste disposal containers, significantly reducing their load-bearing capacity and integrity. According to works [1, 2], the critical temperatures for concrete samples are 280 °C and for metal samples - 500 °C. As a result of exposure to elevated temperatures in concrete and reinforced concrete structures, there is a probable loss of bearing capacity due to deformations caused by asymmetric changes in the physical and mechanical properties of the material as a result of uneven heating in the cross-section of the bearing elements; reduction of the design height of the section due to heating of concrete and reinforced concrete to high temperatures; sliding of reinforcement along the support when the contact layer of concrete and reinforcement is heated to a critical temperature, etc.

In the case of concrete containers, as a result of heat generation during radioactive decay of radionuclides, the self-heating temperature can reach values from 400 to 700 °C (in some cases up to 1000 °C) [3]. As a result of such a temperature increase, due to an increase in the degree of radionuclide delocalization, their transition to a gaseous state with an increase in pressure inside the container, destruction of the cement matrix crystalloid structure due to radiolysis, its internal brittle destruction occurs. As a result, there is a high probability of leaching of radionuclides into the environment. Therefore, the permissible load temperature for concrete is 200–250 °C. This temperature limit helps to limit the internal dimensions of waste containers.

In the case of metal containers, depending on steel grades, the critical temperature values are 450–500 °C. At such temperatures, large plastic deformations occur, as a result of which the metal ceases to perceive the forces of external and internal loads. Given that during radioactive decomposition of radionuclides, the specific heat emission is above 0.1 W/m^3 and the metal has high thermal conductivity, it is likely that heat and radioactive gases will be released into the external space with subsequent negative impact on this environment [4].

Therefore, it is important to design safety and fire protection systems for nuclear power plant structures and products for radioactive waste immobilization and disposal, taking into account various fire and heat release scenarios [5–8]. These measures are primarily aimed at preventing limit states of both concrete and reinforcement in it when exposed to fire and metal products.

Among the variety of fire and heat protection materials used in the aspect under consideration are coatings on cement [9, 10] and geopolymer bases [11, 12].

A common disadvantage of the proposed solutions is the increase in the additional distributed load on concrete and metal structures due to the increase in the mass and thickness of the material, as well as the low fire resistance limit, which does not exceed 1.5 h in a standard fire [13–15]. No such information is available on the fire and heat protection of containers.

The aim of this work is to determine the suitability and effectiveness of fire and thermal insulation mixtures based on geopolymer for the protection of concrete and

metal structures of nuclear power plants in case of fire, and containers for immobilization of radioactive waste from self-heating temperature during heat generation during radioactive decay of radionuclides.

This goal is achieved by solving the problems of fire and thermal insulation of these structures and products by conducting fire tests to assess their effectiveness.

2   Materials and Methods of Research

2.1   Materials

To achieve these goals, an aluminosilicate binder of the composition Na_2O - Al_2O_3 - SiO_2 - H_2O was used in the form of a dispersion, with the ratio of structural oxides being $Na_2O/Al_2O_3 = 1.0$, $SiO_2/Al_2O_3 = 6.0$ and $H_2O/Al_2O_3 = 20$ (hereinafter – geopolymer), which was characterized by a density of 1.427 g/cm^3, a dynamic viscosity of 1987 cP at 25 rpm and a surface tension of 46.9 mN m.

The calculation of the ratios between oxides in the geopolymer binder for synthesis of zeolites was carried out with taking into account the recommendations given in [16, 17].

Aluminosilicate granules based on zeolite-like geopolymer matrices of the above composition with a particle size of 0.63…4.0 mm was also used as an intumescent filler. These granules were obtained by granulation of the geopolymer binder in $CaCl_2$ solution ($\rho = 1350$ kg/m^3), the appearance of these granules is shown in Fig. 1 [18].
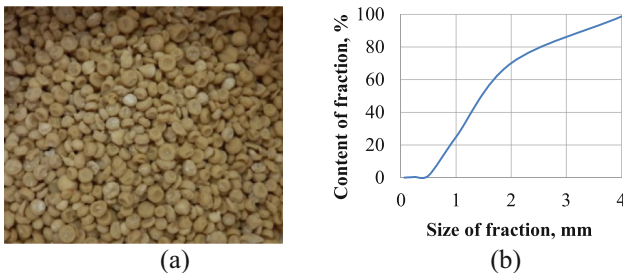
Fig.1. Appearance of the granules (a) and their distribution by fraction (b)

Metakaolin was used as a solid phase component of the binder. The composition of metakaolin, % by mass of mixture: CaO – 0.52, SiO_2 – 53.67, Al_2O_3 – 43.61, Fe_2O_3 – 0.77, MgO – traces, TiO_2 – 0.74, K_2O – 0.75, Na_2O – 0.25, other – 0.14, LOI < 0.5. The specific surface area of the ground metakaolin was 300…350 m^2/kg (by Blaine).

Sodium silicate solution with a silicate modulus $M_s = 3.05$ and $\rho = 1420 \pm 10$ kg/m^3 was used as an alkaline component.

Modification of the zeolite-like cement matrices has been done by adding NaOH, KOH and a rotten-stone (by mass, %: CaO – 3.6, SiO_2 – 88.4, Al_2O_3 – 2.3, Fe_2O_3 – 1.1, MgO – 0.9, TiO_2 – 0.2, K_2O – 0.9, other – 0.6, LOI < 2.0). The specific surface area of the ground rotten-stone is 250…280 m^2/kg (by Blaine).

Limestone (by mass, %: CaO – 44.15, SiO_2 – 7.6, Al_2O_3 – 2.92, Fe_2O_3 – 2.64, MgO – 2.89, TiO_2 – 0.22, K_2O – 1.18, LOI < 39.71) was used as an intumescent and a filler [19, 20]. Its specific surface area after grinding is 70…80 m^2/kg (by Blaine).

Perlite (by mass, %: SiO_2 – 70, TiO_2 – 0.3, Al_2O_3 – 12.5, Fe_2O_3 – 0.6, FeO – 0.95, CaO – 1.0, Na_2O – 3, K_2O – 2.8, H_2O – 5, LOI < 3.85, granules a size of 0.16–1.25 mm, density 2.30 - 2.39 g/cm^3, porosity 1.8 - 70%) was used as a heating filler [20–22].

Organic thickeners and adhesion promoters based on polyacrylates were used to regulate the rheological characteristics of the mixtures and increase the adhesion to the substrates.

For fire protection of concrete products (containers) for radioactive waste disposal the rationally selected composition of the mixture consisting of geopolymer, geopolymer granules and limestone was applied.

For fire and heat protection of metal products (barrels) for radioactive waste disposal the rationally selected composition of the mixture consisting of geopolymer, geopolymer granules, limestone, perlite and polymer additives was applied. These compositions are the authors' know-how and are not disclosed in this paper.

2.2   Testing Methods

After mixing the geopolymer-based matrices with fillers in appropriate proportions, the resulting coating was applied by hand using a trowel to the vertical surface of concrete cube samples (150 mm) with a thickness of 6 mm at 18 mm. After the coating had cured, 2 TT-K-24-SLE type K thermocouples were installed, temperature range 20…1100 °C, accuracy $\pm$ 0.05 °C (Czech Republic). These three thermocouples (T_s, T_c and T_a) (Fig. 2), connected to a KIMO HD 200 HT multifunction device (France), were inserted into specially drilled holes in the concrete samples to a depth of 75 mm and at a distance of 25 mm of reinforcement. A DT 8867H infrared pyrometer (Germany) was used to measure the temperature (T_s) on the surface of uncoated and coated concrete specimens as well as in the depth of the concrete specimen (temperature field distribution). A gasoline burner with a flame temperature at the coating surface of not more than 1100 °C
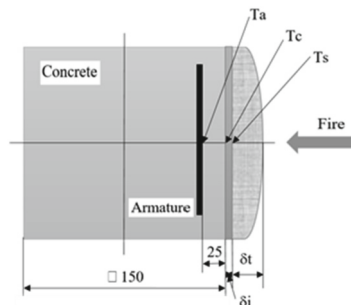
Fig. 2. Location of thermocouples in standard fire tests: T_s - temperature at the surface of the coating; T_c - temperature at the surface of the concrete under the coating; T_a - temperature of the concrete at the depth of laying the reinforcement

was used in the fire test (Fig. 2). The distance of the burner flame to the coating surface was 200 mm [18].

The surface heating temperature T_s, which corresponds to the standard fire temperature, was determined by the formula [18] and provided by changing the distance of the flame of the gasoline burner within 160…200 mm:

$$T = 20 + 345 log_{10}(8t + 1) \tag{1}$$

where T is the flame temperature, °C; t is the duration of thermal exposure during the fire test, min.

For fire and heat protection of metal products (containers) dry and liquid components of the mixture were mixed with a construction mixer in a container for 3 min. Fire tests were carried out on a hot-rolled I-beam made of steel No. 20 GOST 8239–89 (Fig. 3).
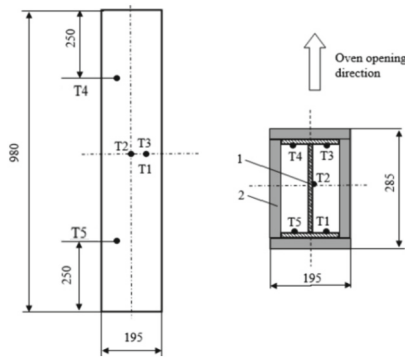
Fig. 3. Schematic representation of the insulated I-beam and of the layout of thermocouples set on it: 1 - I-beam; 2 fire-heat-insulating geopolymer coating; T1-T3 - the main thermocouples for the I-beam; T4-T5 - additional thermocouples for the I-beam.

The anti-corrosion treatment of the shelves and walls of the I-beam was carried out using the "Contrrust" converter (PE "Ruslan and Lyudmila", Kyiv, Ukraine). After rust transformation, a thin layer of geopolymer suspension was applied to the chelated film with a brush to improve the adhesion of the fire-heat-insulating mixture to metal surfaces.

The fire resistance limits of steel structures protected from fire by materials for general construction purposes were determined based on the results of fire tests in accordance with national standards (DSTU B V.1.1-4-98* Fire protection. Building structures. Fire test methods. General requirements; DSTU B V. 1.1-14: 2007 Fire protection - Columns - Fire test method (EN 1365-4: 1999, NEQ)) and calculation methods in accordance with the European design line standards according to the Eurocodes: DSTU-N B EN 1993-1-2: 2010 Eurocode 3. "Design of steel structures. Part 1-2. Basic provisions. Calculation of structures for fire resistance "(EN1993-1-2: 2005, IDT); DSTU-N B EN 1991-1-2: 2010 Eurocode 1. "Actions on structures. Part 1-2. General actions. Actions on a structure during a fire" (EN 1991-1-2: 2002, IDT).

The calculation of the fire resistance limit of steel structures according to Eurocode 3, for which constructive protection methods (plastering) are used as fire protection, is carried out using the thermophysical characteristics of fire-retardant materials in the calculations. The calculation method is based on determining the temperature rise DQat, over a period of time Dt for a uniform temperature distribution in the cross section of the protected steel structure:

$$\Theta_{a,t} = \frac{\lambda_p A_p/V\left(\Theta_{g,t} - \Theta_{a,t}\right)}{d_p c_a \rho_a (1 + \phi/3)} \Delta t - \left(e^{\phi/10} - 1\right)\Delta\Theta_{g,t} \tag{2}$$

at $\Delta\Theta_{a,t} \geq 0$, if $\Delta\Theta_{g,t} > 0$,

$$\phi = \frac{C_p \rho_p}{C_a \rho_a} \cdot \frac{d_p A_p}{V}, \tag{3}$$

where: A_p/V – section coefficient of steel structures coated with fire retardant materials (m^{-1}); A_p – surface area of fire-retardant material per unit length, m^2; V – volume of structures per unit length, m^3; C_a – specific heat capacity of steel, J/kg·K; C_p – specific heat capacity of a fire-retardant material, independent of temperature, J/kg·K; d_p – fire retardant thickness, m; t – time interval, while $\Delta t \leq 30$, s; $\Theta_{a,\,t}$ – steel temperature at time t, °C; $\Theta_{g,\,t}$ – temperature of the environment (nominal fire) at the moment of time t, °C; $\Delta\Theta_{g,\,t}$ – increase in the temperature of the environment (nominal fire) at the moment of time Δt, °C; ρ_a – steel density equal to 7850, kg/m³; λ_p – thermal conductivity coefficient of a fire retardant system, W/m °C; ρ_p – density of fire-retardant material, kg/m³.

Equations for calculating the fire resistance limits of protected steel structures:

$$R = \left[C_1\left(\frac{17W}{p_s}\right) + C_2\right]d_p/25.4 \tag{4}$$

where: R – fire resistance limit, min; W – specific weight of a steel column, kg/m; d_p – the thickness of the sprayed fire-retardant material, mm; P - heated perimeter of the steel column, mm; C_1 and C_2 – coefficients characterizing the thermal conductivity of the sprayed material. For geopolymer-perlite thermal insulation mixtures $C_1 = 33$ and $C_2 = 100$.

The main technological operations for applying the thermal insulation geopolymer-based mixture to the I-beam are shown in (Fig. 4).
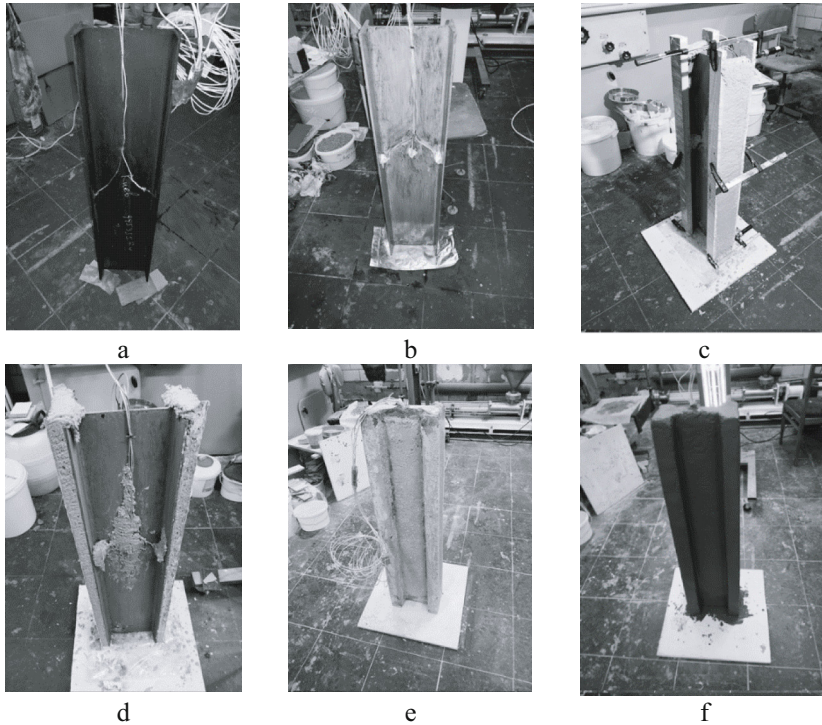
Fig. 4. Scheme of geopolymer mixtures application on an I-beam: a - treatment of the I-beam with Contrrust converter; b - painting of the beam with geopolymer suspension to increase adhesion [23]; c-e - application along the rails with fire and thermal insulation mixture; f - painting the structure with mineral paint on geopolymer-base [24, 25], thickness 125 μm

3   Research Results

At the first stage of the fire tests, concrete samples protected by a geopolymer fire protection coating containing geopolymer granules and limestone were examined. The coating was applied to concrete surfaces with thicknesses of 6, 12, and 18 mm, respectively. The average temperature on the surface of the fire protection coating was 1100 °C during the entire fire test period. The temperature was recorded on the surface of the concrete under the fire protection coating (Fig. 5) and at the depth of reinforcement embedding (Fig. 6).

As can be seen from Fig. 5, the maximum temperature (T1) on the surface of concrete 1110 °C was recorded after 1 h 21 min of heating. This is 4.44 times higher than the temperature of the permissible thermal load on concrete from the heat release of radionuclides during their decay. After completion of the fire test, the concrete surface was characterized by melting and cracks with a width of 1.5 to 2 mm. The cracks were formed as a result of the release of physically bound water from the concrete structure and from the thermal destruction of the hydrosilicate phases of cement hydration products. At the depth of reinforcement embedding (25 mm) (Fig. 6), the maximum temperature

value was recorded - 267.8 °C after concrete heating for 1 h and 52 min, which is 1.1 times higher than the permissible thermal load on concrete from heat release of radionuclides during their decomposition.

The temperature on the concrete surface (T2) under the 6 mm thick coating reached the maximum values - 334 °C after 2 h and 32 min of fire tests (Fig. 5), which is 1.34 times lower than the critical temperature for unprotected concrete and 1.34 times higher than the temperature of the permissible thermal load on concrete from the heat release of radionuclides during their decomposition. It should be noted that in the time interval from 0 to 1 h and 16 min, the value of heating of the concrete surface under the coating did not exceed 250 °C.
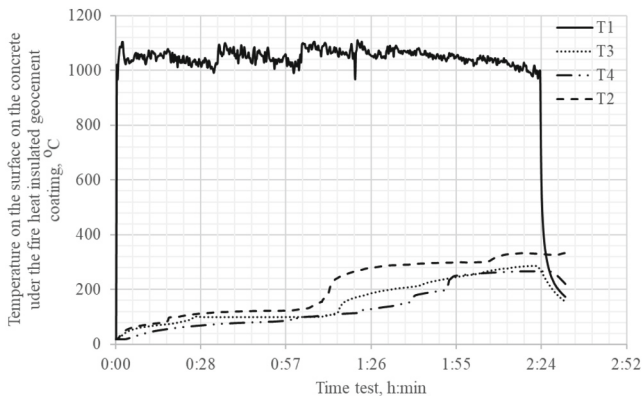
Fig. 5. Evolution of temperature on the concrete surfaces: T1 - temperature on the surface of uncoated concrete; T2 - temperature on the surface of concrete with a coating of 6 mm; T3 - temperature on the surface of concrete with a coating of 12 mm; T4 - temperature on the surface of concrete with a coating of 18 mm

At the depth of reinforcement embedding (25 mm) (Fig. 6), the maximum temperature T2 was recorded at 122.6 °C after concrete heating for 2 h 32 min, which is 2.04 times less than the permissible thermal load on concrete from heat release of radionuclides during their decay.

A similar dependence is observed for the values of concrete temperature (T3) under a 12 mm thick coating (Fig. 5). At the depth of reinforcement embedding (25 mm) (Fig. 6), the maximum value of temperature T3 was recorded - 122.6 °C after concrete heating for 2 h and 32 min, which is 2.04 times less than the permissible thermal load on concrete from heat release of radionuclides during their decay.

The temperature on the concrete surface (T4) under the 18 mm thick coating reached the maximum value of 265.5 °C after 2 h and 21 min of fire tests (Fig. 5), which is 1.43 times lower than the critical temperature for unprotected concrete and 1.06 times higher than the temperature of the permissible thermal load on concrete from the heat release of radionuclides during their decomposition.

At the depth of reinforcement embedment (25 mm) (Fig. 6), the maximum temperature T4 was recorded at 101.8 °C after concrete heating for 2 h and 32 min, which
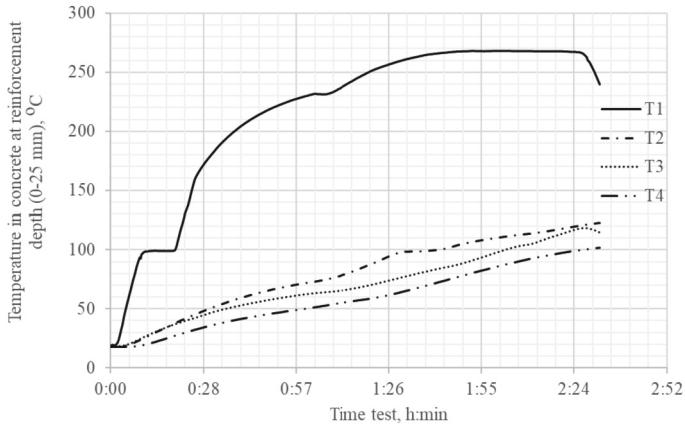
Fig. 6. Distribution of concrete temperature at the depth of reinforcement embedding (25 mm from the sample surface): T1 - uncoated concrete; T2 - 6 mm thick coated concrete; T3 - 12 mm thick coated concrete; T4 - 18 mm thick coated concrete

is 2.47 times less than the permissible thermal load on concrete from heat release of radionuclides during their decay.

The results obtained can be used for fire protection of concrete containers against both external temperature and internal self-heating of immobilized radioactive waste (Fig. 7).
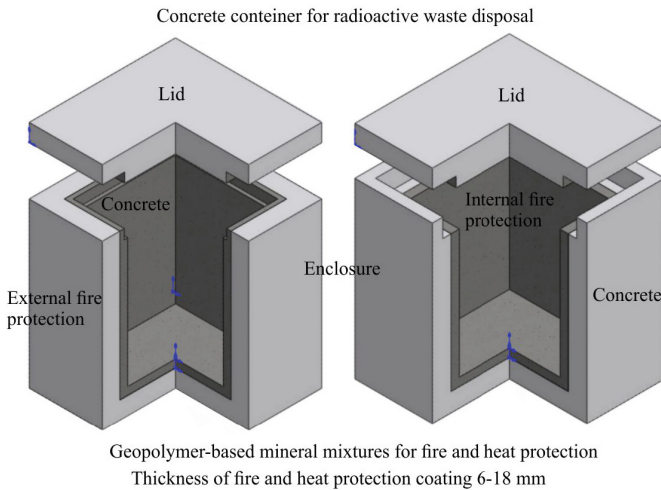
Fig. 7. Schemes of fire protection of external and internal surfaces of concrete containers

In Fig. 7 shows two options for fire protection of concrete surfaces against temperature effects with geopolymer-based fire protection coatings. Thus, in the case of external fire protection, it is recommended to apply a 6 mm thick coating to concrete surfaces; for

internal fire protection (in case of self-heating of radioactive waste), it is recommended to treat surfaces with a coating of 18 mm thickness. This coating thickness will not significantly reduce the active volume of radioactive waste.

At the second stage of the fire tests, a sample of the I-beam was examined, which was protected by a fire and heat-insulating geopolymer mixture containing, in addition to the geopolymer binder, geopolymer granules, limestone, perlite sand, and organic additives-modifiers. After mixing the components with a construction mixer, the mixture was manually applied to the shelves and walls of the 25 mm thick I-beam.

After hardening of the geopolymer-based mineral mixtures, the I-beam was placed in a furnace to undergo firing tests along a standard fire curve. In Fig. 8 shows a graph of the furnace temperature change. It should be noted that the temperature regime was maintained, no significant deviations from the standard temperature curve were recorded, which is confirmed by the data given in the work [1].
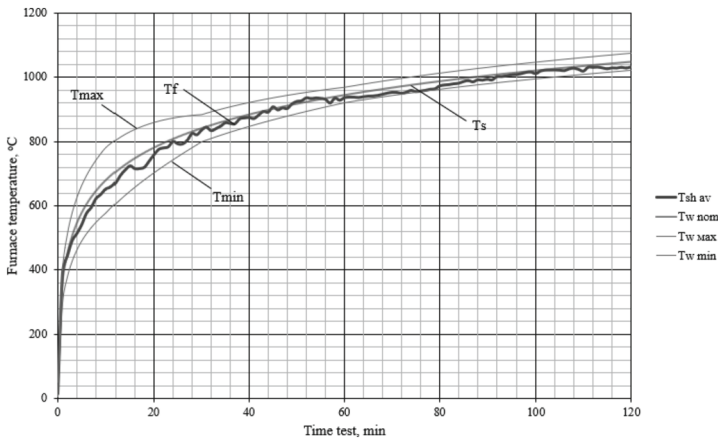
Fig. 8. Variation of the average furnace temperature (Tf) with time. Standard temperature regime (Ts), maximum temperature (Tmax) and minimum temperature (Tmin), are indicated.

In Fig. 9 shows a graph of the temperature distribution on the side flanges and the I-beam wall.

After the completion of the firing tests, a comparison was made between the experimental and calculated data given in the Table 1 and for the given parameters of the mixture.

Experiment data: reaching the critical temperature of heating the I-beam up to 500 °C with a fireproof coating thickness of 25 mm is carried out for 113 min of fire tests; the fire resistance class of the steel column ranges from R90 to R120.

Estimated data for Eurocode 3 and Eq. 3: reaching the critical temperature of heating the I-beam up to 538 °C with a fire-retardant coating thickness of 25 mm is carried out for 116 min; the fire resistance class of the steel column ranges from R90 to R120.

To ensure the fire resistance class R120, in the future, it is necessary to increase the thickness of the geopolymer-based mineral mixtures to 30 mm, which will increase the fire efficiency of the proposed fire-retardant material.
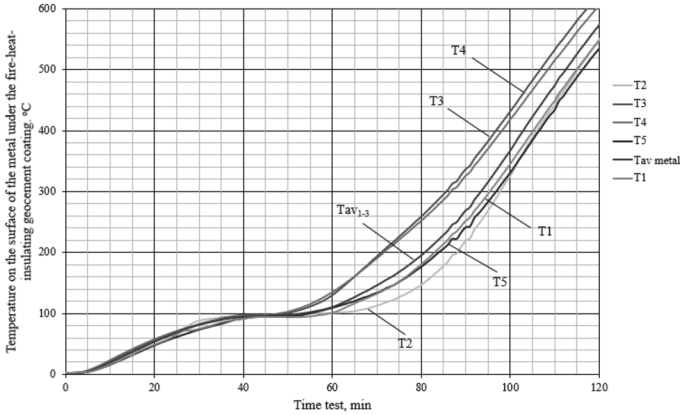
Fig. 9. Evolution of temperature on the metal surfaces of the I-beam: T1-T3 – the main thermocouples adapted on the I-beam; Tav1–3 – average values of thermocouples T1-T3; T4-T5 – additional thermocouples.

Table 1. Comparison of the minimum thicknesses of geocement perlite containing thermal insulation mixture (d_ρ, mm)[1]

Geopolymer-based mineral mixtures, ρ=0.560 [g/cm³], $\lambda_\rho(\lambda_c)$=0.1 [W/m·°C]², Cp=1130 [J/kg·K]					
Profile section coefficient, A_m/V, [m⁻¹]	Calculation method	Fire resistance class			
		R60	R90	R120	R150	R180
345-140	Eurocode 3	12-18	18-24	24-32	30-37	36-44
	Equation 3	12-16	18-22	24-29	30-35	34-41

[1]Contour protection
[2]According to Equation 1, the thermal conductivity of a fire-retardant system is temperature dependent. The calculation took into account the data obtained during tests according to DSTU B V1.1.-17: 2007

The results obtained can be used for fire protection of metal containers against both external temperature and internal self-heating of immobilized radioactive waste (Fig. 10).

In Fig. 7 shows two options for fire protection of metal surfaces against temperature effects with geopolymer-based mineral the fire protection mixtures. Thus, in the case of external fire protection, it is recommended to apply a 25 mm thick coating to metal surfaces; for internal fire protection (in case of self-heating of radioactive waste), it is recommended to treat surfaces with a coating of 30 mm thickness. This mineral the fire protection mixtures thickness will not significantly reduce the active volume of radioactive waste.

Metal conteiner for radioactive waste disposal

Geopolymer-based mineral mixtures for fire and heat protection
Thickness of fire and heat protection coating 25-30 mm
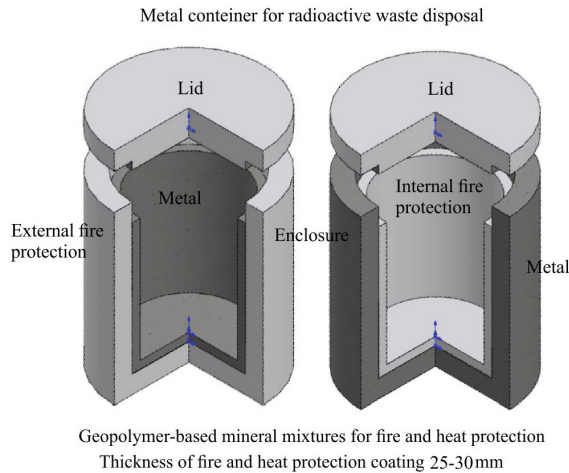
Fig. 10. Schemes of fire protection of external and internal surfaces of metal containers

4   Conclusions

According to the results of fire tests, it was determined that the treatment of concrete surfaces with a fire-retardant geopolymer coating with thicknesses from 6 to 18 mm prevents critical heating of the surface of the coated products (Tfact from 265.5 to 334 °C) to the critical temperature - 380 °C and prevents brittle destruction of its surface. It has been determined that the temperature of concrete at the depth of reinforcement embedding (25 mm) warms up from 101.8 to 122.6 °C, which is 4.08–4.91 times less than the critical temperature of metal heating. It was shown that 6 mm of coating is sufficient for fire protection of external concrete surfaces. And for internal concrete surfaces - 18 mm. The specified thickness of the geopolymer fire protection coating provides protection against the permissible thermal load (250 °C) on concrete from the heat release of radionuclides during their decay. The developed composition of the geopolymer coating provides a fire resistance class of concrete structures and products not lower than R180.

The use of geopolymer fire- and heat-insulating mixtures in the protection of metal structures from fire from both the outside and the temperature from inside metal containers provides a fire resistance class of R90-R120 and a fire protection efficiency group III. It is shown that with a fire-insulating coating thickness of 25 mm, the metal surface of an I-beam is heated to a critical temperature of 500 °C during 113 min of testing. Based on the calculation data in accordance with Eurocode 3, it was found that the critical heating temperature of an I-beam to 538 °C with a fire protection coating thickness of 25 mm is reached in 116 min, which ensures a fire resistance class of R90 - R120 and a fire protection efficiency group III. For fire protection of the outer surfaces of metal containers, 25 mm of coating thickness is sufficient, and for the inner surfaces, 30 mm of coating thickness is sufficient to ensure a fire resistance class of R120.

References

1. Mróz, K., Hager, I., Korniejenko, K.: Material solutions for passive fire protection of buildings and structures and their performances testing. Procedia Eng. **151**, 284–291 (2016). https://doi.org/10.1016/j.proeng.2016.07.388

2. Duquesne, S., Magnet, S., Jama, C., Delobel, R.: Intumescent paints: fire protective coatings for metallic substrates. Surf. Coat. Technol. **180**, 302–307 (2004). https://doi.org/10.1016/j.surfcoat.2003.10.075

3. Martynov, B.N.: Radioactive Waste Management. Kyiv, Technics, p. 107 ((1993))

4. Krylova, N.V., Kulichenko, V.V., Salamatina, R.N.: Influence of thermal past on properties of vitrified high-level waste. Atom. Energies **69**(2), 244–245 (1990)

5. VBN V.1.1-034-2003. Fire protection design standards for nuclear power plants with water-water power reactors

6. NAPB B.01.014-2007 Fire Safety Rules for the Operation of Nuclear Power Plants

7. NAPB 05.028-2004 Fire protection of power enterprises, individual facilities and power units. Design and operating instructions

8. NAPB V.01.061-2011/111 Fire protection of power plant turbine rooms. Rules for design and operation of fire-fighting equipment

9. Kim, J.-H.J., Mook Lim, Y., Won, J.P., Park, H.G.: Fire resistant behavior of newly developed bottom-ash-based cementitious coating applied concrete tunnel lining under RABT fire loading. Constr. Build. Mater. **24**(10), 1984–1994 (2010). https://doi.org/10.1016/j.conbuildmat.2010.04.001

10. Pan, Z., Sanjayan, J.G., Kong, D.L.Y.: Effect of aggregate size on spalling of geopolymer and Portland cement concretes subjected to elevated temperatures. Constr. Build. Mater. **36**, 365–372 (2012). https://doi.org/10.1016/j.conbuildmat.2012.04.120

11. Guerrieri, M., Sanjayan, J.G.: Behavior of combined fly ash/slag-based geopolymers when exposed to high temperatures. Fire Mater. **34**(4), 163–175 (2010). https://doi.org/10.1002/fam.1014

12. Sakkas, K., Sofianos, A., Nomikos, P., Panias, D.: Behaviour of passive fire protection K-Geopolymer under successive severe fire incidents. Materials **8**(9), 6096–6104 (2015). https://doi.org/10.3390/ma8095294

13. Yasir, M., Ahmad, F., Yusoff, P.S.M.M., Ullah, S., Jimenez, M.: Latest trends for structural steel protection by using intumescent fire protective coatings: a review. Surf. Eng. **36**(4), 334–363 (2019). https://doi.org/10.1080/02670844.2019.1636536

14. Krivenko, P., Guzii, S., Bodnarova, L., et al.: Effect of thickness of the intumescent alkali aluminosilicate coating on temperature distribution in reinforced concrete. J. Build. Eng. **8**, 14–19 (2016). https://doi.org/10.1016/j.jobe.2016.09.003

15. Kurska, T., Khodakovskyy, O., Kovalchuk, A., Guzii, S.: Fire protection of steel with thermal insulation granular plate material on geocement-based. Mater. Sci. Forum **1038**, 524–530 (2022). https://doi.org/10.4028/p-a1ae7r

16. Kryvenko, P., Kyrychok, V., Guzii, S.: Influence of the ratio of oxides and temperature on the structure formation of alkaline hydro-aluminosilicates. East.-Eur. J. Enterp. Technol. **5**(5-83), 40–48 (2016). https://doi.org/10.15587/1729-4061.2016.79605

17. Breck, D.W.: Zeolite Molecular Sieves: Structure. Wiley, Chemistry and Use (1973)
18. Krivenko P., Guzii S., Rudenko I., Konstantynovskyi O.: Intumescent fireproof coatings based on zeolite-like cement matrices. ce/papers **6**(5), 923–929 (2023). https://doi.org/10.1002/cepa.2214
19. Bodnarova, L., Guzii, S., Hela, R., et al.: Nano-structured alkaline aluminosilicate binder by carbonate mineral addition. Solid State Phenomena **276**, 192–197 (2018). https://doi.org/10.4028/www.scientific.net/SSP.276.192
20. Kyrychok, V., Kryvenko, P., Guzii, S.: Influence of the CaO-containing modifiers on the properties of alkaline alumosilicate binders. East.-Eur. J. Enterp. Technol. **2**(6-98), 36–42 (2019). https://doi.org/10.15587/1729-4061.2019.161758
21. Small Mining Encyclopaedia. Donetsk, Donbas Publish, 2: L – R: 670 (2007). ISBN 57740-0828-2
22. Kryvenko, P., Guzii, S., Tsapko, J., Kravchenko, A.: Determination of the effect of fillers on the intumescent ability of the organic-inorganic coatings of building constructions. East.-Eur. J. Enterp. Technol. **5**(10-83), 26–31 (2016). https://doi.org/10.15587/1729-4061.2016.79869
23. Rong, X., Wang, Z., Xing, X., Zhao, L.: Review on the adhesion of geopolymer coatings. ACS Omega **6**(8), 5108–5112 (2021). https://doi.org/10.1021/acsomega.0c06343
24. Guzii, S., Bazhelka, I., Svitlychna, N., Lashchivskiy, V.: Protection of wood from burning with paints on alkaline aluminosilicates-based. Mater. Sci. Forum **1006**, 19–24 (2020). https://doi.org/10.4028/www.scientific.net/AMR.688.3
25. Guzii, S., Kurska, T., et al.: Features of the organic-mineral intumescent paints structure formation for wooden constructions fire protection. IOP Conf. Ser. Mater. Sci. Eng. **1162**, 012003 (2021). https://doi.org/10.1088/1757-899X/1162/1/012003

Calculation of Enclosures of Defence Structures Based on the Quasi-static Method

Dmytro Kochkarev[1] , Taliat Azizov[2] , and Tetiana Galinska[3(✉)]

[1] National University of Water and Environment Engineering, Rivne, Ukraine
[2] Pavlo Tychyna Uman State Pedagogical University, Uman, Ukraine
[3] National University "Yurii Kondratyuk Poltava Polytechnic", Poltava, Ukraine
galinska@i.ua

Abstract. The article shows the peculiarities of calculating the walls of defence structures according to Ukraine's new regulatory documents. General information about the calculation of enclosures of defence structures by the direct integration of equations of motion, impulse method and quasi-static method is given. The peculiarities of determining the load from conventional weapons are indicated for each of the proposed calculation methods. For the direct dynamic calculation method, the parameters of the blast air wave pressure diagrams established for the relevant ammunition are used as the load. For the impulse method, the impulse values of the blast air wave are established for the suitable ammunition, and the appropriate form and time of its action are used. When using the direct integration of the equations of motion and the impulse method, performing dynamic calculations of spatial frames of buildings and structures is necessary. The calculation of walls of defence structures for quasi-permanent loads is considered in detail. An example of the calculation of shock blast waves from standard means of destruction of defence walls for quasi-constant loads is given. The methodology for determining the reinforcement of walls and ceilings of typical buildings of defence structures in calculating the impact of an air blast wave under the action of standard means of destruction is shown.

Keywords: defence structures · quasi-constant loads · TNT equivalent · stress-strain state · off-centre compressed elements · bending elements with double reinforcement

1 General Information on the Calculation of Enclosures of Defence Structures

Defence structures play an essential role in protecting the population during air attacks. Defences must protect against air shock waves and shrapnel when conventional weapons are used. This necessitates appropriate calculations, namely:

1. Calculation of enclosures of defence structures for the impact of air shock waves;
2. Calculation of the enclosures of defence structures against the impact of shrapnel.

It is worth noting that certain types of structures are designed to be directly hit by certain munitions. As a rule, these are specialised structures that are of utmost importance. Additional separate calculations are performed for them, which are not considered in this article.

The calculation of the enclosures of defence structures and buildings for the impact of an air shock wave can be performed using one of three methods:

1) The method of direct integration of the equations of motion;
2) The shock pulse method;
3) Quasi-static method.

A corresponding load characterises each of these methods. In particular, the method of directly integrating the equations of motion uses the pressure diagrams of the blast air wave established for the corresponding ammunition as a load. These diagrams make it possible to determine the values of the corresponding surface normal pressures within a specific time range. For the shock pulse method, the value of the corresponding shock wave pulse, shape, and time of action are taken as the main load. The corresponding equivalent static load is assumed for the quasi-static method of designing protective structures for the impact of a blast wave.

The blast wave calculation is performed for a given TNT equivalent W of a munition exploding at a distance R or R_G from a building [1–3] (see Fig. 1).
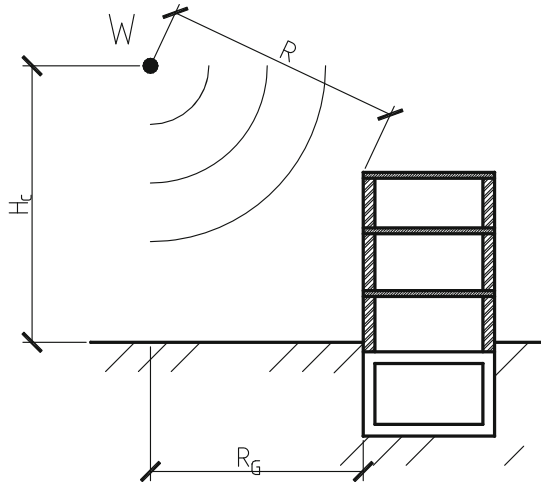
Fig. 1. Defining the parameters of the equation of motion diagrams

The parameters of the diagrams or shock pulses are set depending on the distance entered.

$$Z = \frac{R}{\sqrt[3]{W}}, \tag{1}$$

where R – is the distance from the building to the explosion's epicentre, m; W– is the equivalent mass of the TNT, kg.

A typical pressure diagram of a shock air wave is shown in Fig. 2. Blast diagrams contain two phases: a positive pressure phase and a negative pressure phase (separation). Each phase is characterised by the following parameters: maximum pressure P_r, P^-_r, action time t_0, t^-_0 and shock impulse i_r, i^-_r. The value of the shock pulse corresponds to the area of the corresponding phase of the pressure diagram.

Fig. 2. Pressure diagram of a shock air wave
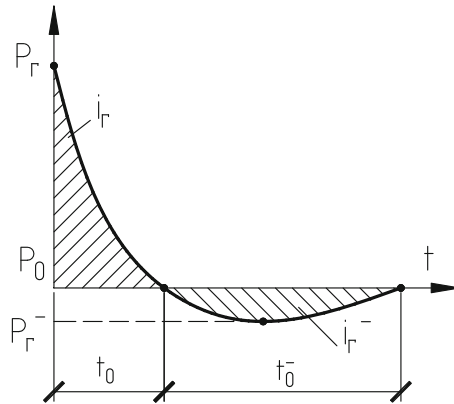
In practical calculations, the use of a nonlinear pulse shape dramatically complicates the process of modelling the blast load. Therefore, in most cases, the pulse shape is assumed to be either triangular or rectangular.

Direct dynamic and shock pulse calculations usually cause particular difficulties for most designers, especially for complex and advanced buildings and structures. Applying dynamic loads is particularly difficult, as there are no formulated recommendations. This leads to a large number of inaccuracies in such calculations. In this regard, they are pretty difficult to verify. That is why the current design standards [4] propose using quasi-static loads to design protective structures.

2   Quasi-static Method of Calculation of Enclosures of Defence Structures

The quasi-static method of calculation replaces dynamic loads with equivalent static loads. The equivalent static loads are assumed to equal the inertial load determined by the dynamic impact. It is known that inertial forces depend on the form of oscillations of the main load-bearing structures of a building or structure. Therefore, for each form, a different value of inertial forces is obtained. That is why obtaining an accurate static load value that fully corresponds to the dynamic impact is quite a challenge. Given this, most scientists consider the quasi-static calculation method the least accurate and is not recommended for use in various dynamic problems. However, satisfactory results can be obtained for typical buildings and structures that are simple in plan.

Equivalent static loads are taken in the form of overpressure and applied generally to the surface of the main enclosing structures of buildings and structures. The value of overpressures depends on the structural features of buildings and their corresponding class of protective structures and is determined according to regulatory documents [4].

The following procedure for calculating civil protection facilities is proposed:

1. .The shelter class (AI–AIV) or shelter group (P-1–P-6) is determined. According to Table A.1 or Table A.2 [4], the overpressure of the air shock wave ΔR_{ex}, kPa, is determined.
2. Determine the load P_{max} on the cover and walls of the protective structure following Table 14.1 and Table 14.2 [4].
3. Calculate the horizontal quasi-static load on the exterior walls using the formula:

$$q_{ex,eqv} = P_{max} K_d K_0, \tag{2}$$

where P_{max} is the reduced horizontal load, kPa; K_d is the dynamic coefficient, which is taken from Table 14.9 [4]; K_0 is a coefficient that takes into account the change in pressure on the walls due to the horizontal component of the mass velocity of soil particles, the attenuation of the compression wave with depth and the pressure reduction due to the movement of the structure and wall deformation. For buried and embedded walls, the value of the coefficient K_0 is taken to be 0.8 when calculated according to design condition IA and 1.0 - according to design condition IB. For unembedded walls and walls located in saturated soils, the coefficient K_0 is 1.

4. The design scheme of the structure or building is modelled, loads are applied generally to the surface of the enclosing structure, and a static calculation is performed. The central thicknesses of the elements are preliminarily accepted, provided that adequate protection against debris is provided.
5. The forces in the main load-bearing elements of a building or structure are determined.
6. Additionally, the dynamical coefficients for the corresponding load-bearing structures are considered in Table 14.10, 14.11 [4].
7. The required reinforcement is selected only for the first group of limit states (bearing capacity).

When determining the reinforcement of defence structures, the coefficients of dynamic strengthening should also be considered, depending on the rate of change of deformation. For conventional means of destruction, the value of the dynamic compressive strength of concrete may be taken as 1.2. Such values are used for dynamic, non-explosive loads. The known expression can specify a more accurate value.

$$\begin{cases} DEF_c = \left(\dfrac{\dot{\varepsilon}}{\dot{\varepsilon}_{sc}}\right)^{1,026\alpha_s} & \rightarrow \quad 30 \times 10^{-6} \le \dot{\varepsilon} \le (30 + 23i)\ c^{-1}; \\[2ex] DEF_c = \eta \left(\dfrac{\dot{\varepsilon}}{\dot{\varepsilon}_{sc}}\right)^{k} & \rightarrow \quad (30 + 23i) \le \dot{\varepsilon} \le 300\ c^{-1}, \end{cases} \tag{3}$$

where $\alpha_s = \frac{1}{5+9f_c/f_{c0}}$, $f_{c0} = 10$ MPa; $\dot{\varepsilon}_{sc} = 30 \times 10^{-6} c^{-1}$, $\gamma_s = 10^{(6,15\alpha_s - 2)}$,

$$\eta = (1 - 0,3392i)\gamma_s, \quad k = \frac{1 + 0,05i}{3}, \quad i = \begin{cases} 0 & - \ concrete; \\ 1 & - \ fibre\ concrete. \end{cases}$$

The value of the strain rate is determined by

$$\dot{\varepsilon} = \frac{\varepsilon_u}{\tau}, \tag{4}$$

where $\dot{\varepsilon}$ – is the strain growth rate, s^{-1}; τ – is the loading time, s; ε_u – is the corresponding ultimate concrete strain.

For most explosions, the load duration of the positive phase of the air blast is 0.020 s. This corresponds to the average value. Most concrete classes' ultimate deformations are assumed to be 350×10^{-5}. Thus, according to expression (4), the value of the strain growth rate will be $\dot{\varepsilon} = 0.175$. For concrete C20/25 with $\alpha_s = 0.055$, , we obtain the value of the dynamic strengthening coefficient equal to $DEF_c = 1.63$.

The reinforcement of defence enclosing structures for bending elements is proposed to be carried out according to the method given in [5, 6].

For bending elements with single reinforcement, the following calculation procedure is proposed:

– determine the required design resistance of reinforced concrete by the expression

$$f_{zM} = \frac{M_{Ed}}{W_c} = \frac{6M_{Ed}}{bd^2}; \tag{5}$$

– define an auxiliary parameter

$$k_z = \frac{f_{zM}}{6 \cdot f_{cd}}; \tag{6}$$

– determine the mechanical coefficient of reinforcement

$$\omega = 1 - \sqrt{1 - 2 \cdot k_z}; \tag{7}$$

– determine the height of the compressed zone and check the condition

$$x/d = 1.25 \cdot \omega < 0.45. \tag{8}$$

If condition (8) is not met, double reinforcement is used or the cross-sectional height of the element is increased.

– Determine the cross-sectional area of the reinforcement and accept the reinforcement:

$$\rho_f = \frac{\omega \cdot f_{cd}}{f_{yd}} > \rho_{\min} = 0.0013. \tag{9}$$

When determining the cross-sectional area of reinforcement with double equal reinforcement of the compressed and tensile zones, use the expression

$$A_s = \frac{M_{Ed}}{0,94 \cdot f_{yd} \cdot d}. \tag{10}$$

The following conditions must be met

$$\rho_f = \frac{A_s}{b \cdot d} > \rho_{\min} = 0.0013. \tag{11}$$

For off-centre compressed elements (walls), we propose to use a modified method of calculating iron resistances, and the following sequence of reinforcement calculation is proposed:

- calculate the initial eccentricity $e_0 = M/N$.
- determine the relative initial eccentricity e_0/d.
- calculate the design resistance $fzN = N_{Ed}/bd$.
- determine the parameter $k_z = f_{zM}/f_{cd}$.
- According to Table 1, depending on the parameter k_z and the relative initial eccentricity e_0/d, we determine the mechanical reinforcement factor ω.
- Calculate the cross-sectional area of the reinforcement $A_s = \frac{\omega f_{cd} bd}{f_{yd}}$.

**Table 1.** Values of k_z for off-centre compressed rectangular cross-sectional elements with symmetrical reinforcement, $\lambda \leq 4$ ($\lambda = 0$).

Mechanical coefficient of reinforcement ω	Relative initial eccentricity of the longitudinal force application e_0/d									
	0.01	0.15	0.30	0.65	1.00	1.50	2.00	3.00	4.00	5.00
0.10	1.16	0.82	0.58	0.21	0.09	0.05	0.03	0.02	0.01	0.01
0.15	1.21	0.88	0.64	0.27	0.13	0.07	0.05	0.03	0.02	0.02
0.20	1.26	0.92	0.68	0.33	0.17	0.09	0.06	0.04	0.03	0.02
0.25	1.31	0.96	0.72	0.38	0.20	0.11	0.08	0.05	0.03	0.03
0.30	1.36	1.00	0.76	0.42	0.24	0.14	0.09	0.06	0.04	0.03
0.35	1.41	1.04	0.79	0.46	0.27	0.16	0.11	0.07	0.05	0.04
0.40	1.46	1.08	0.83	0.50	0.30	0.18	0.12	0.08	0.05	0.04
0.45	1.51	1.11	0.86	0.54	0.33	0.20	0.14	0.08	0.06	0.05
0.50	1.56	1.15	0.90	0.57	0.36	0.22	0.15	0.09	0.07	0.05
0.60	1.66	1.22	0.96	0.62	0.41	0.26	0.18	0.11	0.08	0.06
0.70	1.76	1.28	1.03	0.67	0.46	0.29	0.21	0.13	0.09	0.07
1.00	2.06	1.54	1.22	0.80	0.60	0.40	0.29	0.18	0.13	0.10
2.00	3.06	2.30	1.34	1.22	0.92	0.68	0.54	0.35	0.26	0.21
3.00	4.06	3.07	1.46	1.67	1.26	0.93	0.74	0.52	0.38	0.31

Below is an example of how to calculate a protective structure.

3 Example of Calculation of Enclosing Structures of Protective Buildings and Structures

Example 1: Calculate the area of working reinforcement of the walls and floor of an underground vault under a three-storey frame monolithic building. The walls and floor are made of concrete of class C20/25, $f_{cd} = 14.5$ MPa, $\varepsilon_{cu} = 350 \cdot 10^{-5}$, and steel of class A500C, $f_{yd} = 435$ MPa. The overpressure of the air shock wave ΔP_{ex} is assumed to be 100 kPa. The height of the building floor is assumed to be 3 m. The design scheme of the building is shown in Fig. 3.
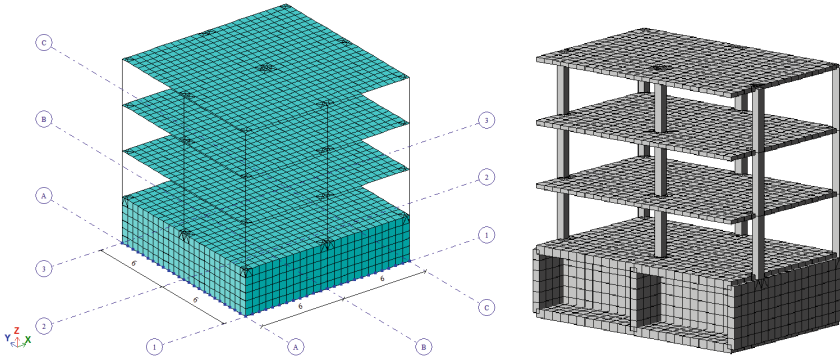
Fig. 3. Design layout of the building

Solution.

1. We specify all design loads on the above-ground part of the building: dead and live loads. We do not include snow and wind loads here.
2. Set a constant load on the underground part of the building from the weight of the soil. Pre-determine the coefficient of lateral friction of the soil. All constant loads will be set in the first load.
3. Create a second load for the payloads. Let's assume a payload of 4 kPa on the floors on all floors.
4. The thickness of the walls and ceiling above the vault is assumed to be 350 mm (for concrete class C20/25, Table [4]), provided that it is not penetrated by debris.
5. For scheme a of Fig. 14.1 [1], using Table 14.1 and Table 14.2, we determine the values of the overloads P1 and P2: $P1 = \Delta P_{ex} = 100$ kPa; $P2 = K_\sigma \times \Delta P_{ex} = 1 \times 100$ kPa $= 100$ kPa. Next, we calculate the horizontal quasi-static load using expression (2).
6. Generate a particular shock wave load by setting the appropriate values of evenly distributed pressure on the floors and walls.
7. Download schemes are shown in Fig. 4.

a)   b)   c)
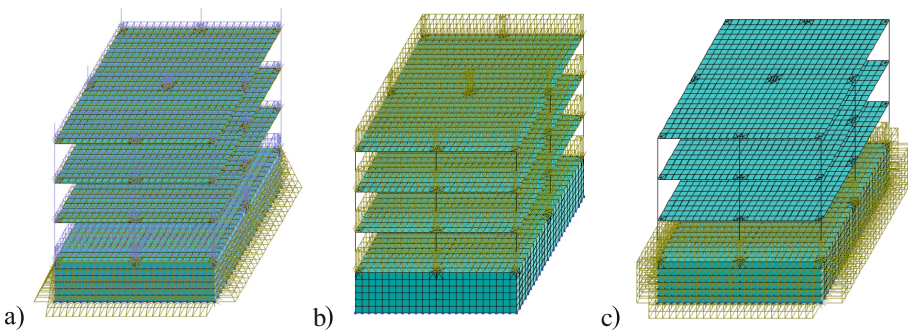
Fig. 4. Loading patterns: a) Constant; b) Useful; c) Explosive.

8. Perform a static calculation and determine the force from the most untenable combination of forces.
9. The largest values of forces in the wall per 1 MP: Nx = 1120 kN, My = 18.8 KN·m.
10. The largest values of forces in the slab Mx = 106 KN·m.
11. Determine the required area of reinforcement for the vault wall. To do this, we first determine the relative initial eccentricity

$$\frac{e_0}{d} = \frac{M_{Ed}}{N_{Ed}d} = \frac{18.8 \times 10^2}{1120 \times 32} = 0.052;$$

Let's calculate the required design compressive strength of reinforced concrete and the parameter k_z

$$f_{zN} = \frac{N_{Ed}}{bd} = \frac{1120}{100 \times 32} \times 10 = 3.5 \; MPa; \quad k_z = \frac{f_{zM}}{DEF_c \cdot f_{cd}} = \frac{3.5}{1.63 \cdot 14.5} = 0.15.$$

According to Table 1, using interpolation by k_z and the relative initial ex-centricity e_0/d, we determine $\omega \leq 0,1$.

Calculate the reinforcement factor

$$\rho_f = \frac{DEF_c \cdot f_{cd}}{f_{yd}} \omega = \frac{1.63 \cdot 14.5}{435} 0.1 = 0,0054.$$

The required cross-sectional area of the reinforcement $A_s = A_{sc} = \rho_f \times b \times d/2 = 0,0054 \times 1000 \times 320/2 = 869 \; mm^2$.

According to the product range, we accept 5Ø16 A500C, As = 1005 mm². (That is, Ø16 A500C with a pitch of 200 mm.)

12. Determine the required area of reinforcement in the slab. To do this, determine the required design resistance of reinforced concrete

$$f_{zM} = \frac{M_{Ed}}{W_c} = \frac{6M_{Ed}}{bd^2} = \frac{6 \times 106 \times 10^6}{1000 \times 320^2} = 6.21 \; MPa;$$

Define an auxiliary parameter

$$k_z = \frac{f_{zM}}{6 \cdot f_{cd} \cdot DEF_c} = \frac{6.21}{6 \cdot 14.5 \cdot 1.63} = 0.044.$$

Determine the mechanical coefficient of reinforcement

$$\omega = 1 - \sqrt{1 - 2 \cdot k_z} = 1 - \sqrt{1 - 2 \cdot 0.044} = 0.045;$$

Determine the height of the compressed zone

$$x/d = 1.25 \cdot \omega = 1.25 \cdot 0.045 = 0.056 < 0.45.$$

Determine the cross-sectional area of the reinforcement and accept the reinforcement:

$$\rho_f = \frac{\omega \cdot f_{cd} \cdot DEF_c}{f_{yd}} = \frac{0.045 \cdot 14.5 \cdot 1.63}{435} = 0.0024 > \rho_{\min} = 0.0013.$$

$$A_s = \rho_f \cdot b \cdot d = 0.0024 \cdot 1000 \cdot 320 = 782, 4 \text{ mm}^2.$$

According to the product range, we accept 5Ø16 A500C, As = 1005 mm². (That is, Ø16 A500C with a pitch of 200 mm.)

It is not necessary to calculate the slab for impact loads from overlying floor structures. It is believed that one monolithic floor in case of partial collapse creates an equivalent pressure of 10 kPa, so the maximum pressure from the collapse of the upper floors on the floor of the repository may not be 30 kPa, which is significantly less than the 100 kPa for which the previous calculations were performed.

4   Conclusions

It is shown that the quasi-static method of calculation is the least accurate but the most accessible for designers. A methodology for determining the reinforcement of walls and ceilings of typical buildings of protective structures in the calculation of the impact of an explosive air wave under the action of conventional weapons is shown. The quasi-static method for determining the forces and the method of calculated reinforced concrete resistances for determining the required reinforcement are used. A step-by-step algorithm for calculating the protective structure and an example of the calculation of its enclosing structures are presented.

References

1. Unified Facilities Criteria: UFC 3-340-02 Structures to Resist the Effects of Accidental Explosions. U.S. Army Corps of Engineers, Naval Facilities Engineering Command, Air Force Civil Engineer Support Agency (2008)
2. Kingery, C.N., Bulmash, G.: Technical report ARBRL-TR-02555: Air blastparameters from TNT spherical air burst and hemispherical burst, AD-B082 713,U.S. Army Ballistic Research Laboratory, Aberdeen Proving Ground, MD (1984)
3. Yan, S., Wang, J.-H., Wang, D., Zhang, L.: Mechanism analysis on progressive collapse of RC frame structure under blast effect. Gongcheng Lixue/Eng. Mech. **26**(Suppl. 1), 119–123, 129 (2009)
4. DBN V.2.2-5:2023 Protective Buildings of Civil Defense
5. Rizak, V., Kochkarev, D., Azizova, A., Galinska, T.: Approximation models of the method of design resistance of reinforced concrete for bending elements with double and multirow reinforcement. In: Onyshchenko, V., Mammadova, G., Sivitska, S., Gasimov, A. (eds.) Proceedings of the 4th International Conference on Building Innovations: ICBI 2022, pp. 285–292. Springer, Cham (2023). https://doi.org/10.1007/978-3-031-17385-1_23
6. Kosior-Kazberuk, M., Kochkarev, D., Azizov, T., Galinska, T.: Approximation model of the method of design resistance of reinforced concrete for bending elements. In: Onyshchenko, V., Mammadova, G., Sivitska, S., Gasimov, A. (eds.) Proceedings of the 3rd International Conference on Building Innovations, ICBI 2020. LNCE, vol. 181, pp. 245–254. Springer, Cham (2022). https://doi.org/10.1007/978-3-030-85043-2_23

Research of Processes Sedimentation Sludge Radioactive Waters and the Improvement of Treatment Technology

Dmytro Korsun[(✉)] [iD]

Khmelnytskyi Nuclear Power Plant, Netishyn 30100, Ukraine
korsun.dmitriy@khnpp.atom.gov.ua

Abstract. It can be literally said that further development of nuclear-power engineering will be finally determined by a possibility of safe treatment of radioactive wastes with prevention of their contact with the biosphere.

Isolation and prevention of environment radioactive contamination determined a necessity of concentration and solidification of radionuclide, which could be disposed over a long period of time. One of the main and necessary conditions for creating stable and safe radioactive wastes is maximal moisture removal with a maximal degree of their concentration in the binder [1].

The experience of operating existing systems of preliminary radioactive water purification at Nuclear Power Plant showed that one of the important and unsolved problems is improving the efficiency of removal of dispersed admixture from radioactive water. Low rate of suspension removal of the existing technology leads to sludge getting into radioactive wastes that makes the operation of the vaporizer difficult, to setting of deep concentration by evaporation, and, what is also very important, it leads to increase in quantity of liquid radioactive wastes.

Keywords: Radioactive Waste · Sludge Cleaning · Nuclear Power Plant

1 Research on Properties of Radioactive Waters Suspension

The technology of radioactive waters purification from insoluble admixture provides:

- sedimentation of suspension in the sump tank, sedimentation tank and radioactive waters tank,
- filtration of radioactive water through mechanical filter [2].

The diversity of technological processes with various influences of physicochemical and radioactive factors on Nuclear Power Plant objects leads to formation of radioactive waters containing complicated dispersed systems with little-studied properties.

It is necessary to have information about physicochemical properties of dispersed systems as well as calculation of instability (25…100 m^3/h) of radioactive water discharge rate for recycling in the sedimentation tank while analyzing the efficiency of removal of insoluble admixture from radioactive waters.

The analyses of literature shows the lack of such data and the necessity of conducting experimental research on properties of real radioactive waters suspension while recycling [1].

Depending on the nature of the dispersed phase and dispersed environment, dimensions of dispersed particles, their bulk concentration and a number of other properties dispersed systems are divided into classes that can have completely different properties [3].

The main of them, which influence the efficiency of purification, are typical for all similar systems [3]. Among them:

– total concentration of suspended particles;
– phase-dispersed composition of suspension;
– unitized stability of suspensions;
– viscosity of the liquid phase;
– solidity difference between dispersing and dispersed environment;
– suspension particles distribution function according to hydraulic size or distribution density of suspension particles.

During the experimental work on defining properties of suspensions the analyses of phase-dispersed composition of sludge in sump tank, sedimentation tank and radioactive waters tank as well as analyses of concentration of suspended particles and dispersed composition in the purified water were hold according to the technological chain of purification [4]. There was a method was chosen to define dispersed composition of the solid phase and construct differential and integral curves of density of particles distribution according to the size. It is based on separation of suspension by filtering through a line of membrane filters, on which dispersed solid phase was kept with further drying and weighing on the analytical weights [5]. Suspension filtering was hold sequentially through membrane filters with gradual reduction of filter cells size (Table 1). Total concentration of suspended particles was defined as a sum of all suspensions kept by the filters. The relative average weight of suspensions fractions in radioactive water was calculated as a sum of relative dispersions of the sludge of sump tank, sedimentation tank and radioactive waters tank.

The poured density of sludge, which was calculated by weighing a sludge sample after drying in the muffle furnace at 105 °C, weighing on analytical weighs, by defining the volume using a measuring cylinder, constituted for: sump tank 1,26 t/m^3, sedimentation tank 1,27 t/m^3, radioactive waters tank 1,28 t/m^3. The density of suspensions was calculated taking into account real occupied volume which was in the measuring cylinder after adding weighed amount of sludge and constituted for: sump tank 2,42 t/m^3, sedimentation tank 2,13 t/m^3, radioactive waters tank 1,84 t/m^3. The macrostructure of fallouts, size and form of particles were defined by the method of optical microscopy using the microscope of "Ervahal" type. It was determined that the bulk of sludge was composed of small-dispersed particles, partially coagulated into units. The form of the particles is irregular. The majority of the particles have elongated form with the isomeric rate about two. The minimal dimensions of these sludge particles are: sump tank 15 μ, sedimentation tank 8 μ, radioactive waters tank 1,6 μ. The median dimensions of the particles are: sump tank 132 μ, sedimentation tank 78 μ, radioactive waters tank 27 μ. In the sludge of the sump tank and sedimentation tank some big particles with the size of

Table 1. Table captions should be placed above the tables.

Fraction size, μ	Relative average weigh of suspensions fractions in the radioactive water	Relative weigh of sludge fraction, %		
		sump tank	sedimentation tank	radioactive waters tank
>500	11,6	28,5	6,2	0,0
250…500	15,5	22,6	13,9	10,1
100…250	22,7	22,8	28,9	15,7
40…100	22,0	14,6	27,1	24,3
10…40	18,9	8,2	14,8	33,6
1…10	9,3	3,3	9,1	16,3

more than 1 mm can be observed. The maximum size of the particles of the radioactive waters tank is 340…380 μ. Therefore, the solid phase of sludge of the sump tank and sedimentation tank is several times more large-dispersed compared to the solid phase of sludge of the radioactive waters tank. However there are rather big particles in the radioactive waters tank, and in the sump tank and sedimentation tank only suspensions with the size over 380 μ can be efficiently purified.

The measuring of the hydraulic size was performed by Stocks' formula. The Stocks' formula is applicable to Newtonian liquid at small Reynolds numbers (Re < 2) as well as to diluted suspensions with high unit stability of the system and stability of the internal properties of the particles [7]. The hydraulic size must be reduced with the reduction of the equivalent diameter of a particle, which has been proved by the calculations based on the test data (Table 2).

Table 2. The hydraulic size of Nuclear Power Plant radioactive waters sludge suspensions.

Median particle size, μ	The hydraulic size of suspensions, mm/sec		
	sump tank	sedimentation tank	radioactive waters tank
500	286,0	215,0	154,0
375	161,0	121,0	86,8
175	35,0	26,3	18,0
70	5,6	4,2	3,0
25	0,71	0,54	0,39
5	0,029	0,022	0,015

However U is also a function from viscosity and density. Therefore, it is also from temperature, salt-containment, concentration, composition of suspended particles and

other factors. Thus the test data calculated by Stocks' formula provides a range of values, which define domain of dependence of hydraulic size of the radioactive water suspensions on equivalent diameters of suspensions (see Fig. 1). The present domain is built on the basis of test data of suspensions properties and operational characteristics of the sedimentation tank in Khmelnytskyi Nuclear Power Plant.
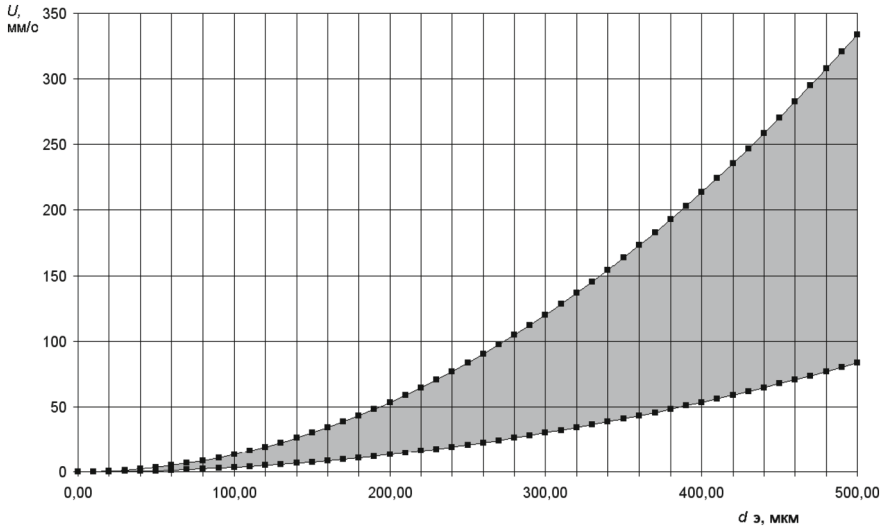
Fig. 1. Range of values of hydraulic size U, mm/sec, depending on suspensions diameter $d_э$, microns: *1 - favourable conditions of operation, 2 – unfavourable conditions of operation*

There was a connection between diameter of suspension entrainment and discharge of the recycled radioactive water (see Fig. 2) set to define dependence of the purification quality on the discharge rate of water supplied to the sedimentation tank. Taking into account Stock's formula these dependences characterize also the necessary hydraulic size of suspensions. The range of diameter of entrainment can be put down as an in equation.

$$d_{y\ min} \leq d_y \leq d_{y\ max}, \tag{1}$$

d_y - is an equivalent diameter of entrainment, microns;
$d_{y\ min}$ - is an equivalent diameter of entrainment under the most favourable conditions of sedimentation tank operation, microns;
$d_{y\ max}$ - is an equivalent diameter of entrainment under the most unfavourable conditions of sedimentation tank operation, microns.

While defining dependences a combined coordinate system was used: natural logarithm dy, microns and radioactive water flow F, m³/min (see Fig. 2). The interval of change of radioactive water rate in the sedimentation tank was 0,4 … 1,7 m³/min. Semi-logarithmic coordinate system allowed to describe the calculation data by equation of

lines out of which the empirical dependences of $d_{y\,max}$ and $d_{y\,min}$ on F for the tested sedimentation tank were found.
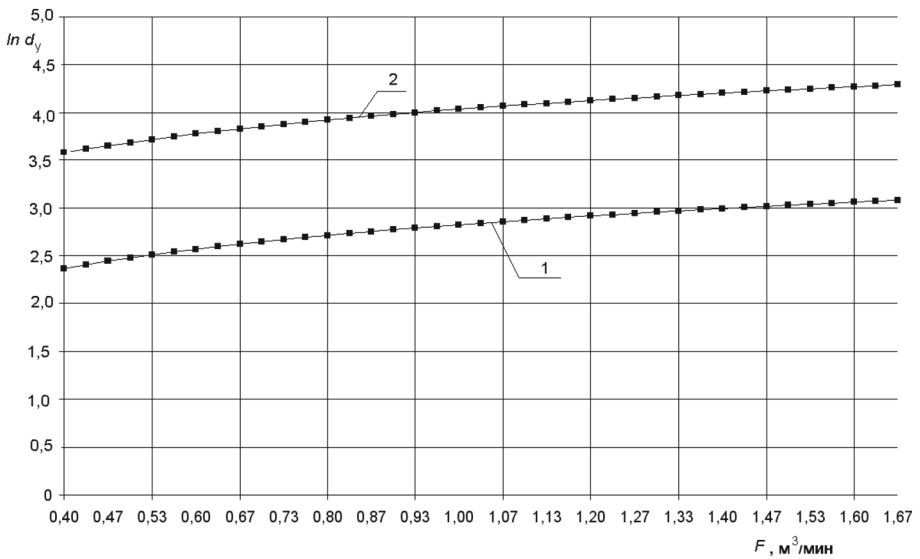
$$d_{y\,max} = 35,80\exp(1,76F), \qquad (2)$$

$$d_{y\,min} = 10,65\exp(1,76F). \qquad (3)$$

Taking into consideration that F = SV, where S - is a square of the sedimentation tank, m², V - is a speed of rise, than relation between (4) and (5) can be shown as follows

$$d_{y\,max} = 35,80\exp(0,83\frac{F}{S}), \qquad (4)$$

$$d_{y\,min} = 10,65\exp(0,83\frac{F}{S}). \qquad (5)$$

Fig. 2. Dependence of diameter of entrainment dy, microns on radioactive water rate F, m³/min: 1 – the most favourable conditions of operation, 2 – the most unfavourable conditions of operation

Those are true for a sedimentation tank with any settling square.
Dependences (4), (5) allow rewriting the in Eq. (1) as follows

$$35,80\exp(0,83\frac{F}{S}) \geq d_y \geq 10,65\exp(0,83\frac{F}{S}). \qquad (6)$$

Analyzing the data received (see Tables 1, 2 and drawings 1, 2) and in Eq. (6) it can be stated that regardless high calculation sedimentation speed of suspensions sludge the majority of them is not drawn out of radioactive waters and comes to the radioactive waters tank.

A reason of such suspensions behaviour in the NPP radioactive waters lies in deviation of their stream from the Newtonian that correspond to [8, 9]. This determines difficult for understanding and description rheological properties. Their explanation and prediction demand creation and application of complex approaches and numerous methods.

2   Research on Sludge Compression Processes

Research results [4] give an idea about dispersed composition and macrostructure of NPP radioactive waters sludge, process of their sedimentation and allow to define the hydraulic size of diluted suspensions with high unit stability of the system and stability of the internal properties of the particles.

However single settling of the particles is possible only in the mono-dispersed unit-stable system, when the particles during sedimentation do not change their form and size. At the same time, while settling NPP radioactive waters, the process runs in poly-dispersed system with a wide range of particles sizes, which become bigger, change their form, density and dimensions during the process of sedimentation. As a result of this the speed of their sedimentation changes.

Because of the unit instability (and sedimentation instability of NPP radioactive waters sludge consequently) the kinetics of their clarification and compression was defined by means of technological simulation of settling real sludge of the sedimentation tank of Khmel'nitsk NPP in the laboratory cylinders of different height. The cylinders were made of Plexiglas and were graduated along the full height in order to measure the volume of the compressed sludge [12]. To prepare a sludge solution, samples of sludge were prepared and thoroughly mixed in water with the volume equal to the volume of the cylinder (Table 3). The weigh of the sample was chosen depending on the sludge concentration in the high-concentrated sludge streams coming into the sedimentation tank.

Table 3. Initial values for simulating a process of sludge compression.

Model number	Cylinder height, mm	Weigh of sludge sample, g	Cylinder volume V_0, decimeters3	Sludge concentration in the prepared solution C_0, g/decimeters3
Model 1	400	20,0	2,00	10,0
Model 2	800	40,0	4,00	10,0
Model 3	1200	60,0	6,00	10,0

After mixing the tested sludge solution was put into cylinders, in which periodically, after specific time intervals of settling they marked the movement of border line between purified water and compressed sludge. The typical peculiarity of small-dispersed sludge

is their compression, not sedimentation, i.e. the movement of border line between liquid and sediment downwards with sediment density increase. Movement of the border line between liquid and sediment was measured every two minutes. Test was stop if there border line between liquid and sediment was not moving during 10 min.

At quite long time of compression the process slows down, the value of solid phase concentration (C_τ) moves to some constant.

$$\text{At } \tau = 0, C_\tau = C_0, \text{ and at } \tau \to \infty, C_\tau \to C_\infty, \tag{7}$$

where
Co - is sludge concentration at initial moment, g/decimeters^3;
C_τ - is sludge concentration at present moment, g/decimeters^3;
C_∞ - is sludge concentration at infinite compression, g/decimeters^3;
τ - compression time, minutes.

The average sludge concentration was calculated basing on the initial sludge concentration in the volume occupied by the sludge at present moment of time. As sludge weigh is constant and during the process of compression only the volume occupied by it changes, then the following comes from the equation of the balance:

$$C_\tau = \frac{C_0 \cdot V_0}{V_\tau}, \tag{8}$$

Where
Vo - is the volume of sludge solution at initial moment, decimeters3;
Vτ - is the volume of sludge solution at present moment, decimeters3;

In order to make interpretation of the test data completely accurate and to raise reliability of the conclusions made, the most probable value of the tested value and calculations by (8) of the sludge solidification process the curves (see Fig. 3) were constructed based on the results of the curves averaging using the method of the smallest squares.

The test data of the NPP radioactive waters sludge compression process was processed with method of approximation using the exponential function

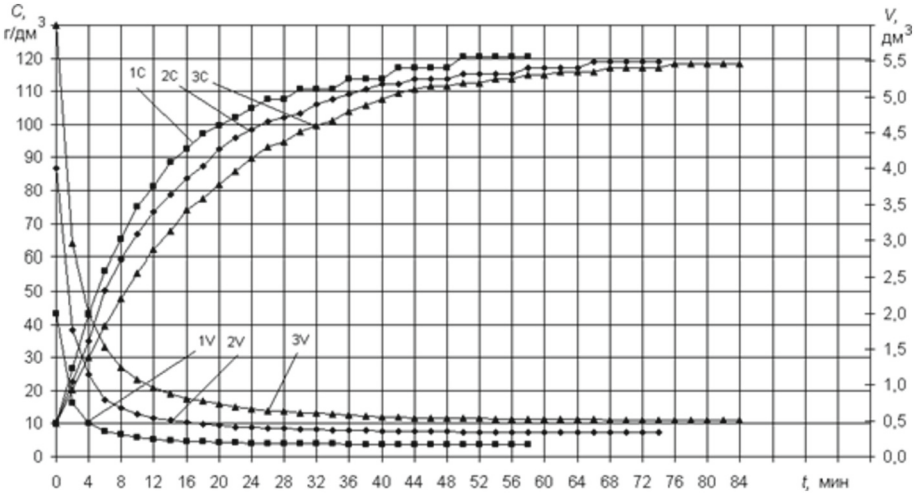$$C_\tau = C_0 + (C_\infty - C_0)\left(1 - \exp\left[-\frac{\tau}{k}\right]\right), \tag{9}$$

where
k - a constant of sedimentation speed, minutes-1.
Expression (9) in the view:

$$C_\tau = B - A esp\left(-\frac{\tau}{k}\right), \tag{10}$$

Where B and A are coefficients connected with the values C_0 and C_∞ of the expression (9) in the following way:

$$A = C_\infty - C_0; \tag{11}$$

Fig. 3. Change of sludge concentration C (g/decimeter^3) and sludge volume V (decimeter^3) while compression from time t (min): 1c, 1v – model 1; 2c, 2v – model 2; 3c, 3v – model 3.

$$B = C_\infty. \qquad (12)$$

Values A, B (Table 5) were calculated on the basis of initial sludge concentration in the model solution and stabilization of the volume of the compressed sludge (stopping the border line between liquid and sediment). The value of the constant of the concentration speed k (see Table 4) was calculated using in (10) substitution of the values of the found A, B, and the value $C\tau$ that lies on the curve (see Fig. 3) at $\tau = 30$ min.

Table 4. Coefficients values of the equations of compression simulation of high-concentrated NPP radioactive waters sludge.

Model number	A	B	k	n
Model 1	111	121	12,68	0,323
Model 2	110	120	15,86	0,349
Model 3	109	119	18,27	0,333

As the depth of settling Ho in the operating sedimentation tanks constitutes 4…6 m then in order to recalculate the kinetics of clarification of radioactive waters drawn in the laboratory models for the depth of the real sedimentation tanks, they used a condition of sedimentation similarity, under which equation of clarification effects in the model and real sedimentation tank is observed.

$$\frac{T_o}{t_m} = \left(\frac{H_o}{h_m}\right)^n, \qquad (13)$$

where

To - is clarification duration in real, sec;

Ho- is clarification depth in real, m;

tm - is clarification duration in the model, sec;

hm - is clarification depth in the model, m;

n - index in the sedimentation similarity, which reflects capability of suspension to agglomeration during the process of clarification.

Indexes of the sedimentation similarity were calculated after comparing the processes of sludge compression for the models with different depth out of the following equation:

$$n = \log_{\left(\frac{h_1}{h_2}\right)}\left(\frac{\tau_1}{\tau_2}\right), \qquad (14)$$

where

h_1, h_2 are cylinder heights of the models 1 and 2 correspondingly.

τ_1, τ_2 are time of sludge compression before concentrating $C\tau = 110$ g/decimeter^3 of the models 1 and 2.

High convergence of the sedimentation similarity index calculation results shows its independence from relation of the real and model depth of sludge compression (see Table 4).

Formula of approximation (10) and calculation (13) allows to define dependence of change compressed sludge concentration on time:

$$C_\tau = C_\infty - (C_\infty - C_0) \exp\left[-\frac{\tau}{k}\left(\frac{H_0}{h_m}\right)^n\right], \qquad (15)$$

where coefficients k and n are defined during simulation of the compression process on the models.

After data processing of KhNPP high-concentrated radioactive sludge of the sedimentation tank compression simulation this dependence may have the following view:

$$C_\tau = 121 - 111 \exp\left(-\frac{\tau}{6.52}\right). \qquad (16)$$

The speed of suspended solid particles and liquids may be increased by the action of centrifugal forces. The essence of water clarification in hydrocyclones and centrifuges is based on moving a particle to the periphery by the centrifugal force during water rotation.

The method of filtering through a mechanical filter was replaced with a two-stage centrifuging, and this was chosen as an optimal way of improving the technology of radioactive waters suspension purification.

3   Conclusions

So, the results shown give an idea about process of sedimentation and solidification of high-concentrated NPP radioactive waters sludge as well as after running a laboratory simulation, give a possibility to estimate compression processes with real heights of sedimentation tank.

The results give an idea about dispersed composition and macrostructure of NPP radioactive waters sludge, process of their sedimentation and allow to define dependency of efficient entrainment diameter on suspensions properties and of sedimentation tank characteristics.

Using centrifuging plant solves the following problems:

– radioactive waters clarification from heterogeneous admixture;
– accumulated sludge recycling;
– free bulk in Liquid Waste Storage.

Moreover, the suggested technology reduces radioactive wastes to 1 m^3/year of the solidified wastes and 195 m^3/year of the spillages bottoms, allows to significantly save on heat, water, reagents, tar as well as provides long-time and safe storage of radioactive wastes under simplified conditions.

References

1. Andronov, O., Stikhar, O.: Purification of liquid radioactive waste. Review of methods and technologies. Chornobyl (2001)
2. Korsun, D.: Investigation of the properties of suspensions of radioactive drain waters of nuclear power plants in order to improve the technology of their purification. In: Proceedings of the Odessa Polytechnic University (sp4): p. 108 – for Purification of Radioactive Trapping Waters of Nuclear Power Plants. Proceedings of the Odessa Polytechnic University (21), Odesa, pp. 40–43 (2004)
3. Kulskii, L.: Handbook on the properties, methods of analysis and purification of water. Scientific though, Kyiv (1980)
4. Sautin, S.: Experiment planning in chemistry and chemical technology. Chemistry (1975)
5. Pavlov, K.: Examples and tasks for the course of processes and apparatus of chemical technology. Study in their own way for universities. Chemistry (1987)
6. Boger, D., Walters, K.: Rheological Phenomena in Focus. Elsevier, New York (1993)
7. Tanner, R., Walters, K.: Rheolodgy: An Historical Perspective. Elsevier, Amsterdam (1998)
8. Portnov, L.: Kinetic model of sedimentation of polydisperse suspensions (1990)
9. Yakovlev, S.: Water drainage and wastewater treatment (1996)
10. Кишневский, В.А., Korsun, D.: Investigation of processes of sedimentation and compaction of sludges of radioactive waters of nuclear power plants. In: Proceedings of the Odessa Polytechnic University, vol. 22, pp. 48–52 (2004)
11. Kulskii, L.: Technology of water treatment at nuclear power plants. Scientific though, Kyiv (1986)

Management of Radioactively Contaminated Water at the Shelter Object of Chernobyl NPP

Viktor Krasnov [iD], Anatolii Doroshenko[(✉)] [iD], Mykola Pavlyuchenko [iD],
Daria Muliar [iD], and Serhii Kupriianchuk [iD]

Institute for Safety Problems of Nuclear Power Plant, National Academy of Sciences of Ukraine,
Chornobyl, Ukraine
a.doroshenko@ispnpp.kiev.ua

Abstract. In this paper decryptsand analyzedresults of radioactively contaminated water from the "Shelter" object in the period from 1998 to 2022 years witch was pumped out. A search was made for information on the sources of radioactive water and the amount of radioactive water pumped out of the volume of the "Shelter" object and the New Safe Confinement. The volumes and activity content of radioactively contaminated water that were pumped and collected to temporary storage in the Chornobyl NPP liquid radioactive waste storage facility were analyzed. A regression and correlation analysis was carried out between the indicators of the arrival of water solutions and the volumes of radioactive water pumped out. A strong connection (according to the Chaddock scale) between atmospheric precipitation and pumping out of hazardous waste was revealed. The main source of radioactive water, before the construction and installation in the project position New Safe Confinement was atmospheric precipitation, after that it is dust-fixing mixtures. However, their volumes are insignificant and have been decreasing every year since 2013.

Keywords: Radioactively contaminated water · Atmospheric precipitation ·
Dust-fixing mixtures · Activity · "Shelter" object · Regression analysis ·
Correlation coefficient

1 Introduction

Water from various sources penetrates the "Shelter" object (SO), moves from the upper to the lower levels on its way, interacts (contacts) with structural and fuel-containing materials and is contaminated with radioactive substances and accumulates at the lower levels.

In the paper examines the process of water (liquid aqueous solutions) entering the nuclear power plant in the period from 1998 to 2022, excluding the period of the active stage of accident elimination before the construction of the nuclear power plant (November 1986), when atmospheric precipitation fell into the destroyed reactor ("breakdown" of the reactor hole). For example, from August 6, 1986 to September 4, 1986, 540 t of trisodium phosphate mixture (to wash away radioactive dust) and 540 t of polymer coating mixture [1] were poured into the "breakdown" reactor hole of the 4th Unit ChNPP

from helicopters. Also, during the period from the end of 1989 to 1998, the dust suppression system regularly operated, from the operation of which about 250 cubic meters entered the SO annually of man-made mixture.

Radioactively contaminated water (RCW) generated in the SO contains a significant number of organic impurities and transuranic elements (TUE), which exceed permissible limits and cannot be directly sent for processing to the ChNPP evaporators, which complicates it's handling.

2   Material and Methods

In this work was used information from next sources:

– the annual "Report on the state of safety of the "Shelter" object (NSC-SO)", which contains information on the handling of radioactive materials from 1998 to 2022 (25 books);
– acts of completed works on the implementation of dust suppression and supply of neutron-absorbing mixture.

The sources are official documents, registered and stored in the Technical Department of the ChNPP. The analysis and interpretation of data on the handling of radioactively contaminated water based on the information obtained by searching for sources and analyzing the given ChNPP data, verifying and systematizing.

3   Results and Discussion

3.1   Sources of Water Supply to the SO

Water and aqueous solutions coming inside due to the leakiness of the roof of the SO during precipitation and the annual operation of the modernized dust suppression system (MDSS), the supply system of the gadolinium nitrate solution (SGNS), the injector of which is located under the pipe roll (roof). In certain periods, these systems sprayed from 70 to 180 t of dust fixing mixtures into the under-roof space of the SO annually.

As of 1998 and earlier, the sources of water (liquid solutions) in the SO were:

– atmospheric precipitation (until 2017) that entered the interior before the installation of the New Safe Confinement (NSC);
– stationary systems of MDSS, SGNS, which are active now;
– other secondary sources with insignificant volumes of RCW.

Insignificant volumes of hazardous waste are created by: condensate water, works on decontamination of room and operation (maintenance, repair, modernization) of systems and equipment of NSC-SO.

The upper limit of the inflow of atmospheric precipitation inside the SO due to the leakiness of the roof is estimated at almost 4,000 cubic meters per year [2] (before NSC was installed in project position), and the amount of water, accumulative, localizing mixtures, and gadolinium solutions fed into the "breakdown" reactor hole amounted to almost 2,000 cubic meters in the period from 1989 to 2013.

After 2013, dust suppression cycles were carried out situationally (1 cycle in 2 years) and with a small amount of localizing solution, accordingly, and flushing water (up to 30 cubic meters of liquid per cycle).

As a result of the contact of aqueous mixture with the materials of SO, dissolution and leaching of radionuclides occurs, and RCW is formed, which accumulates on the lower levels of SO. Most of the radioactive waste that is formed inside is collected in room 001/3, seeps through the partition wall and ultimately accumulates in the pit of room 0005 of the auxiliary systems of the reactor compartment of the 3rd Unit [3].

In order to prevent the ingress of radioactive substances into the groundwater and improve the radiation situation, the radioactive waste is collected and pumped to the Radioactive Waste Management Plant (RWMP) of the ChNPP for temporary storage in tanks X02, X04 of the liquid radioactive waste storage facility.

3.2 Characteristics of Radioactively Contaminated Water

Table 1 shows the volumes and content of activity in RCW, which was collected and pumped from the SO to the RWMP for temporary storage in the liquid radioactive waste facility from 1998 to 2022. Figures 1 and 2 shows their annual dynamics of activity and volumes.

According to the table, from 1998 to 2022 (25 years), 67,010 cubic meters were pumped and collected from the SO to the RWMP for temporary storage in the repository RCW, their total activity is $2.29E + 09$ kBq (γ, β-emitters, TUE), while the specific activity of radionuclides was in the range of $1.25E + 04 \div 8.89E + 04$ kBq/m^3.

According to the content of activity, RCW belong to the category of medium and low activity, the content of TUE in the total activity does not exceed 0.17%, the minimum values are below 0.05% (according to the "Basic sanitary rules for ensuring radiation safety of Ukraine" in the table "Classification of categories of solid and liquid radioactive waste according to the criterion of specific activity"). Interval of specific activity values of liquid radioactive waste in PCB$_{ingest}$ multiplicity units: low-active $> 1 < 10^2$, medium-active $\geq 10^2 < 10^6$ (PCB$_{ingest}$ for TUE $= 1.E + 03$ Bq/m^3, PCB$_{ingest}$ for Sr-90 $= 1.E + 04$ Bk/m^3) [5].

The analysis of the dynamics of the specific activity of the RCW showed the following: a noticeable decline in the specific activity from 2002 to 2006 is explained by the testing and commissioning of the MDSS, which significantly increased the area of the protective polymer coating of the "breakdown" reactor hole of the 4th Unit and, accordingly, reduced the washing, leaching of radionuclides from the surfaces "breakdown" reactor hole and the coefficient of variation of specific activity after 2006 decreased from 36% to 22% (Fig. 3).

It should be noted that the volumes of solid waste pumped from the SO decreased sharply in 2017, which is due to the NSC being installed into the design position, i.e. from 2017, the SO is isolated from the atmospheric precipitation, and the technological solutions that spray the MDSS and SGNS, do not have a significant impact on the volumes of RCW. For example, the contribution of technological mixture to the volumes of pumping in the period from 2004 to 2012 was approximately 4%. At the same time, since 2013, the volumes and frequency of spraying solutions have significantly decreased, and

Table 1. Characteristics of radioactively contaminated water, which was collected and pumped from the SO to the RWMP for temporary storage in the liquid radioactive waste facility from 1998 to 2022.

Year	Specific activity, kBq/m³	Total activity, kBq/year	Volume RCW, m³	Atmospheric precipitation, mm/year	Accumulative-localizing mixtures, m³
1998	8.89E+04	2.75E+08	3095		
1999	5.11E+04	1.45E+08	2830	653.2	
2000	5.73E+04	1.68E+08	2930	585.5	
2001	6.34E+04	1.84E+08	2900	668.7	
2002	3.82E+04	8.17E+07	2140	507	
2003	4.46E+04	9.45E+07	2120	345.4	96.8
2004	3.42E+04	1.47E+08	4295	664.3	159.3
2005	3.95E+04	1.40E+08	3543		69.3
2006	3.17E+04	1.15E+08	3627	652.1	144.3
2007	2.61E+04	7.40E+07	2838	641.9	214.5
2008	2.68E+04	7.54E+07	2818	657.4	119.6
2009	1.94E+04	5.85E+07	3015	620.4	119.6
2010	2.01E+04	7.33E+07	3650	599.8	173.7
2011	2.30E+04	6.85E+07	2976	660	179.3
2012	2.47E+04	1.73E+08	7006	953.8	179.3
2013	2.97E+04	1.62E+08	5442	654	
2014	2.26E+04	6.27E+07	2775	534.9	
2015	1.79E+04	3.89E+07	2175	493	
2016	2.54E+04	1.22E+08	4803	760.9	
2017	1.60E+04	1.40E+07	872	470.4	
2018	1.46E+04	7.91E+06	541	1166	
2019	1.25E+04	3.90E+06	311		
2020	2.08E+04	1.64E+06	79	618.1	
2021	2.48E+04	3.50E+06	141	558	
2022	2.09E+04	2.39E+06	114	817	

the average volumes of pumping from 2017 to 2022 fell more than 10 times compared to the average in previous years.
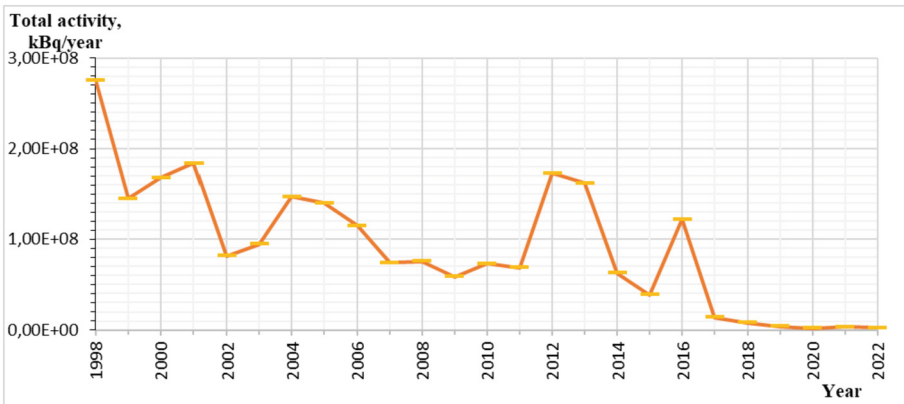
3.3 Correlation Analysis

In Fig. 4 according to the data in the Table 1 shows a linear regression and a correlation field of scattering. This allows us to put forward a hypothesis about a possible analytical correlation between atmospheric precipitation (mm) and RCW pumping (m³).
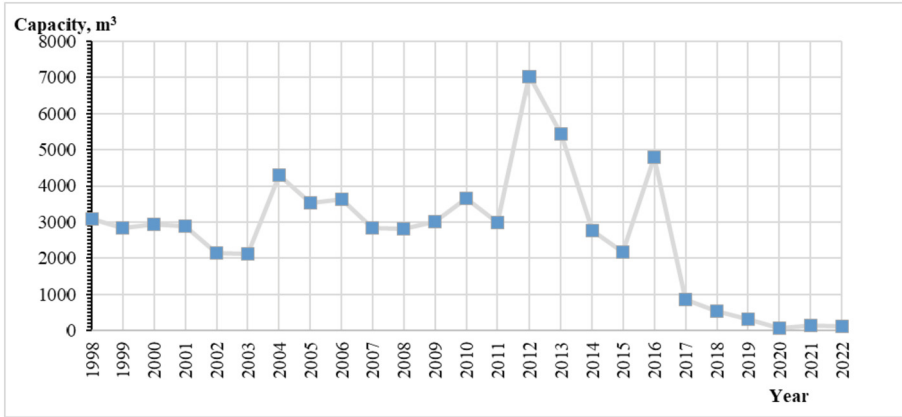
Fig. 1. Annual volumes (cubic meters) of RCW pumping to the RWMP.

Fig. 2. Dynamics of annual total activity of γ, β -emitters and TUE.

The pairwise correlation coefficient was determined for the period 1998–2016 (that is, before the building of the NSC), its numerical value is 0.81, which, according to the Chaddock scale, corresponds to a strong connection between the values.

Since the sample is randomly selected from the two-dimensional general population, it cannot be concluded that the correlation coefficient of the general population (r) is also different from zero (H1 = {r ≠ 0}). The null hypothesis H0 = {r = 0} was tested at the level of significance α = 0.001, the Student's criterion was determined according to the table t_{cri} {0,001; 15} ≈ 4,073, the empirical value of the criterion t_{emp} ≈ 5,35 was calculated [4]. Thus, the $|t_{emp}| > t_{cri}$ null hypothesis is rejected, and "atmospheric precipitation" and "pumping" are correlated, that is, connected by a linear contribution, as well connected between the values is considered significant.
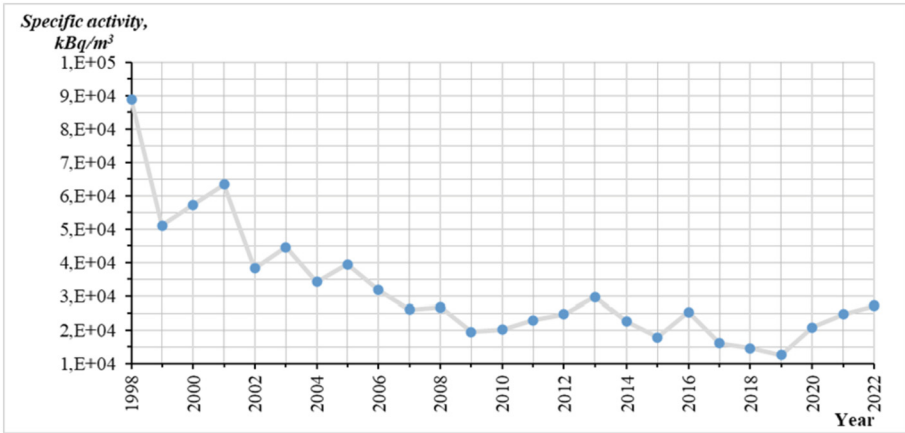
Fig. 3. Dynamics of annual specific total activity of γ, β-emitters and TUE (kBq/m³).
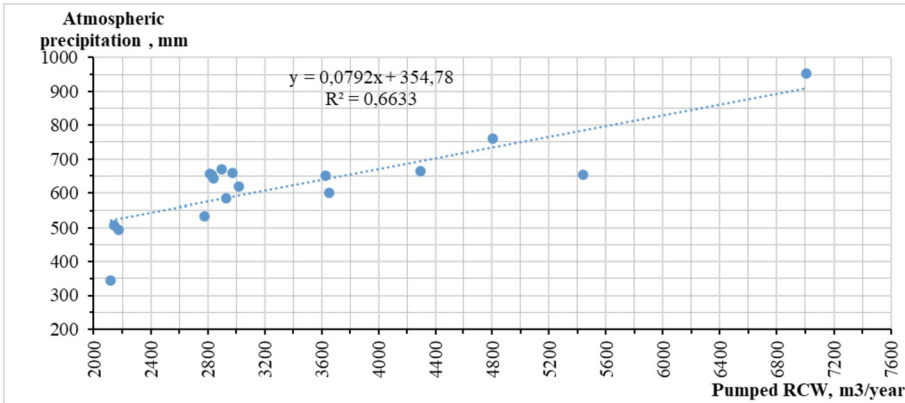

Fig. 4. Linear regression and correlation field of "pumping" (horizontal axis, m³) and atmospheric precipitation, (vertical axis, mm/year) parameters.

3.4   Assessment of the RCW Balance

The balance of "precipitation - pumped" of the RCW is calculated for the area of the roof of the SO equal to 6500 square meters, located within the building coordinates in axes 39-53 and B-S.

In the period from 1999 to 2016 inclusive, 69,200 cubic meters fell on the specified roof area of atmospheric precipitation, 2005 is excluded from the calculation, where there are no data on the amount of precipitation. During this period, 58,300 cubic meters were pumped out. m of RCW to RWMP for temporary storage.

Thus, about 16% less was pumped out than the precipitation. If we take into account Accumulative-localizing mixtures (≈4%), then ≈80% of atmospheric precipitation penetrated into the SO due to the leaky roof.

4   Conclusions

In order to prevent the inflow of radioactive substances into groundwater and improve the radiation situation, 67,010 cubic meters were pumped out from 1998 to 2022 of RCW to the ChNPP RWMP for temporary storage. RCW generated in the SO contains a significant amount of organic impurities and TUE, which exceed permissible limits and cannot be directly sent for processing to the ChNPP evaporators, which complicates its handling.

The problem of reprocessing the specified solid waste pumped out for temporary storage is still relevant at the present time.

After the building of the NSC, the volumes of the formed wastes decreased significantly and in the period from 2017 to 2022 did not exceed 900 cubic meters per year, and the minimum in 2020 reached 79 cubic meters, their average volume during this period decreased by more than an order of magnitude compared to the previous period of 2011–2016. Thus, the NSC blocked the access of atmospheric precipitation to the SO (inside the SO penetrated ≈80% of atmospheric precipitation due to the leaky roof) and eliminated the dominant source of RCW formation in SO - atmospheric precipitation, the contribution of which to the formation of RCW was approximately 95%. The pairwise correlation coefficient "precipitation- pumping" calculated for the period 1998–2016 (i.e., before the building of the NSC) is $r_{xy} = 0.81$, which, according to the Chaddock scale, corresponds to a strong connected between the values, at the level of significance $\alpha = 0.001$ distribution between values is considered significant.

The total activity of radionuclides in RCW is 2.29E + 09 kBq or 2.29E + 03 MBq (γ, β-emitters, TUE), while the specific activity of radionuclides was in the range of 1.25E + 04 ÷ 8.89E + 04 kBq/m^3. According to the [5], according to the activity content of RCW, they belong to the category of medium and low activity, the content of TUE in the total activity does not exceed 0.17%, their minimum values are below 0.05%.

The introduction of the MDSS into operation reduced the intensity of radionuclide washing and water infiltration through the contaminated materials of the precipitation and, according to the decrease of the average specific activity in the period from 2007 to 2022, by 2.3 times in comparison with the period 1998–2006, the impact of the work of the MDSS in the existing regime, the volume of RCW is minimal.

References

1. Samoylenko, Yu.N., Chernouchenko, V.M.: The use of polymer coatings to improve the radiation situation during the liquidation of the consequences of the Chernobyl accident // Chernobyl '88. Reports of the I All-Union Scientific and Technical Conference on the results of the liquidation of the consequences of the accident at the Chernobyl nuclear power plant/Under the general editorship of d.t.s. E. I. Ignatenko. T.7 Localization of the consequences of the accident at unit No. 4, the industrial site of the Chernobyl nuclear power plant and adjacent territories Part II. Chernobyl, pp. 152–184 (1989)
2. Shcherbin, V.N., Krinitsyn, A.P., Strikhar, O.L.: Determination of 235U in "Ukryttia" object water flows – Chornobyl, 8 p. (1999). - (Prepr. /National Academy of Sciences of Ukraine. Interdisciplinary Scientific and Technical Centre "Shelter"; 99-1)

3. Krinitsyn, A.P., Strikhar, O.L., Shcherbin, V.N.: On the mechanics of the formation of liquid radioactive waste in the room of Block B and VSRO. Prob. Chornobyl (9), 98–104 (2002)
4. Bolshov, L.N., Smirnov, L.V.: Mathematical statistics tables. The science (1983)
5. Basic sanitary rules for ensuring radiation safety in Ukraine. Order of the Ministry of Health of Ukraine 02.02.2005, no. 54. https://zakon.rada.gov.ua/laws/show/z0552-05(UA)

Restoration of Roofing and Slabs of Buildings Damaged as a Result of Military Operations in Ukraine

Oleksandr Lapenko[1]([✉]) [iD], Nataliia Tabarkevych[1] [iD], Vasiliy Makarov[2] [iD], and Oleksandr Palyvoda[2] [iD]

[1] National Aviation University, Kyiv, Ukraine
my-partner@ukr.net
[2] Kryvyi Rih National University, Kryvyi Rih, Ukraine

Abstract. The article presents an example of reconstruction of interfloor floors of residential buildings damaged or destroyed as a result of military operations. Monolithic slabs with sheet reinforcement are steel-concrete structures that use external sheet reinforcement placed on the extreme edges of the cross-section. When these slabs are constructed, steel profiles are assembled in the form of a deck and used as formwork. After the concrete has hardened and reached its design strength, the profiled steel sheet is incorporated into the slab as working reinforcement. The deck is incorporated into the reinforcement of the slab by means of anchors of various designs or by embedding the deck itself in the concrete.

Keywords: Steel-reinforced concrete · Slabs · Reconstruction

1 Introduction

The operation of monolithic slabs on steel profiled decks has been studied quite well so far. However, there are practically no design developments of anchoring means to ensure compatible operation of sheet reinforcement with concrete when the slabs are supported on concrete, reinforced concrete or brick structures, or in these cases, conventional rod anchors are used, which are fixed to the deck by welding and require additional embedded parts. Existing calculation methods do not take into account all the features of such structures, especially when using non-standard anchoring means.

An analysis of the results of the research conducted so far and the experience of using steel-reinforced concrete slabs on steel profiled decks show that, with a sufficient level of feasibility study, monolithic slabs on steel profiled decks are quite effective (they can save up to 30% of steel compared to conventional reinforced concrete slabs). They have a number of advantages and, despite some disadvantages, meet all the requirements of modern construction.

2 Aim and Objectives

The aim of the work is to restore the interfloor slab and roofing of buildings as soon as possible during the elimination of the consequences of emergencies in Ukraine.

The article presents examples of restoration of roofs and floors of residential buildings developed on the basis of systems with fixed formwork with profiled sheet.

It is expected that the proposed solutions will be used in the future to restore coatings and floors of residential buildings.

3   Presentation of the Main Material

Restoration work is a set of works related to the restoration of buildings, structures, enterprises, institutions and organisations, regardless of ownership, which were destroyed or damaged as a result of an emergency, including military operations.

Justificaiion for the restoration of floor slabs and ceilings.

The floor slab of a residential building was damaged by a shell fragment. The consequences of the damage are shown (see Fig. 1).

Fig. 1.   Nataliia Tabarkevych. The consequences of a shell fragment hitting the floor slab of a residential building.

Since a crane was required to install new roof slabs and the damaged roof slabs needed to be repaired as soon as possible before the start of seasonal rainfall, a solution of fixed formwork with profiled sheet was proposed.

Fixed profiled sheet formwork has sufficient hardness and is an excellent base, it is laid directly on the metal floor beams. After that, the profiled sheet is used as a base for reinforcing frames and pouring concrete mix. In this case, the entire load acting on the floor is transferred to the metal frame of the building. Load-bearing corrugated sheeting is used as formwork for the installation of interfloor floors and flat roofs. [10–12].

The profiled sheet used for these purposes has a profile height of more than 44 mm and is usually reinforced with additional stiffeners to increase its load-bearing capacity. When constructing flat roofs, a layer of vapour barrier, insulation and waterproofing is laid on the surface of the profiled sheet. The corrugated sheets should be perpendicular to the load-bearing beam. Formwork using corrugated sheeting will be more expensive than wood-based construction, but also much more reliable.

The elements of the system are mounted in the following order:

beam for formwork (channel No. 16 or I-beam No. 20);

corrugated sheeting - laid so that the sheet edges are perpendicular to the direction of the supporting beam;

reinforcement.

Next, the assembled metal structure is poured with concrete and compacted.

The height of the profile sheet is calculated individually for each floor. As a rule, a sheet within the range of grades H60-H75 is used. The use of metal sheets in the formwork makes it possible to obtain a strong floor, save on reinforcement, reduce the weight of the structure, and thus reduce the load on the foundation. The design of fixed formwork is shown in Fig. 2.
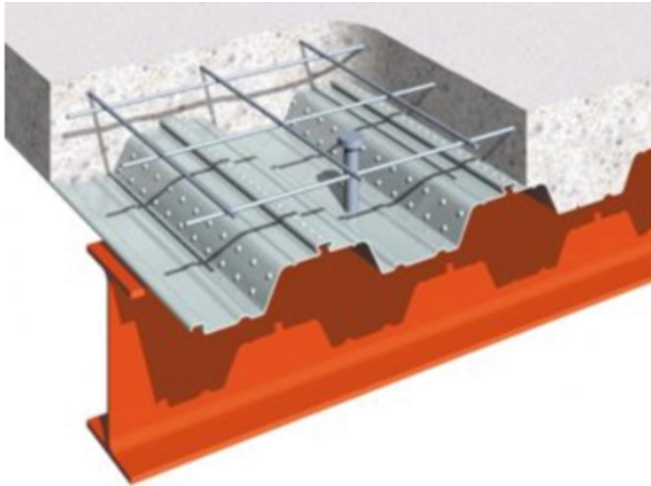

Fig. 2. - Design of fixed formwork [14]

In the walls of a residential building, strobes are made into which metal channels with a cross section of No. 16 are inserted; with a large span between the walls, channels with a cross section of No. 16 are welded in the opposite direction to the channel with a cross section of No. 12. Metal frame elements should be treated with anti-corrosion agents such as PF119 [14].

After the metal frame elements have been installed on the top of the channels with a cross-section of 16 (or, in case of large spans, on additional channels of 12), install H-75
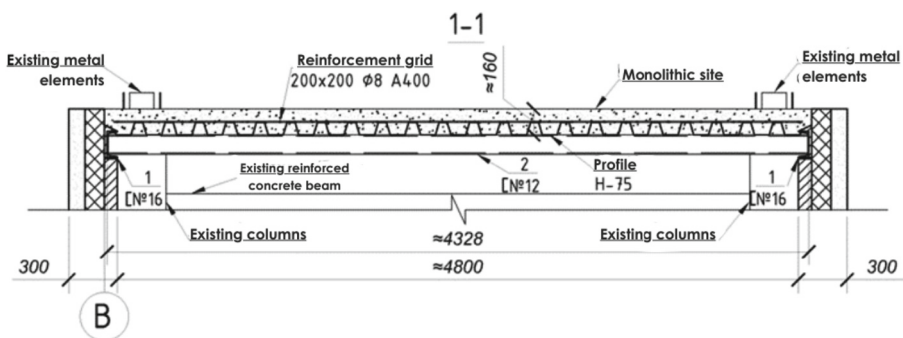

Fig. 3. Scheme of arrangement of fixed formwork and cover slab. Cut 1–1.

corrugated board and attach it to the channels using spacer dowels, install reinforcing mesh with a cross-section of 200 × 200 □ 8 A400 on the surface of the corrugated board and concrete with concrete of class C16/20 [15, 16].

In the same way, it is possible to restore damaged interfloor slabs with large spans in residential buildings. These solutions will save time and costs for the restoration of floor slabs and floors in residential buildings. The layout of the floor slabs is shown in Figs. 3–5.
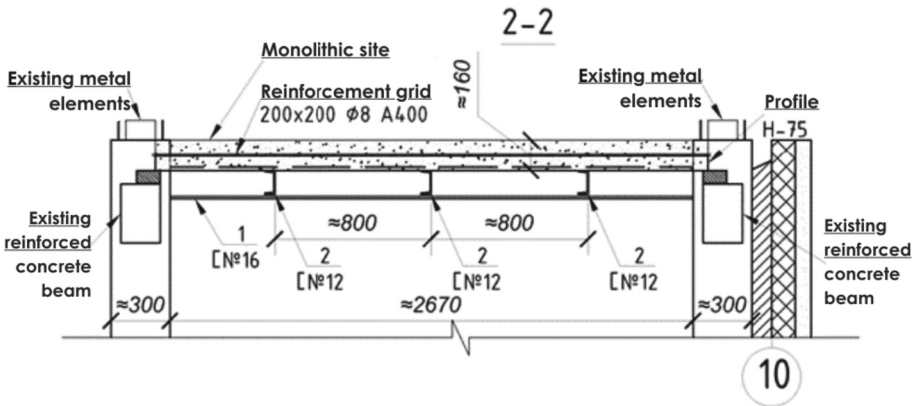

Fig. 4. Scheme of arrangement of fixed formwork and cover slab. Cut 2–2.
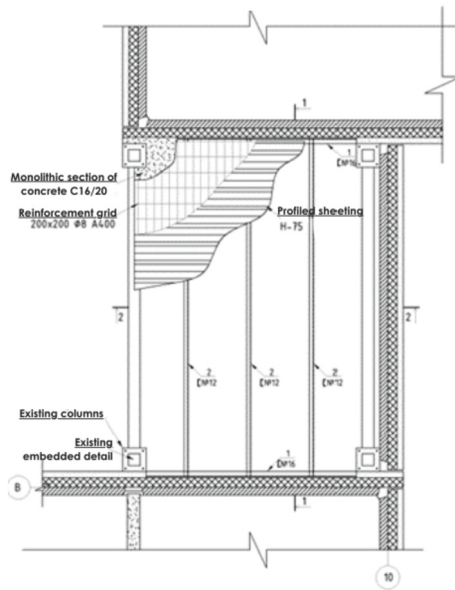

Fig. 5. Scheme for refinishing the coating elements.[9, 13]

4 Conclusion

Steel-reinforced concrete structures, i.e. structures using rolled steel and monolithic reinforced concrete, are widely used in construction in Ukraine and the CIS countries. These structures combine the flexibility of shapes and sizes of monolithic reinforced concrete and steel structures, while at the same time they do not require expensive formwork and are highly fire-resistant.

The experience of many years of widespread use of various types of steel reinforced concrete structures (pipe concrete, monolithic reinforced concrete slabs over corrugated board, load-bearing beams and posts that combine concrete and rolled steel in industrial and civil buildings) in Kyiv, Poltava, Lviv, Kryvyi Rih, Kremenchuk, Komsomolsk and other cities of Ukraine allows us to assert high reliability, ease and speed of installation, and good performance of steel reinforced concrete.

Based on the analysis of existing studies, the advantages of steel-reinforced concrete slabs were identified. The complexity of designing the proposed structures depends on their structural solution. To increase interest in these structures, it is necessary to study the main issues related to the features of the proposed structures, their types and structural solutions. To implement the proposed structures in the reconstruction, it is necessary to solve the problem of finding the optimal geometric parameters of the pavement that would satisfy the conditions of its operation.

References

1. DSTU-N B V.1.2–18:2016. Guidelines for the inspection of buildings and structures to determine and assess their technical condition. Kyiv. UkrNDNC SE (2017)
2. DSTU B B.2.6.-210: 2016 "Assessment of the technical condition of steel building structures in operation" / Ministry of Regional Development of Ukraine, Kyiv 2016 -56 p.
3. DBN V.1.2–14–2009. System of ensuring the reliability and safety of construction facilities. General principles of ensuring the reliability and structural safety of buildings, structures, building structures and foundations / Ministry of Regional Development of Ukraine - Kyiv: Ukrarkhbudinform, 2009. 37 p.
4. DBN V.2.6–98: 2009. Concrete and reinforced concrete structures. Main provisions / Ministry of Regional Development of Ukraine. - Kyiv: Ukrarhbudinform, 2011. - 71 p.
5. DSTU B.2.6–156: 2010. Concrete and reinforced concrete structures of heavy concrete. Design rules. Kyiv, Ministry of Regional Development of Ukraine. 2010
6. DBN B.2.6–162: 2010 Stone and reinforced stone structures. Main provisions. Ministry of Regional Development of Ukraine. Kyiv-2011
7. DBN B.2.6–160:2010 - Steel and reinforced concrete structures. Basic provisions
8. DSTU B.1.2–3:2006 Deflections and displacements. Design requirements. Ministry of Construction of Ukraine. - K., 2006. - 40 p.
9. Storozhenko, L., Yermolenko, D., Pents, V.: Steel and reinforced concrete frames of one-storey buildings for universal use. - Poltava, pp. 221–225 (2018)
10. Azizov, T.N., Kochkarev, D.V., Galinska, T.A.: New design concepts for strengthening of continuous reinforced-concrete beams. IOP Conf. Series: Materials Sci. Eng. **708**(1), 012040 (2019). https://doi.org/10.1088/1757-899X/708/1/012040
11. Azizov, T., Kochkarev, D., Galinska, T.: Reinforced concrete rod elements stiffness considering concrete nonlinear properties. Lecture Notes in Civil Eng. **47**, 1–6 (2020). https://doi.org/10.1007/978-3-030-27011-7_1

12. Kochkarev, D., Azizov, T., Galinska, T.: Design of effective statically indeterminate reinforced concrete beams. Lecture Notes in Civil Eng. **73**, 83–93 (2020). https://doi.org/10.1007/978-3-030-42939-3_10

13. Storozhenko, L., Butsky, V., Taranovsky, O.: Stability of compressed steel concrete composite tubular columns with centrifuged cores. J. Constr. Steel Res. **46**(1–3), 484 (1998)

14. Baranetska, D.: Stress-strain state of steel-reinforced concrete slabs with external reinforcement by different types of profiled flooring (2018). [PhD Thesis, National Aviation University]

15. Lapenko, O.: Reinforced concrete structures with working reinforcement with fixed formwork. Poltava: ACMI (2009)

16. Lapenko, O.: Problems of reinforcing reinforced concrete with fixed formwork. Constr., Material Sci., Eng. Collect. **50**, 279–284 (2009)

Study of Mechanical Properties of Shipbuilding Pipe Steels for Cooling Systems of Long-Term Operation in a Wide Range of Sub-zero Temperatures

Valery Makarenko[1] , Viktor Khoruzhiy[1] , Serhiy Maksymov[2] ,
Tetiana Khomutetska[1] , Tetiana Galinska[3(✉)] , and Yuliya Makarenko[4]

[1] Kyiv National University of Construction and Architecture, 31 Povitroflotskyi Avenue, Kyiv, Ukraine

[2] E.O. Paton Electric Welding Institute of the National Academy of Sciences of Ukraine, Kyiv, Ukraine

[3] National University «Yuri Kondratyuk Poltava Polytechnic», Pershotravnevyj Ave. 24, Poltava 36011, Ukraine
`galinska@i.ua`

[4] University of Manitoba, Winnipeg, Canada

Abstract. Comprehensive studies have shown that with the increase in the service life of both pipelines for transporting the cooling medium and pipes of cooling systems, metal is enriched with hydrogen with an increase in the structure of non-metallic inclusions, which leads to its embrittlement and weakening, resulting in a decrease in the parameters of crack resistance, which indicates a reduction in the resistance of the metal to the formation of cracks leading to structural damage.

Keywords: Crack resistance · Viscosity · Plasticity · Crack nucleation · Fracture · Destruction

1 Introduction

The change in the stress level of shipbuilding steels with different service life was determined on standard (flat) samples, which were made with a working part size of $35 \times 4 \times 1.5$ mm. The samples were cut from the steel billets and subjected to uniaxial stretching at a strain rate of $\varepsilon = 10^{-5}c^{-1}$ [1–5]. Mechanical tests were performed on a universal tensile machine, "Instron-1251" (UK), at a constant temperature of 22^0C. Based on the results of experimental tests, standard indicators of the mechanical properties of steels were determined for each sample: tensile strength (σ_v), yield strength ($\sigma_{0.2}$), transverse (ψ) and longitudinal (δ) deformation [5]. It is believed that [1–4, 15, 16] the mechanical characteristics $\sigma_{0.2}$ and ψ are the most sensitive to metal embrittlement.

2   Research Methodology and Materials

One of the characteristic indicators of resistance to brittle fracture of steels is impact strength. Samples with a V-shaped cut – КСV (Charpy) were used to study impact strength. The samples' direction and the cuts' location were the same. GOST 9454–78 and GOST 1497–84 tested the specimens for dynamic bending in a wide temperature range.

To determine the impact strength, samples of 55 mm in length and a cross-sectional area of 8×8 mm2 with a V-shaped cut of 2 mm in size and a 45º bending angle [5], cut from pipe steel in different states, were used. The tests were conducted using a well-known method [1–5]. The test results were averaged over at least three tests.

In addition, as a criterion of crack resistance, we used the R_{Mc} index, known from modern mechanics of fracture of metal structures, which is the resistance of steel to micro-cracking, which depends on the structural state of steel, in particular on the grain size and thickness of cementite inclusions and does not depend on external factors, unlike other integral criteria of mechanical properties, i.e., temperature, deformation rate, geometric dimensions and shape of the sample, and the type of stress state [1–4]. The determination of R_{Mc} was carried out according to the method described in [1].

The crack resistance characteristics, i.e., the fracture toughness parameters K_{1c} and δ_c, were also determined, for which samples of standard sizes were prepared [1–5]. Fatigue cracks in the pieces were created using a hydraulic pulsator CDM-10 (Germany) at a loading frequency of 10…15 Hz, and a cycle asymmetry factor r = 0.1…0.2. Tests to determine the fracture toughness parameters K_{1c} and δ_c were carried out at the UME-10 and "Instron" (UK) installations according to standard methods [5, 15, 16].

In addition, the residual hydrogen content in the metal was determined by local mass spectral analysis (LMSA) with a laser microprobe.

The research objects were samples of steel grades D32, 10KhSND, and 20KhSND intended for shipbuilding during operation from 0 to 12 years in a corrosive environment in a wide range of temperature changes (from + 20 °C to -50 °C) [1–16].

During forced or scheduled repairs, the samples were prepared using pipe fragments from emergency pipelines or cooling system pipes.

3   Research Results and their Discussion

The results of mechanical tests of pipe samples to determine the stress intensity factor parameters of crack resistance in a wide range of changes in subzero temperatures are shown in Figs. 1–7.

Figure 1 shows that with an increase in service life over the entire temperature range from + 20 to −50 °C, the stress intensity factor R_{Mc} of D32 steel decreases, and this is noticeably manifested for pipe samples with a service life of 10 years or more and temperatures of -35… $\times$ −50 °C. Thus, for pieces made from emergency stock pipes, the R_{Mc} parameter at temperatures of + 20 and $\times$ −20 °C is equal to 580 and 560 MPa, and at a temperature of $\times$ −50 °C, this parameter has the following values: 400 and 460 MPa, respectively, i.e. the R_{Mc} value decreases by 1.2–1.45 times. At the same time, the R_{Mc} parameter at temperatures of −35 −50 °C for samples of unused D32 steel has

the following values: 530 and 500 MPa, and after 30 years of operation, respectively, 250 and 200 MPa, i.e. the value of R_{MC} decreases by 1.6–2.0 times. Moreover, this trend persists over the entire range of changes in sub-zero temperatures and the service life of pipe structures.
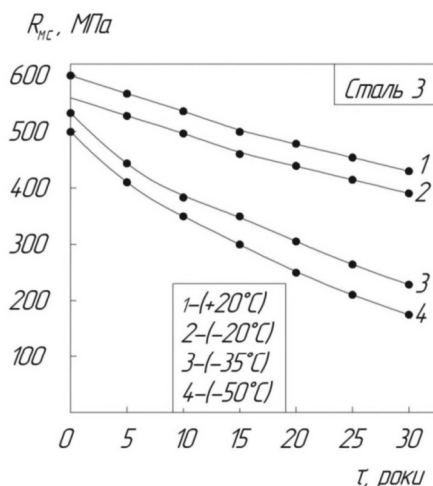

Fig. 1. Graphical dependence of micro-crack stress of D32 steel on the service life of pipelines for pumping refrigerant at a processing industry enterprise. Test temperature designation (in 0 C): 1 - (+20); 2 - (-20); 3 - (-35); 4 - (-50).

The negative effect of lowering the test temperature from + 20 to −50 °C on the crack resistance parameters K_{1c} and δ_c is observed throughout the entire period of long-term operation of pipelines. The analysis of the data shown in Figs. 2 and 3 shows that for non-operated steel at a temperature of + 20 °C, the values of K_{1c} and δ_c are 115 MPa-m$^{1/2}$ and 0.79 mm, respectively, and for pipe steel, which was exploited throughout, for example, 25 years, the same parameters at the same temperature have the corresponding values: 74 MPa-m$^{1/2}$ and 0.39 mm, i.e. the crack resistance of steels decreases by 2.2 times (K_{1c}) and two times (δ_c). For non-operated steel at a temperature of -50 °C, the values of the parameters K_{1c} and δ_c are equal to 95 MPa-m$^{1/2}$ and 0.67 mm, while for steel with a service life of, for example, 30 years, the same parameters have the following values: 41 MPa-m$^{1/2}$ and 0.17 mm, respectively, i.e. they decrease by 2.3 times (K_{1c}) and by ≈four times (δ_c), i.e. at a sub-zero temperature of −50 °C, the resistance of D32 steel against cracking with subsequent destruction of pipe structures, which are in direct contact with the aggressive technological environment of shipbuilding production, is significantly reduced.

The graphs shown in Fig. 4 indicate a significant change in the fracture toughness parameter КCV in a wide range of changes in the pipe structures' service life and the samples' test temperature. For non-operated steel at a temperature of + 20 °C (curve 1), the КCV parameter is 0.68 mJ/m^2. An increase in the service life, for example, up to 30 years, leads to a decrease in the КCV parameter, the value of which in this case is
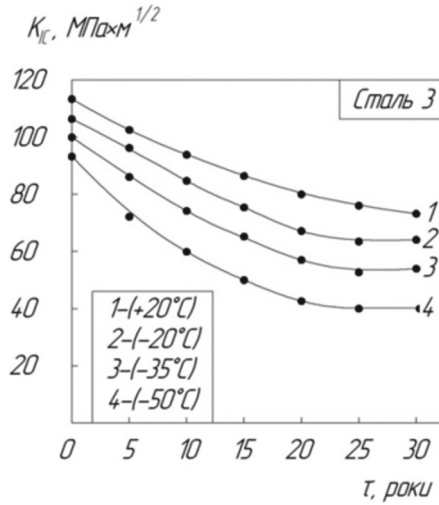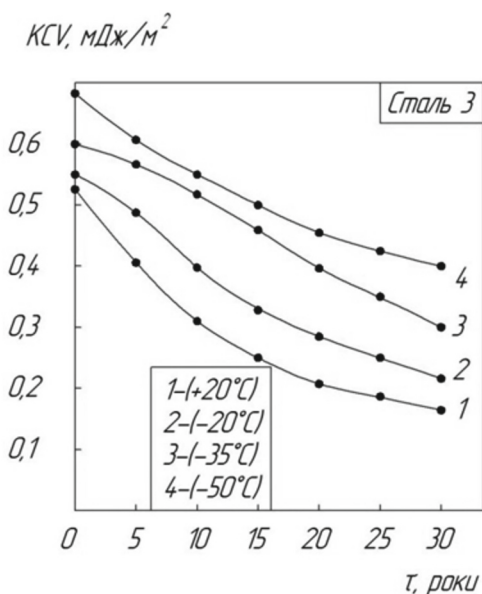
Fig. 2. Graphical dependences of the stress intensity coefficient K1c on the service life of pipelines at a shipbuilding enterprise. Test temperature designation (in ^{0}C): 1 - (+20); 2 − (−20); 3 - (−35); 4 - (−50).
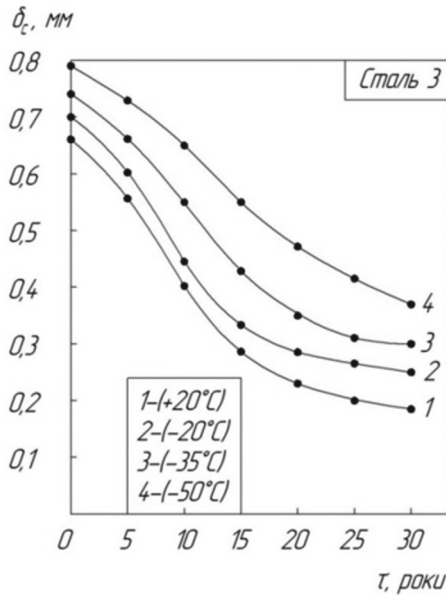
Fig. 3. Graphical dependences of the critical crack opening coefficient on the service life of pipelines at a shipbuilding company. Test temperature designation (in ^{0}C): 1 - (+20); 2 - (−20); 3 - (−35); 4 - (−50).

0.38 mJ/m², i.e., a 1.7-fold decrease. At the same time, at a test temperature of −50 °C, the КCV parameter has a value of 0.54 mJ/m² (non-operated steel) and 0.15 mJ/m² (steel service life of 30 years), which decreases by 3.6 times. Notably, the same trend is observed for steels with different service lives (from 0 to 30 years) in the temperature range of the test (from + 20 to −50 °C).

Fig. 4. Graphical dependence of the impact strength (Charpy test) of metal on the service life of pipelines at a shipbuilding company. Test temperature designation (in ⁰C): 1 - (+20); 2 - (-20); 3 - (-35); 4 - (-50).

Figure 5 shows that as the service life of the D32 steel pipeline changes from 0 to 30 years, the values of the strength limit σ_B hardly change, but the values of the yield strength σt decrease from 240 MPa (non-operated steel) to 170 MPa (30 years of service), i.e. almost 1.5 times. The values of the longitudinal δ and transverse ψ deformation, respectively, vary from 33% (δ) and 75% (ψ) (non-operated steel) to 14% (δ) and 50.5% (ψ) (service life of 30 years), i.e. a 2.2 (δ) and 1.48 (ψ) times reduction in the plasticity of the steel with long service life.

For Fig. 6 shows the graphical dependences of the plasticity parameter $\sigma_{0.2}$ and the degree enrichment with hydrogen [H] on the service life of D32, 10KhSND and 20KhSND steels for the shipbuilding industry. It can be seen that 20KhSND steel has the highest plastic properties, while 10KhSND steel showed the lowest values of σ0.2 throughout the entire service life of the pipelines. The analysis of Fig. 6.25 shows that an increase in the service life leads to a decrease in $\sigma_{0.2}$; in particular, for D32 steel, the value of $\sigma_{0.2}$ for non-operated steel is 220 MPa, and for used steel with a service life of 30 years it is already equal to 140 MPa, i.e. the plasticity of the steel decreases by 1.57 times. The same trend is observed for 10KhSND and 20KhSND steels. For example, in
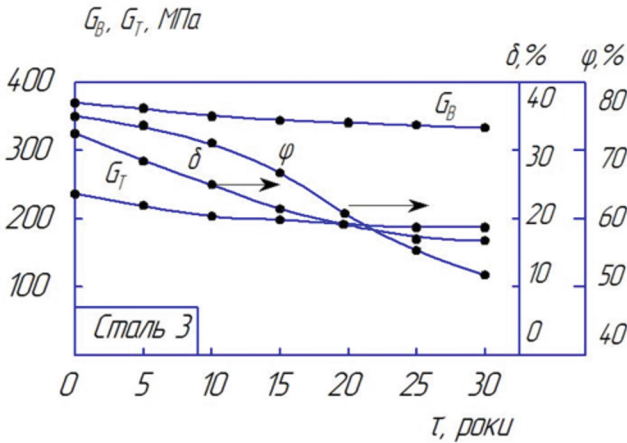
Fig. 5. Graphical dependences of the tensile strength (σt) and yield strength (σt), longitudinal (δ) and transverse (ψ) deformation of metal on the service life of pipelines at shipbuilding enterprises.

the case of non-operated steels, the values of the $\sigma_{0.2}$ parameter are 210 MPa (steel 10) and 250 MPa (steel 20). For steels in use with a service life of 30 years, the σ0.2 parameter is 115 MPa (steel 10) and 180 MPa (steel 20), i.e. the plastic properties decrease by 1.82 (steel 10) and 1.38 (steel 20) times, respectively.

The above data indicate a possible enrichment of shipbuilding steels with hydrogen during long-term operation, which is confirmed by the results of measurements of residual hydrogen [H] in the metal of existing pipelines (Fig. 6).

For example, for non-operational steels of D32, 10KhSND and 20KhSND grades, the [H] values are (in ppm): 4.1 (D32 steel); 3.1 (10KhSND steel) and 1.5 (20KhSND steel), and for the same steels with 30-year service life, the [H] values are respectively (in ppm): 14.3 (D32 steel); 12.5 (10KhSND steel) and 10.2 (20KhSND steel), i.e. the enrichment of shipbuilding steels with hydrogen with an increase in service life from 0 (emergency reserve) to 30 years increases by 3.5 times (D32 steel); 4 times (10KhSND steel) and 6.8 times (20KhSND steel), respectively.consecutive.

The same trend is generally observed when analysing the data in Fig. 7, which shows graphs of the dependence of the plasticity parameter $\sigma_{0.2}$ and hydrogen concentration [H] in D32, 10HSND and 20HSND steels on the service life of cooling systems in shipbuilding.

The data shown in Fig. 7 shows that the values of the plasticity parameter σ0.2 for 20KhSND steel decrease much less than other D32 and 10KhSND steels. Thus, the values of σ0.2 for non-operated steels are equal to (in MPa): 250 (20KhSND steel), 240 (D32 steel) and 205 (10KhSND steel), and for used steels with a service life of 30 years, the σ0.2 parameter has the following values (in MPa): 190 (20KhSND steel), 155 (D32 steel) and 105 (10KhSND steel), i.e. the values of σ0.2 decrease by 1.32 times (20KhSND steel), 1.55 times (D32 steel) and ≈two times (10KhSND steel), respectively. Similar to the above data for pipelines, the data indicate that pipe steels are waterlogged during their long-term operation, which is confirmed by the results of determining the concentration of residual hydrogen in the steels.
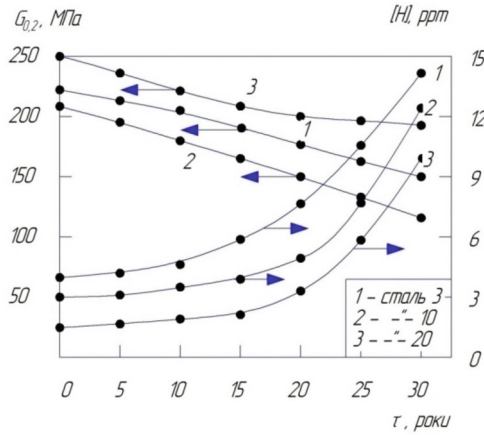
Fig. 6. Graphs of changes in plasticity and the degree of enrichment of shipbuilding steel depending on the service life of pipelines at a shipbuilding company.
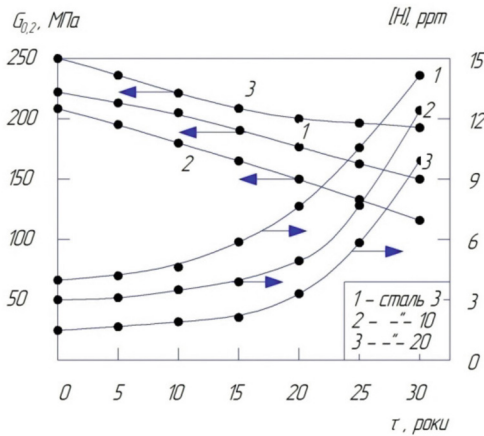
Fig. 7. Graphs of changes in plasticity and the degree of enrichment of shipbuilding steel depending on the service life of cooling systems in industrial production.

Analysis of the data in Fig. 7 shows the following. For non-operated steels, the hydrogen content [H] is equal to (in ppm): 3.2 (D32 steel), 1.0 (10HSND steel) and 2.1 (20HSND steel), and for steels with a service life of 30 years, the [H] values are (ppm): 19.3 (D32 steel), 15.8 (10KhSND steel) and 11.0 (20KhSND steel), i.e. with an increase in service life from 0 (no service life) to 12 years, the enrichment of shipbuilding steel increases by a factor of 6 (D32 steel), 15.8 (10KhSND steel) and 5.2 (20KhSND steel), respectively.

4   Conclusions and Prospects

Thus, it can be concluded that as the service life of both pipelines for transporting the cooling medium and pipes of cooling systems increases, metal flooding occurs with an increase in the structure of non-metallic inclusions, which leads to its embrittlement and weakening, resulting in a decrease in crack resistance parameters, which indicates a reduction in the metal's resistance to crack initiation, leading to structural failure.

References

1. Meshkov Yu, Ya.: Fizicheskie osnovyi razrusheniya stalnyih konstruktsiy. –Kiev: Naukova dumka. – 229s (1981)
2. Vasilenko, I.I., Melehov, O.D.: Korrozionnoe rastreskivanie stali. – Kiev: Naukova dumka. – 265 s (1997)
3. Zolotorevskiy, V.S.: Mehanicheskie svoystva metallov.–M.: Metallurgiya. – 350 s (2013)
4. Kalachev, B.A.: Vodorodnaya hrupkost metallov. – Metallurgiya. – 216 s (2009)
5. Makarenko, V.D., Moroz, A.I., Petrenko, I.V.: Metodi otsInki bezpechnogo resursu obladnannya agropererobnogo v virobnitstva//NIzhin NDU Im.Mikoli Gogolya. – 133s (2017)
6. Marinin, A.N.: Soprotivlenie zhelezobetonnyih konstruktsiy vozdeystviyu hloridnoy korrozii i karbonizatsii / A.N. Marinin, R.B. Garibov, I.G. Ovchinnikov. Saratov: Izdat. tsentr «RATA» –296 s (2008)
7. Moskvin, V.M.: Korroziya betona i zhelezobetona, metodyi ih zaschityi / V.M. Moskvin, F.M. Ivanov, S.N. Alekseev, E.A. Guzeev. – 536 s (1980)
8. Pichugin, A.G., Hritankov, V.F.: i dr.: Puti obespecheniya dolgovechnosti rechnyih portovyih sooruzheniy //IVVseros. Nauch.-praktich. konferentsiya "Sovremennyie problemyi stroitelstva i zhizneobespecheniya", Y. – S.271–275 (2016)
9. Markovich, R.A., Kolgushkin, A.V.: Korroziya morskih gidrotehnicheskih sooruzheniy// Gidrotehnicheskoe stroitelstvo.- 2(15).–S.72–75 (2000)
10. Rozental, N.K., Chornyiy, G.V., Porshnya, I.I.: Korroziya betonnyih i zhelezobetonnyih konstruktsiy v presnyih i morskih vodah//Vestnik NITs "Stroitelstvo". - 1(2). – S.43–53 (2017)
11. Kovalenko, R.G.: Analiz izmeneniya nesuschey sposobnosti "Bolverka" s uchetom korrozii shpuntovoy stenki//Gidrotehnicheskoe stroitelstvo.-4(16). – S.43–51 (2000)
12. Dubrovskiy, M.P.: AnalIz suchasnogo stanu ekspluatovanih prichalnih sporud morskih portIv UkraYini//VIsnik Odeskogo natsIonalnogo morskogo unIversitetu.- (33) (2018)
13. Dyadur, L.S.: Korrozionnoe vozdeystvie kak suschestvennyiy faktor tehnicheskoy ekspluatatsii portovih prichalnih sooruzheniy tipa "Bolverk"//VIsnik Odeskogo natsIonalnogo morskogo unIversitetu.- 1(47). – S.136–144 (2016)
14. Okada, T., Hattori, S.: Zavisimost mezhdu kontsentratsiey soli v vode i soprotivleniem korrozschionnoy ustalosti konstruktsionnoy stali//Journal of Engineering Materials and Technology, vol.107. – P.235–239 (1985)
15. .Makarenko, V.D., BIlik, S.I., Maksimov S.Yu.: I In.(2021) KorozIynI ruynuvannya morskih prichalIv// KiYiv: NUBIP UkraYini. – 296s
16. Makarenko, V.D., Maksimov S.Yu., Vinnikov Yu.L. I In.: KorozIynI ruynuvannya kanalIzatsIynih sistem UkraYini// KiYiv: NUBIP UkraYini. – 294s (2021)

The Research of the Nature of Surface Compaction of Polymer Concrete by a Vibration Working Body with Electric Drive

Oleksandr Maslov , Dmytro Savielov$^{(\boxtimes)}$, and Roman Vakulenko

Kremenchuk Mykhailo Ostrohradskyi National University, Kremenchuk, Ukraine
dvsavelov@gmail.com

Abstract. Based on the analysis of existing methods of surface vibration compaction, a vibration working body is proposed, made in the form of a horizontal vibration plate, on which an electric drive is mounted on top, consisting of an asynchronous electric motor with unbalances installed at the ends of the rotor shaft. To analytically determine the nature of the interaction of a vibrating plate equipped with an electric drive with polymer concrete, the research was made of the dynamic system "vibration plate - polymer concrete", in which polymer concrete is presented as a system with distributed parameters, taking into account the action of elastic and dissipative resistance forces from polymer concrete with its surface compaction. In accordance with the accepted rheological model of polymer concrete, a wave equation of vibrations was compiled that describes the movement of compacted polymer concrete, the solution of which made it possible to determine the law of propagation of elastic-viscous deformation waves in polymer concrete, the physical and mechanical characteristics of polymer concrete, the vibration amplitude of the vibrating plate and the law of stress change in compacted layer of polymer concrete.

Keywords: Electric drive · Asynchronous motor · Polymer concrete · Stresses · Deformation

1 Introduction

At surface compaction of polymer concrete by a vibration method, the vibrating plate of the working body interacts with the compacted medium. At the same time, the physical and mechanical characteristics of the compacted polymer concrete have a significant impact on the behavior of the dynamic system of vibration equipment and the choice of its main operating parameters. Determination of the physical and mechanical characteristics of the compacted polymer concrete will make it possible to establish a rational law of motion of a vibrating plate interacting with polymer concrete, to assess the operating modes of a vibrating plate, to correctly select the technological parameters of vibration action, the use of which will ensure effective compaction of polymer concrete.

At present, research has been carried out on the process of vibration compaction of polymer concrete on a vibrating plate with vertically directed vibrations. [1–5]. In papers

[1, 2], a mathematical model of a dynamic system of a vibrating plate interacting with polymer concrete was created. As a result of the research, analytical expressions were obtained to determine the dynamic moduli of elastic deformation and the coefficient of dynamic viscosity of polymer concrete [3, 4], the law of motion of the movable frame of the vibrating plate and polymer concrete, depending on its physical and mechanical characteristics, the amplitude and frequency of forced vibrations and the height of the compacted layers. In paper [5], the design scheme of the dynamic system "vibrating working body - polymer concrete" is substantiated.

For the effective operation of vibration compaction equipment, it is necessary to accurately determine its main parameters and modes of vibration action, depending on the physical and mechanical characteristics of the compacted medium, which can be represented by various types of rheological models [6–9]. In [1–5], the physical and mechanical characteristics of polymer concrete compacted by vibration load are presented by the Zener rheological model, which, along with reversible and irreversible deformation, describes reversible highly elastic deformation, which is most clearly manifested in media containing polymers [10–12]. At the same time, for the most accurate description, polymer concrete is presented in the form of a system with distributed parameters, taking into account its elastic and viscous properties.

All these results were obtained to determine the rational parameters of vibration areas and cannot be applied to surface vibration compactors of polymer concrete.

Therefore, carrying out further theoretical research aimed at accurately determining the law of motion of vibration equipment for surface compaction of polymer concrete, determining the modes of vibration impact depending on the physical and mechanical characteristics of the compacted material and the size of the products is a very topical task.

The purpose of this research is to theoretically determine the law of motion of the vibrating plate of the.
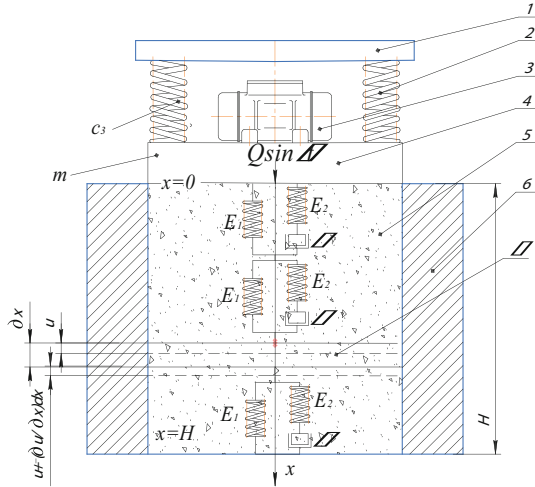
2 Main Body

To theoretically determine the resistance forces acting during surface compaction in the vertical direction from the polymer concrete on the vibrating plate, let us consider the design scheme of the dynamic system "vibrating plate - polymer concrete", in which polymer concrete is presented in the form of a system with distributed parameters [4] (Fig. 1).

In the operating mode, the vibration plate 4 of the working body, which is suspended on elastic shock absorbers 2 to the support frame 1, is subjected to disturbance in the form of a vertically directed harmonic force $Q \sin \omega t$. As a result, vibrating plate 3 vibrates in the vertical plane and vibrates the polymer concrete 5 in the mold 6. With this interaction, a stress state occurs in the deformable layer of polymer concrete 5.

In accordance with the proposed rheological model of polymer concrete [6], the relationship between stress and deformation in polymer concrete has the form [1]:

$$\sigma(x, t) = E_1 \frac{\partial u(x, t)}{\partial x} + \eta \cdot \left(\frac{E_1 + E_2}{E_2} \right) \frac{\partial^2 u(x, t)}{\partial x \partial t} - \left(\frac{\eta \cdot \rho}{E_2} \right) \frac{\partial^3 u(x, t)}{\partial t^3}, \qquad (1)$$

Fig. 1. Design diagram of the dynamic system "vibration plate - polymer concrete": 1 – support frame; 2 – elastic shock absorber; 3 –asynchronous electric motor; 4 – vibrating plate; 5 – polymer concrete; 6 – mold.

where $\sigma(x, t)$ – stresses arising in the compacted layer of polymer concrete; u and x – Euler and Lagrangian coordinates; E_1 and E_2 – dynamic moduli of elastic deformation of polymer concrete; η – dynamic viscosity coefficient taking into account internal friction in polymer concrete; ω – forced angular frequency; t – current time.

Functional values of dynamic modules E_1, E_2 and η based on paper [4] can be found due to the following expressions:

$$E_1 = E_{01} \cdot \left[1 + \mu \cdot \left(\frac{\rho - \rho_0}{\rho_k - \rho} \right)^z \right]; \tag{2}$$

$$E_2 = E_{02} \cdot \left[1 + \mu \cdot \left(\frac{\rho - \rho_0}{\rho_k - \rho} \right)^z \right]; \tag{3}$$

$$\eta = H_1 \cdot \sqrt{(E_1 + E_2)\rho}, \tag{4}$$

where E_{01} and E_{02} – dynamic moduli of elastic deformation of uncompacted polymer concrete at initial density ρ_0 ($E_{01} = 3,12$ MPa, $E_{02} = 4,28$ MPa); μ and z – experimental coefficients taken accordingly 3,5 and 3; ρ – the current value of the density of polymer concrete corresponding to the applied dynamic load P, kg/m^3; ρ_0 – initial density of polymer concrete, kg/m^3; ρ_k – density of polymer concrete mixture under load $P_k = 40$ MPa; H_1 –reduced thickness of the compacted layer of polymer concrete, taken depending on the direction of vibration and the ratio between the wavelength of the disturbance and the thickness of the layer [4].

Vibrations of a layer of polymer concrete in the direction of coordinate x in time t will be of the form [1, 2]:

$$\frac{\partial \sigma(x, t)}{\partial x} = \rho \frac{\partial^2 u(x, t)}{\partial t^2}, \tag{5}$$

where ρ – density of polymer concrete.

Substituting expression (1) into (5), we obtain the differential equation of motion of the compacted polymer concrete in the form [1]:

$$\frac{\partial^2 u(x,t)}{\partial x^2} + \eta \cdot \left(\frac{E_1 + E_2}{E_1 \cdot E_2}\right) \cdot \frac{\partial^3 u(x,t)}{\partial x^2 \partial t} - \left(\frac{\eta \cdot \rho}{E_1 \cdot E_2}\right) \cdot \frac{\partial^3 u(x,t)}{\partial t^3} = \left(\frac{\rho}{E_1}\right) \cdot \frac{\partial^2 u(x,t)}{\partial t^2}$$
(6)

To solve the wave equation of vibrations (6), we use the following boundary conditions resulting from the design scheme in Fig. 1:

at $x = 0$:

$$-m\frac{\partial^2 u(0,t)}{\partial t^2} - c_3 u(0,t) + E_1 F \frac{\partial u(0,t)}{\partial x} + \left(\frac{E_1 + E_2}{E_2}\right) \times$$

$$\times \eta F \frac{\partial^2 u(0,t)}{\partial x \partial t} - \left(\frac{\eta \rho F}{E_2}\right) \frac{\partial^3 u(0,t)}{\partial t^3} = -Q \sin(\omega t),$$
(7)

at $x = H$:

$$u(H,t) = 0,$$
(8)

where m – vibrating plate mass; c_3 – coefficient of stiffness of elastic shock absorbers in the vertical direction in the suspension of a vibrating plate; F – vibrating plate bearing surface area; Q – disturbing force amplitude; H – height of the compacted layer of polymer concrete.

Boundary condition (7) describes the interaction of the vibrating plate with the surface of the compacted polymer concrete. Boundary condition (8) indicates that the displacement of the compacted layer of polymer concrete at distance H from the surface of the vibrating plate is zero.

We represent the solution to Eq. (6) in the form of the imaginary part of the complex number [1]:

$$u(x,t) = u(x) \cdot e^{i\omega \cdot t},$$
(9)

where $u(x)$– complex vibration amplitude meeting the boundary conditions for the design diagram shown in Fig. 1.

Using the technique described in [1], we find a solution to Eq. (6) in the complex form:

$$u(x,t) = \left[B \cdot e^{-(ik+\alpha) \cdot x} + D \cdot e^{(ik+\alpha) \cdot x}\right] \cdot e^{i\omega \cdot t},$$
(10)

where B and D – integration constants (complex amplitudes) determined by boundary conditions (7) and (8).

The functional values of coefficients α and k are determined in [1].

To determine integration constants B and D we substitute expression (10) into the boundary condition (8) and, after transforming, we find the relation between the complex amplitudes in the form:

$$B = -D \cdot \frac{e^{(ik+\alpha) \cdot H}}{e^{-(ik+\alpha) \cdot H}}.$$
(11)

Substituting the found value B from relation (11) into expression (10), we find a solution to Eq. (6) in the form:

$$u(x, t) = D\left[\frac{-e^{(ik+\alpha)\cdot(H-x)} + e^{-(ik+\alpha)\cdot(H-x)}}{e^{-(ik+\alpha)\cdot H}}\right]e^{i\omega\cdot t}. \quad (12)$$

Substitute expression (12) into the boundary condition (7). Based on (9) expression $Q\sin(\omega t)$ in boundary condition (7) can be represented as the imaginary part of a complex function, namely $Q\sin(\omega t) = Q \cdot e^{i\omega t}$. After the transformations, we get the following expression:

$$2D \cdot \left\{ sh[(ik + \alpha)H] \cdot \left(c_3 - m\omega^2 - i\frac{\omega^3\rho F}{E^2}\right) - \right.$$

$$\left. - ch[(ik + \alpha)H] \cdot (ik + \alpha) \cdot F \cdot \left(E_1 + i\omega\eta\left(\frac{E_1 + E_2}{E_2}\right)\right)\right\} = Q \cdot e^{-(ik+\alpha)H}. \quad (13)$$

Transforming expression (13), we determine the integration constant D in the following form:

$$D = \frac{Q \cdot e^{-(ik+\alpha)H}}{2sh[(ik + \alpha)H](c_3 + c_n - (m + m_n)\omega^2 + i\omega b_n)}, \quad (14)$$

where c_n – reduced coefficient of stiffness of compacted polymer concrete; m_n – reduced mass of compacted polymer concrete; b_n – reduced coefficient of dissipative resistance of compacted polymer concrete:

$$c_n = \frac{F\left[(E_1\alpha)sh(2\alpha H) + \left(E_1 k + \eta\omega\alpha\left(\frac{E_1+E_2}{E_2}\right)\right)\sin(2kH)\right]}{[ch(2\alpha H) - \cos(2kH)]}; \quad (15)$$

$$m_n = \frac{Fk\eta\left(\frac{E_1+E_2}{E_2}\right)sh(2\alpha H)}{\omega \cdot [ch(2\alpha H) - \cos(2kH)]}; \quad (16)$$

$$b_n = \frac{1}{\omega}\left[\frac{F\left[\left(E_1 k + \eta\omega\alpha\left(\frac{E_1+E_2}{E_2}\right)\right)sh(2\alpha H) - \left(E_1\alpha - \omega\eta k\left(\frac{E_1+E_2}{E_2}\right)\right)\sin(2kH)\right]}{[ch(2\alpha H) - \cos(2kH)]} - \frac{F\omega^3\rho}{E_2}\right]. \quad (17)$$

It follows from expressions (15) – (17) that numerical values of coefficients c_n, b_n and m_n will depend on the area of the supporting surface F of the vibrating plate; dynamic moduli of elastic deformation of polymer concrete E_1 and E_2; dynamic viscosity coefficient η; angular frequency of forced vibrations ω; the height of the compacted layer of polymer concrete H, vibration absorption coefficient α and wave number k. Substituting the value of integration constant D from (14) into expression (11), we determine integration constant B:

$$B = -\frac{Qe^{(ik+\alpha)H}}{2sh[(ik + \alpha)H](c_3 + c_n - (m + m_n)\omega^2 + i\omega b_n)}. \quad (18)$$

Substituting the found integration constants (14) and (18) into dependence (10), we find in the complex form the solution to the wave equation of vibrations (6), meeting the boundary conditions (7) and (8):

$$u(x, t) = \frac{Qsh[(ik + \alpha)(H - x)]e^{i\omega \cdot t}}{sh[(ik + \alpha)H](c_3 + c_n - (m + m_n)\omega^2 + i\omega b_n)}. \tag{19}$$

Multiply the numerator and denominator of expression (19) by a complex number $(c_3 + c_n - (m + m_n)\omega^2 - i\omega b_n)$, after performing the decomposition of expressions $sh[(ik + \alpha)(H - x)]$ in the numerator and $sh[(ik + \alpha)H]$ in the denominator, and, separating the imaginary part of the complex function from the obtained expression, we get a solution to the wave equation of oscillations (6) meeting the boundary conditions (7) and (8) in the following form:

$$u(x, t) = \frac{A}{\sqrt{(sh\alpha H \cos kH)^2 + (ch\alpha H \sin kH)^2}} \times [sh[\alpha(H - x)] \cos[k(H - x)] \sin(\omega t - \theta) +$$

$$+ ch[\alpha(H - x)] \sin[k(H - x)] \cos(\omega t - \theta)], \tag{20}$$

where A – amplitude of forced vibrations of the vibrating plate and the upper layer of polymer concrete:

$$A = \frac{Q}{\sqrt{[c_3 + c_n - (m + m_n)\omega^2]^2 + \omega^2 b_n^2}}; \tag{21}$$

$$\theta = \phi_1 + \phi_2; \tag{22}$$

$$\phi_1 = arctg\left(\frac{\omega \cdot b_n}{c_3 + c_n - (m + m_n)\omega^2}\right); \tag{23}$$

$$\phi_2 = arctg(cth(\alpha H) \cdot tg(kH)). \tag{24}$$

Expression (19) describes the law of motion of the polymer concrete compacted by a vibrating plate of the researched dynamic system "vibrating plate - polymer concrete" in the direction of the coordinate x depending on the angular frequency of forced vibrations ω, the amplitude of the disturbing force Q, thickness of the compacted layer H and the current time value t.

At $x = 0$ expression (19) describes the law of motion of the vibrating plate of the surface vibrating working body in the form:

$$u(0, t) = A \cdot \sin(\omega t - \phi_1). \tag{25}$$

Taking into account the physical and mechanical characteristics of the compacted polymer concrete makes it possible to quite accurately determine the law of motion of the vibrating plate and select the modes of vibration action, which ensure the most effective compaction of polymer concrete. The obtained expressions (15)-(17) enable the determination of the physical and mechanical characteristics of polymer concrete in its model representation, which can be used in the research of complex dynamic systems.

Specific reduced weight m_{ny}, as well as specific reduced coefficients of resistance b_{ny} and rigidity c_{ny} of polymer concrete at vibrations of the movable frame of the vibrating platform in the vertical direction is determined by dividing m_{ny}, b_n and c_n by the area F of the base of the molded product:

$$m_{ny} = m_n/F; \ b_{ny} = b_n/F; \ C_{ny} = C_n/F. \tag{26}$$

3 Experimental Research

The theoretical provisions were tested on a laboratory vibrating working body with the following main parameters: the mass of the vibrating plate $m = 75$ kg; disturbing force amplitude $Q = 4415$ N; forced angular frequency $\omega = 293$ rad/s; stiffness of elastic shock absorbers $c_3 = 470880$ N/m; amplitude of vibrations of the movable frame of the vibrating plate in idle mode $A_{x.x} = 0.68$ mm. This vibrating working body was used to compact polymer concrete in a mold being a size in plan 0.2×0.4 m^2, of the following structural composition [14]: crushed granite fraction 5–20 (50% of the total volume of the mixture), river sand with a fineness module $M_k = 1.8$ (22–27%); marshal with fraction 0.05 mm (10–15%); polyester resin Filabond 2000 PA (5%); hardener MEKP-HA-2 (0,5…1%).

Height H of the compacted layer was taken equal to 50, 60, 80, 100, 120 and 150 mm.

Figures 2 and 3 show the change in the coefficients of specific reduced stiffness c_{ny} and dissipative resistance b_{ny} of polymer concrete with vertical vibrations of a vibrating plate depending on the relative density ε and the height of the compacted layer H.
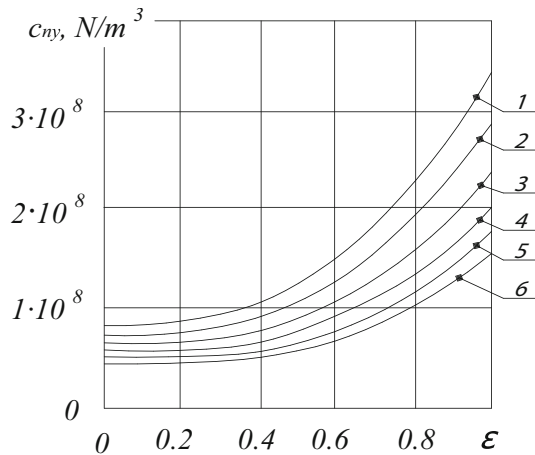
Fig. 2. Change in the specific reduced stiffness coefficient c_{ny} of polymer concrete depending on the relative density ε and the height of the compacted layer H: 1 – at $H = 50$ mm; 2 – at $H = 60$ mm; 3 – at $H = 80$ mm; 4 – at $H = 100$ mm; 5 – at $H = 120$ mm; 6 – at $H = 150$ mm

The analysis of the obtained data reveals that the specific reduced stiffness coefficients significantly depend on the height of the compacted layer H and relative density
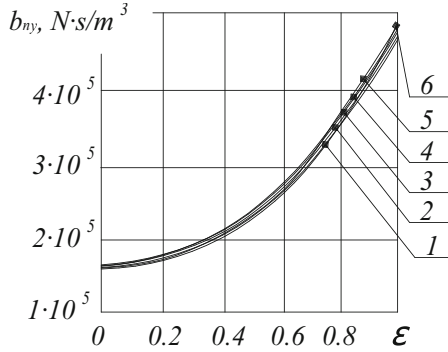
Fig. 3. Change in the specific reduced coefficient of dissipative resistance b_{ny} of polymer concrete depending on the relative density ε and the height of the compacted layer H: 1 – at $H = 50$ mm; 2 – at $H = 60$ mm; 3 – at $H = 80$ mm; 4 – at $H = 100$ mm; 5 – at $H = 120$ mm; 6 – at $H = 150$ mm.

ε of the polymer concrete. In this case, the specific reduced coefficient of dissipative resistance b_{ny} at surface compaction significantly depends on the relative density ε of polymer concrete and to a lesser extent depends on the height of the compacted layer H.

Figure 4 shows the change in the vibration amplitude of the vibrating plate A depending on the relative density ε and the height of the compacted layer H.

Curves in Fig. 4 show that the physical and mechanical characteristics of polymer concrete and the height of the compacted layer H have a significant effect on the vibration amplitude A of the vibrating plate.
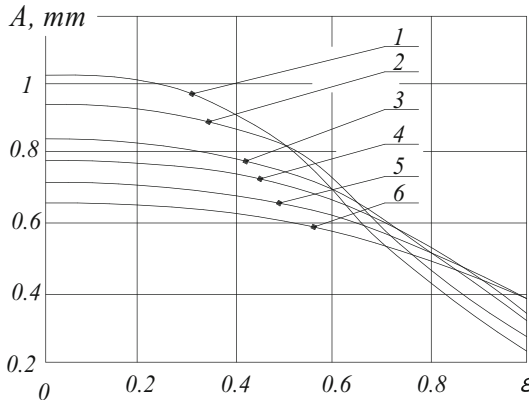
Fig. 4. Change in vibration amplitude A of vibrating plate depending on the relative density ε and the height of the compacted layer H: 1 – at $H = 50$ mm; 2 – at $H = 60$ mm; 3 – at $H = 80$ mm; 4 – at $H = 100$ mm; 5 – at $H = 120$ mm; 6 – at $H = 150$ mm.

With an increase in the thickness of the compacted layer H from 50 to 150 mm and relative density ε of polymer concrete, the vibration amplitude of the vibrating plate decreases.

At the very beginning of the vibration compaction process with the values of the layer heights H 50 and 60 mm and relative density ε from 0 to 0.5 there is a decrease in the vibration amplitude A of the vibrating plate, respectively, from 1.01 to 0.82 mm and from 0.93 to 0.82 mm. With a further increase in the relative density ε from 0.5 to 1 there is a significant decrease in the vibration amplitude A of the vibrating plate, respectively, to 0.23 and 0.27 mm.

During vibration compaction of polymer concrete of the specified composition with a layer thickness of 80, 100, 120 and 150 mm at a relative density ε from 0 to 0.5, a smoother decrease in the vibration amplitude of the vibration plate occurs. For the specified values ε the vibration amplitude changes from 0.83 to 0.76 mm at thickness $H = 80$ mm; from 0.77 to 0.71 mm – at $H = 100$ mm; from 0.72 to 0.67 mm at $H = 120$ mm and from 0.66 to 0.62 mm at $H = 150$ mm. With a further increase in the relative density ε from 0.5 to 1 there is a significant decrease in the vibration amplitude A of the vibrating plate to 0.39… 0.33 mm.

The obtained results make it possible to conclude that at the very beginning of the vibration compaction process at a relative density ε from 0 to 0.5 vibrating plate works in vibration mode. When this operating mode is implemented, the vibrating plate does not detach from the surface of the compacted layer of polymer concrete.

With a further increase in the relative density ε from 0.5 to 1 the dynamic system goes into vibration-impact mode of operation, in which the vibrating plate breaks off from the surface of the compacted layer of polymer concrete and moves in the air until the next impact. In this case, it is advisable to further research the discrete vibroimpact mode of operation of the vibrating plate interacting with the compacted plate, represented by the found physical and mechanical characteristics.

Thus, based on the study of the propagation of deformation waves in compacted polymer concrete, presented in the form of a system with distributed parameters, theoretical expressions were obtained to determine the physical and mechanical characteristics of the compacted medium (polymer concrete): stiffness and dissipative resistance coefficients. These coefficients make it possible to accurately determine the main parameters of the vibrating working body for surface compaction of polymer concrete, take them into account in the expression to establish the law of motion and determine rational modes of vibration impact on polymer concrete, depending on the type of polymer concrete and its relative density, the height of the compacted layer, the vibration frequency and the amplitude of the disturbing force.

The described electric drive is practically applied to the vibrating press (Fig. 5). In this equipment, the electric drive includes two electromechanical vibrators mounted on a plate with a punch. They consist of electric motors with unbalances mounted on the ends of the rotor shafts, which rotate with the rotor shaft and create a disturbing force.

Polymer concrete samples were obtained on this press (Fig. 6).

Fig. 5. General view of the press with electric vibration drive

Fig. 6. Polymer concrete samples for presented structural composition [14]

4 Conclusion

A physical and mechanical model has been developed as a result of a theoretical research of the dynamic system "vibrating plate - polymer concrete". Polymer concrete is presented in it as a system with distributed parameters. The model enables rather accurate determination of elastic and dissipative forces acting from polymer concrete on vertical vibrating plate moving in the vertical plane. The law of motion of the vibrating plate of

the working body is established depending on the found physical and mechanical characteristics of the compacted polymer concrete, the angular frequency of forced vibrations and the thickness of the compacted layer. The obtained theoretical expressions make it possible to reasonably choose the rational parameters of the working body for surface vibration compaction of polymer concrete. The found results can be used in theoretical research on the analytical determination of the law of change in stresses arising in the compacted layer of polymer concrete, as well as in the analysis and synthesis of the obtained vibro-shock mode of operation of the vibrating plate.

References

1. Maslov, O., Savielov, D.: Theoretical definition of the law of motion for mobile frame of a vibrating platform with polymer concrete when compacting it. Trans. Kremenchuk Mykhailo Ostrohradskyi National University **4**, 84–90 (2020). https://doi.org/10.30929/1995-0519.2020.4.84-90

2. Maslov, O., Savielov, D.: Theoretical studies of the strain-deformed state of the compacted medium of the dynamic system "vibrating platform - polymer concrete." Trans. Kremenchuk Mykhailo Ostrohradskyi National Univ. **1**, 92–97 (2021). https://doi.org/10.30929/1995-0519.2021.1.92-97

3. Maslov, A.H., Savelov, D.V., Puzyr, R.: Investigation of the interaction of the movable frame of a vibrating platform with polymer concrete in its model representation. «Building innovations-2020» - Collection of scientific papers based on the materials of the III International Azerbaijani-Ukrainian conference scientific and practical conference June 1–2 2020. - Baku-Poltava, 2020. - pp. 127–130 (2020)

4. Maslov, O., Savielov, D., Salenko, Y., Javadova, M.: Theoretical Study of the Dynamic System «Vibration Platform − Polymer Concrete» Stress–Strain State. In: Onyshchenko, V., Mammadova, G., Sivitska, S., Gasimov, A. (eds.) Proceedings of the 3rd International Conference on Building Innovations: ICBI 2020, pp. 191–201. Springer International Publishing, Cham (2022). https://doi.org/10.1007/978-3-030-85043-2_19

5. Savielov, D.: Development of interaction surface selective working body with polymer concrete during its modeling theory. Trans. Kremenchuk Mykhailo Ostrohradskyi National Univ. **6**, 126–132 (2019). https://doi.org/10.30929/1995-0519.2019.6.126-132

6. Juradin, S., Baloević, G., Harapin, A.: Impact of vibrations on the final characteristics of normal and self-compacting concrete. J. Mater. Res. **17**(1), 178–185 (2014)

7. Sudarshan, N.M., Chandrashekar Rao, T.: Vibration Impact on Fresh Concrete of Conventional and UHPFRC. International Journal of Applied Engineering Research. 2017, Vol. 12, 8thedn, pp. 1683–1690 (2017)

8. Koh, H.B., Yeoh, D., Shahidan, S.: Effect of revibration on the compressive strength and surface hardness of concrete. IOP Conf. Series: Materials Sci. Eng. **271**, 012057, 1–6 (2017)

9. Gutierrez, J., Ruiz, E., Trochu, F.: High-frequency vibrations on the compaction of dry fibrous reinforcements. J. Adv. Compos. Materials. **22**(1), 13–27 (2013)

10. Maslov, A., Savielov, D.: Rheological model of polymer concrete that vibrates. Trans. Kremenchuk Mykhailo Ostrohradskyi National Univ. **5**, 135–141 (2019). https://doi.org/10.30929/1995-0519.2019.5.135-141

11. Bobryshev, A.N., Voronov, P.V., Galimov, E.R., Lakhno, A.V., Abdullin, I.A.: Kinetic models of stress relaxation in composites. Bull. Technol. Univ.17/2014 (14). P. 431–434 (2014)

12. Bogomolov, V., Zhdanyuk, V.A., Tsynka, P.G.: Viscoelastic structural model of asphalt concrete. Автомобильный транспорт, 2016. Вып. 2016. P. 117–123 (2016)

13. Haikova, T., Puzyr, R., Savelov, D., Dragobetsky, V., Argat, R., Sivak, R.: The Research of the Morphology and Mechanical Characteristics of Electric Bimetallic Contacts. In: Conference 2020, PAEP, pp. 579–582, IEEE, Kremenchuk, Ukraine (2020) https://doi.org/10.1109/PAEP49887.2020.9240847

14. Maslov, A., Savielov, D.: Development of structural composition of polymer concrete. Trans. Kremenchuk Mykhailo Ostrohradskyi National Univ. **4**, 94–99 (2018). https://doi.org/10.30929/1995-0519.2018.4.94-99

The Scheme for Optimizing the Liquid Radioactive Waste Management of Ukrainian NPPs

Yuriy Olkhovyk(✉)

National Aviation University, Kyiv, Ukraine
yolkhovik@gmail.com

Abstract. The optimal scheme of the hypothetical package acceptable for the disposal of salt melt without its processing are considered in detail. It is noted that the main protective barrier during package disposal in a near-surface disposal facility will be a geocement matrix, which can be considered as a promising environment for the immobilization of the liquid salt concentrate or spent filter materials.

It is concluded that the use of an insulating geocement barrier is the main condition for forming the package for safe and environmentally friendly disposal of salt melt in near-surface disposal facilities.

The given scheme does not require the creation of new equipment at the NPP sites.

Keywords: Salt melt · Still bottoms · Geocement matrix · Container · Near-surface disposal facility

1 Introduction

The production of electricity at nuclear power plants is based on the transformation of nuclear fuel fission energy first into heat and then into electrical energy, which requires a huge amount of water. Large volumes of water are also used in the processes of storing nuclear fuel in holding pools, during washing of ion-exchange filters, decontamination of plant equipment and premises, washing of work clothes, etc. Each source generates a corresponding volume of liquid radioactive waste with a specific chemical and radionuclide composition. According to the author's assessment, the production of 1 MWh of electricity at a Ukrainian nuclear power plant with WWER reactors forms 1.5 m^3 of homogeneous weakly active aqueous solutions with a low salt content. The indicated radioactively contaminated environments are collected by the special sewage system and sent for processing to special water treatment facilities. The construction projects of the operating power units of the Ukrainian nuclear power plants did not include the construction of facilities for the deep processing of LRW with the obtaining of a processing product whose characteristics meet the criteria of acceptance for final disposal.

2 Presentation of the Main Research Material

At the nuclear power plants of Ukraine, after appropriate processing by evaporation the so-called still bottoms (SB)—a liquid concentrate of salts—is formed. According to the chemical composition, SB is a multicomponent system, the composition of which is determined by the presence of soluble salts ($NaNO_3$, Na_2CO_3, $NaBO_2$, sodium phosphates and oxalates), suspensions (manganese hydroxides, iron and insoluble oxalates and phosphates), organic substances (detergents and complexones). The average salt content of SB stored in NPP storages is 300–400 g/dm^3.

The performed analysis of the specific generation of radioactive waste showed that the further operation of power units with WWER reactors will lead to a sufficiently stable level of formation of liquid radioactive waste, which provides grounds for forecasting the volumes of their accumulation and the implementation of appropriate measures for their conditioning with subsequent transfer to disposal [1].

As a result of the ultimate simplification of the LRW management schemes at NPPs of Ukraine included in the project, the decision was implemented that the SB is processed in deep evaporation units, forming an even more concentrated product – salt melt (SM), which solidifies to a solid state during the cooling process. It should be emphasized that currently the tanks for the storage liquid radioactive waste and storages for SM at the nuclear power plants of Ukraine are 70–95% full [2].

Currently, changes have been made regarding the classification of SM and its classification as solid radioactive waste.

The decision to assign SM to solid radioactive waste provides grounds for abandoning the use of sorption cleaning technologies for highly mineralized liquid medium with a complex chemical composition, which is the still bottoms. It is known that the multicomponent composition of organic substances present in trapped waters and, accordingly, concentrated in the still bottoms, negatively affects the efficiency of sorption processes used to clean LRW from radioactive cations. Therefore, the implementation of sorption technologies requires preliminary treatment of liquid RAW, which includes oxidation, filtration of sediment formed during oxidation and subsequent selective purification from radiocesium by ferrocyanide sorbents and from ^{90}Sr by sorbents based on manganese hydroxide. The existing experience of using sorption technologies on an industrial scale (Paksh NPP, Hungary; Kola NPP, Russian Federation) shows that the used technological equipment has a rather low productivity, high cost and, accordingly, requires significant financial costs [3].

The above makes it possible to consider it as the most likely and economically feasible option for conditioning SB by means of deep evaporation with the formation of SM. In this case, the management of SM will require the fulfillment of special conditions during disposal. Such a condition that will ensure the isolation of radionuclides from the environment for 500–600 years can be the formation of RW packaging in the universal protective reinforced concrete container UZZK TU У 29.2–26444970–005, intended for the transportation and disposal of low- and medium-level RW in near-surface storage facilities, with by placing KRO-200 containers with salt melt in it.

The internal volume of the UZZK is 2.25 m^3, which allows to accommodate four KRO-200 containers with SM with a total volume of 800 l and 1.45 m^3 of slag-alkaline

cement compound. Assuming a density of cemented RW of 2.2 t/m^3, it is calculated that 800 kg of salts can be placed in the UZZK container [4].

Thus, the classification of SM as solid radioactive waste provides grounds for the creation of a simple, reliable and economically acceptable technology for processing the main mass of LRW of nuclear power plants with WWER reactors into a safe form suitable for disposal. According to the author, this scheme should provide for:

• transfer of all currently accumulated and future SB to SM using deep evaporation units available at the NPP;
• packaging of SM in certified KRO-200 containers;
• placement of filled KRO-200 containers in universal protective reinforced concrete containers UZZK TU U 29.2–26444970-005, intended for transportation and disposal of low- and medium-level radioactive waste in near-surface storage facilities;
• filling the voids of the container with a slag-alkaline compound, which acts as an additional engineering barrier, which will ensure the stability of the package and the isolation of radionuclides from the environment for 500–600 years;
• in addition, the slag-alkaline compound can be used as a stable matrix for the immobilization of spent filter materials (SMF) accumulated in nuclear power plant storages. This makes it possible to simultaneously disposal in one package of SM and SMF;
• temporary storage of radioactive waste packages at the NPP site until transportation for disposal in the storage facilities of the Central Enterprise for the Processing of Radioactive Waste. (Fig. 1)
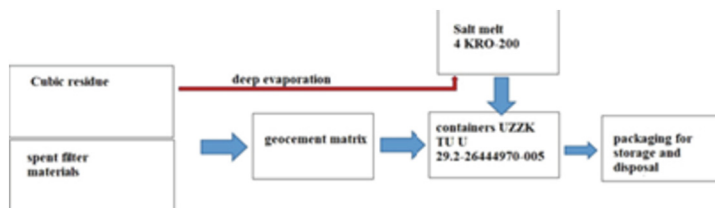
Fig. 1. The scheme for optimizing the management of liquid radioactive waste of the NPP of Ukraine.

The given scheme does not require the creation of new equipment at the NPP sites, as deep evaporation installations are currently implemented at all stations, the production of containers is ensured by the production capacities of SE "NAEK" "Energoatom", the cementing installation is implemented as part of the solid RW processing complex at the Rivne NPP. However, there is a problem of transporting a heavy 15-ton reinforced concrete container of UZZK in the production premises of the special buildings of the nuclear power plant.

The created packaging will be quite acceptable from the point of view of radiation-protective properties even if "fresh" salt water with a noticeable content (up to 20% of the total activity) of radionuclide ^{60}Co is placed in the KRO–200 containers [5].

Undoubtedly, the creation of a liquid radioactive waste conditioning system will be associated with significant financial costs - because for the placement of more than

50,000 currently accumulated containers of the KRO–200 type, 18,000 UZZK reinforced concrete containers with a total cost of approximately \$18 million will be needed, and during the operation of power units with WWER reactors the volume of SM in the NPP storages will only increase. SM is the main factor that determines the further choice of development and implementation of RW conditioning technologies and, accordingly, the amount of expenses of the operator of reactor installations both for the purchase and operation of equipment, and for the logistics of transporting RW packages to storage facilities for disposal.

An urgent task is to carry out a technical and economic analysis to determine the optimal composition of a hypothetical safe package, namely: what is more appropriate - immobilization of the accumulated SB in geopolymer or deep evaporation of the entire salt solution with subsequent disposal in the form of SM. The main factor that will determine the priority of the technology for implementation at the NPP should be the economic assessment of the cost of the complex of measures for conditioning and logistics of packages from RW to storage facilities in the exclusion zone. The requirements to minimize the volumes of conditioned RW, which must be accepted for disposal by the repository operator, have no logical connection with the current system of taxation for the generation of RW at NPPs.

3 Conclusions

The above-mentioned scheme for conditioning liquid raw materials of NPPs of Ukraine without a doubt should receive a technical and economic justification, taking into account the prospects for the development of nuclear energy in Ukraine, the extension of the operating terms of existing units, the creation of new units and the introduction of small modular reactors.

References

1. Olkhovyk, Y.: Salt melt as a determining factor in the conditioning system development of liquid radioactive waste of NPPs in Ukraine. Nuclear Power Environ. **2**(24), 37–42 (2022)
2. Management of radioactive waste during the operation of NPP of NNEGC "Energoatom" (as of 31.12.2019). www.energoatom.com.ua/uploads/2020/%D0%98%D0%BB%D0%BB.% 20%D0%BE%D1%82%D1%87%D0%B5%D1%82_2019.pdf. (in Ukr.)
3. Olkhovyk, Y.: Perspective schemes of conditioning of liquid radioactive waste of Ukrainian nuclear power plants. Nuclear Power Environ. No **3**(18), 48–56 (2020)
4. Olkhovyk, Y., Fedorenko, Y., Rozko, A., Rudychev, Y.: Regarding the properties of package 1for disposal of salt melt from Ukrainian NPPs with WWER reactors in near-surface disposal facilities. Nuclear Radiation Safety **2**(90), 65–73 (2021)
5. Rudychev, Y., Olkhovyk, Y.: Radiation and protective properties of containers for NPPs' salt melt conditioning in Ukraine. Geochem. Technogenesis **5**, 100–104 (2021)

Trends of Development of Combined Steel Trusses of the New Generation

Oleksandr Shimanovsky[1] , Myron Hohol[2](✉) , Igor Melnyk[2] ,
and Dmytro Sydorak[2]

[1] Ltd«UkrinstalkonV.M.Szymanowski», V.Szymanowski Str. 2/1, Kyiv, Ukraine
[2] Lviv Polytechnic National University, S. Bandera Str. 12, Lviv 79013, Ukraine
gogolmyron@i.ua

Abstract. New rational combined trusses of covering systems with spans of 12–30 m with smaller dimensions and material capacity in comparison with existing analogues are proposed. A review of works in improving structural forms of steel trusses was made. General approaches to the development of a new generation of steel trusses are shown. Such designs allow to save 17–32% from the cost of their production. The actual task of selection of the main parameters (regulation of stress strain state) of the combined truss, the solution of which allows finding the optimal structural solution with minimal weight is considered. The indicated result was achieved by the usage of high-strength steels and new design forms. Schemes of the developed ones constructions are presented. The use of high-strength reinforcement is proposed for stretched truss elements. A model of the truss with a span of 30 m with such elements for stress-testing has been designed. Ways of saving material in structures are given. Among such methods the development low-element structures is presented, as well as the use of modern ones calculation methods.

Keywords: combined truss · rational truss · stress strain state · regulation · low-element truss · stiffness girder

1 Introduction

One of the effective ways of increasing the technical level of construction or constructions, including combined steel trusses, is a development of new designing forms, improvement of their calculations and design methods. Accumulated experience in the use of rational steel structures revealed their indisputable advantages, which are manifested to a special extent in combined structures (girder, sprengel, truss, hanging and wire ropes), which are calculated using the calculation method regulation [19]. This method will allow to obtain a structure of equal strength when designing construction structures, that is, the most rational system [6]. Combined steel structures are progressive designing forms that have been dynamically developing in recent times, both in the our country and abroad [12, 17].

Fig. 1. Combined steel truss with a span of 30 m [17]

2 Analysis of Basic Research and Publications

In order to improve steel truss structures, various researchers are currently developing and proposing their structural optimization [1, 18, 20]. However, the iterative approach in structural optimization in which sequential linear programming is used to simultaneously solve the size and section type optimization sub problems subject to normative constraints is not always rational. This leads to a huge but linear programming problem. The proposed method produces optimized structures that only are close to the solutions obtained using the nonlinear formulation of the problem.

Optimization problems with highly nonlinear formulations of truss structures with global stability constraints are too difficult for engineering use [8, 16, 21].

The analysis of works on the design of combined steel structures with calculated adjustment of forces in them showed that the problem of finding a system of minimum weight with a rational distribution of internal forces has been most fully investigated to date [6, 7, 9, 13]. However, rational design provides only one, not necessarily the smallest value [10, 15].

At present, a calculation method for adjusting the stress strain state (SSS) in combined steel structures has been developed, which allows not only to determine the rational topology and stiffness characteristics of the cross sections of the structural elements, but also to adjust the distribution of forces in the stiffness girder in such a way that their limit values are reached simultaneously in more than one, and in many cross-sections, that is, to get a rational design [11, 12].

Therefore, the problem of the development of new-generation combined steel trusses with consideration of the redistribution of internal tension when changing their parameters, in accordance with regulatory documents in design and construction, requires further research.
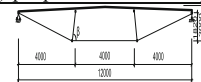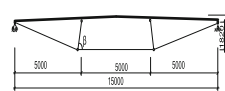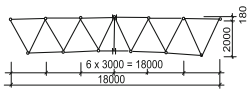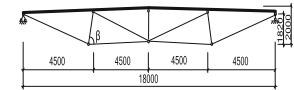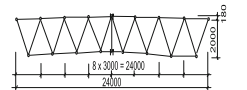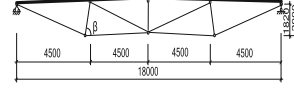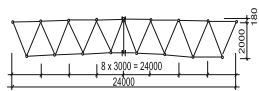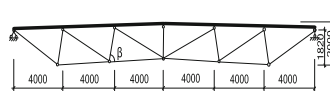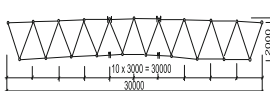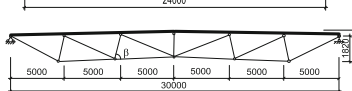
3   Presentation of the Main Research Material

We have developed new rational combined designing forms of roof systems, with smaller dimensions and material consumption in comparison with existing analogues (Table 1, b).

Combined steel structures [6, 19] with designing forms adapted to their actual SSS due to calculated adjustment, rational design can achieve 17–32% lower cost and material consumption compared to typical ones. But at present, there is no clear program for their development and improvement in order to significantly increase their effectiveness.

At the same time, with such a wide application of combined steel systems, the problem of their rational design, calculated regulation of internal stresses in them is not sufficiently covered in the special literature, and the existing experience of its solution is not sufficiently generalized.

**Table 1.** Schemes of rational combined trusses for spans of 12–30 m

The main tasks of scientific and technical progress in the field of steel structures are saving steel, using high-quality steels and profiles, increasing productivity and efficiency [15, 19]. There are several ways to steel saving.

First, the wider use of high-strength steels for stretched elements out of typical sections, which are in short supply in wartime conditions, with their replacement by less scarce and more effective reinforcing bars A300C, A400C, etc. [2, 4, 5]. For example, typical steel trusses are replaced by combined steel trusses with stretched diagonals of class A400C (Fig. 1). This provides low number of elements in trusses. More rational

methods of increasing the efficiency of steel combined systems, using such important features as low-element, minimum number of nodes and weight.

For example, for a truss with a span of 30 m, with a set topology (Fig. 2), the truss consists of six panels, which made it possible to reduce the number of elements in the truss by 38% compared to a typical design (Table 1, a).
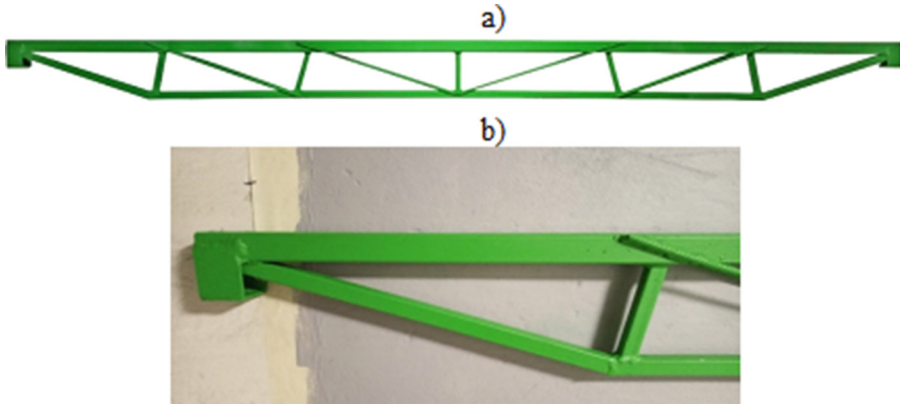

Fig. 2. A model of a combined truss with a span of 30 m with rational parameters and stretched elements from reinforcement rods of the A400C class: a) model; b) node

Secondly, the development of new low-element structural forms and with a concentration of material in the upper chord (stiffness girder), the weight of which is about 60–80% of the structure weight, as well as their design with low-elements (Table 1, b). That is, the implementation of the principle of material concentration in the main supporting systems системах [6]. A numerical experiment was also conducted to find a rational weight ratio of the stiffness girder of the combined truss to the total weight of the truss. The minimum weight of trusses is accepted as a fully stress design criterion. The calculation of models of combined trusses was carried out in the software environment "LIRA-CAD 2016 R5" for a load of $q = 12.75$ kN/m, with a rational angle of inclination of the compressed bars of the grid of the combined truss equal to 800. The models of combined trusses had a span of 3.0 m and a height of 0.2 m (Fig. 3) was calculated at different ratios (in percentages) of the weight of the stiffness girder of the combined truss to the total weight of the truss, equal to: 40%; 50%; 60% and 70%. Based on the results of the calculations, a graph of the truss weight dependence on the ratio of the weight of the stiffening girder to the truss weight was constructed (Fig. 3).

So, according to the results of a numerical experiment for truss models with a span of 3 m for $q = 12.75$ kN/m, the minimum weight of the combined truss was at a ratio of the weight of the stiffening girder to the weight of the truss of about 50% (Fig. 3). So, a 50% ratio is rational for different heights and spans of combined trusses.

Thirdly, minimize the difference between the building and functional space while meeting the regulatory design conditions for ensuring the technological process by using the minimum height of the load-carrying structures to. According to the DSTU [2], the rational and minimum height of steel rafter trusses made of bent-welded profiles of
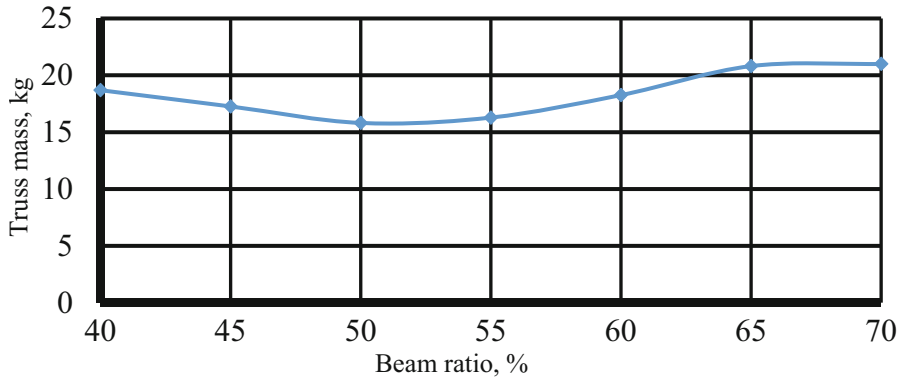
Fig. 3. Graph of the dependence of the weight of the combined truss on the percentage of the weight of the stiffening girder

rectangular cross-section spans of 18–30 m is 2 m, therefore the height of combined steel trusses is taken to be of a similar height (Table 1, a, b).

Fourthly, the saving of steel is achieved by using the scientifically based expediency of the calculation method of regulating the stress-strain state (SSS) of combined steel structures [6, 10, 14, 19]. To ensure the main task in the design of combined building structures, which the engineer faces, is obtaining a uniformly strong structure, that is, the most rational system. At the same time, the main fully stress design criterion can be formulated as follows: the formation of a combined steel structure will be rational only when this structure will have the lowest cost "in practice" of all possible forms of known structures for the same load and span and ensuring the required strength and rigidity of the structures.

Having obtained a rational structural form of a combined steel truss with geometric parameters, they have not yet achieved it according to the fully stress design criterion - the equality of stresses in all characteristic cross-sections in the stiffness girder.

Therefore, for this purpose, the calculation method of adjusting the SSS of the stiffness girder using optimal design is recommended.

The main method (first) of calculated adjustment of SSS in the girder of a rigid-rational combined truss is the creation of support moments on the extreme supports, which are opposite to the action of the external load (Fig. 4). The variable parameter is the value of the calculated eccentricity for creating a reference moment.

In order to check the efficiency and search for rational values of eccentricity, studies of such a regulation method were conducted. The results showed that for a given design, the rational eccentricity is equal to half the height of the upper chord. Accordingly, this value of eccentricity was also adopted for the pilot sample of the scale model.

The second method is a variable parameter - changing the cross-sections of braces and diagonals and the lower chord (a rational ratio of the weight of the stiffness girder to the whole truss weight −50%). Rational selection of cross-sections of middle braces, made it possible to actually balance the bending moment on the second intermediate support and in central spans.
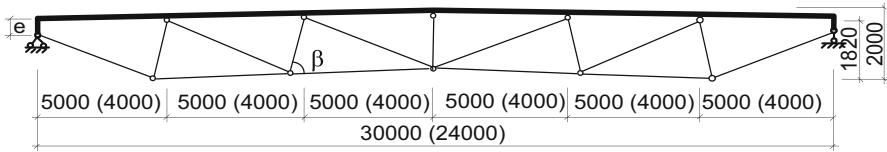
Fig. 4. Scheme for adjusting the SSS by the supporting eccentricity e

The third method is the special application of eccentricity in the junctions of the suspension system to the stiffness girder (Fig. 5). The variable parameter is the eccentricity value.
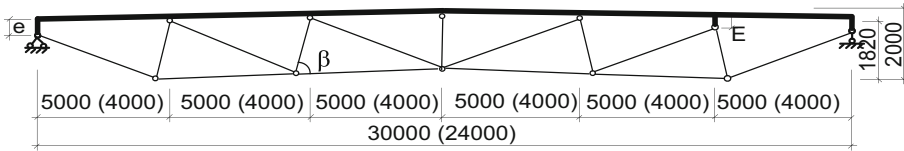
Fig. 5. Nodal eccentricity E (shown on the example of one node)

Fifth, steel savings are obtained as a result of the improvement of engineering calculations of the load-carrying capacity of combined systems based on the energy variation principle (Lagrange's principle), the development of new provisions for the design of rational combined steel structures. In order to provide the process of rational design of combined steel structures with the necessary scientific validity and to minimize the element of subjectivity when choosing design solutions, it is necessary to define the main methodological principles of such design and its sequence.

Sixth, the results of the research will open wide opportunities for purposeful design of rational combined steel structures, also will allow to make comprehensively justified decisions, which will ensure better design and implementation of competitive solutions, wider use in buildings and structures, which will cause a general economic effect. The developed technical solutions of new generation combined steel trusses are competitive in terms of steel consumption, economical in terms of energy consumption, and technological in manufacturing.

4　Conclusions and Prospects

New rational structural combined trusses are proposed and developed roof systems with spans of 12–30 m, with smaller dimensions and material consumption compared to typical existing analogues. The methods of use are shown high-strength reinforcement in stretched elements of combined trusses. Designed a model of a rational combined truss with a span of 30 m with stress strain state (SSS) regulation by such elements. Calculation methods are given regulation of SSS in the stiffness girder of a rational combined truss that allows to achieve equality of stresses in all characteristic sections in the stiffness girder. In order to increase productivity and efficiency, provision savings of steel in steel

combined trusses, use of high-quality six steels and profiles in steel combined structures are proposed ways of solving them. This will increase their cost competitiveness of steel, will provide energy savings and make technological manufacturing.

References

1. Brüttinga, J., Desruellea, J., Senatoreb, G., Corentin, F.C.: Design of truss structures through reuse. Structures **18**, 128–137 (2019). https://doi.org/10.1016/J.ISTRUC.2018.11.006
2. DBN B.2.6-198: 2014. Steel structures. Design standards. - Kyiv: Ministry of Regional Development of Ukraine (2014)
3. DSTU B B.2.6-74: 2008. Constructions of houses and buildings. Trusses steel truss from bent-welded profiles of rectangular section. Kyiv (2009)
4. DSTU 3760:2019. Rolled products for reinforcement of ferroconcrete structures. General specification. . Kyiv (2019)
5. EN1993–1–8. "Eurocode 3: Design of Steel Structures. Part 1-8: Design of joints". CEN (2005)
6. Gogol. M.: Stress regulation in steel combined structures: Monograph. Steel, Kyiv (2018)
7. Gogol, M., Zygun, A., Maksiuta, N.: New effective combined steel structures. Int. J. Eng. Technol. **3.2**(7), 343–348 (2018). https://doi.org/10.14419/ijet.v7i3.2.14432
8. Giger, M., Ermanni, P.: Evolutionary truss topology optimization using a graph-based parameterization concept. Struct. Multidiscip. Optim. Multidiscip. Optim. **32**, 313–326 (2006). https://doi.org/10.1007/s00158-006-0028-8
9. Gogol, M., Kropyvnytska, T., Galinska, T., Hajiyev, M.: Ways to improve the combined steel structures of coatings. In: Onyshchenko, V., Mammadova, G., Sivitska, S., Gasimov, A. (eds.) ICBI 2019. LNCE, vol. 73, pp. 53–58. Springer, Cham (2020). https://doi.org/10.1007/978-3-030-42939-3_6
10. He, L., Gilbert, M.: Rationalization of trusses generated via layout optimization. Struct. Multidiscip. Optim.. Multidiscip. Optim. **52**(4), 677–694 (2015). https://doi.org/10.1007/s00158-015-1260-x
11. Hohol, M., Gasii, G., Pents, V., Sydorak, D.: Structural—parametric synthesis of steel combined trusses. In: Onyshchenko, V., Mammadova, G., Sivitska, S., Gasimov, A. (eds.) Proceedings of the 3rd International Conference on Building Innovations: ICBI 2020, pp. 163–171. Springer International Publishing, Cham (2022). https://doi.org/10.1007/978-3-030-85043-2_16
12. Hohol, M., Marushchak, U., Peleshko, I., Sydorak, D.: Rationalization of the topology of steel combined truss. In: Bieliatynskyi, A., Breskich, V. (eds.) Safety in Aviation and Space Technologies. LNME, pp. 97–106. Springer, Cham (2022). https://doi.org/10.1007/978-3-030-85057-9_9
13. Lavrinenko, L., Zotina, A.: Effective parameters of low-element sprung trusses with the use of I-beams with corrugated walls. Build. Struct. Theo. Pract. **4**, 56–69 (2019). https://doi.org/10.32347/2522-4182.4.2019.56-59.
14. Pichugin, S.F., Semko, O.V., Trusov. G.M.: Modern problems of designing steel load-bearing structures in industrial and civil construction. Mod. Ind. Civil Construct. **1**(1), 53–66 (2005). (in Ukrainian)
15. Pichugin, S.: Reliability estimation of industrial building structures. Mag. Civil Eng. **83**(7), 24–37 (2018). https://doi.org/10.18720/MCE.83.3.
16. Rojíˇcek, J., et al: Optimization of a truss structure used to design of the manipulator arm from a set of components. Appl. Sci. **2021**(11), 10193 (2021). https://doi.org/10.3390/app112110193

17. Saito, M.: Conceptual design of hybrid string structures. In: SEWC2011, Italy (2011)
18. Schwarz, J., Chen, T., Shea, K., Stanković, T.: Efficient size and shape optimization of truss structures subject to stress and local buckling constraints using sequential linear programming. Struct. Multi. Optim. **58**(1), 171–184 (2018). https://doi.org/10.1007/s00158-017-1885-z
19. Shymanovskiy, O.V. Optimization of spatial combined systems. Edited by OV Shimanovsky/OV Shimanovsky, VK Tsykhanovsky, SM Talakh. - Kyiv, Steel, 462 p. (2012)
20. Sokół. T., Rozvany, G.I.N.: On the adaptive ground structure approach for multi-load truss topology optimization. In: 10th World Congresses of Structural and Multidisciplinary Optimization. 5428 (2013). https://repo.pw.edu.pl/info/article/WUTe50f5bda57024d8fae8dff9f48ba9f53/
21. Weldeyesus, A.G., Gondzio, J., He, L., et al.: Truss geometry and topology optimization with global stability constraints. Struct. Multidisc. Optim. **62**, 1721–1737 (2020). https://doi.org/10.1007/s00158-020-02634-z

Reconstruction of Reinforced Concrete Pylons and Reinforcement with Metal Cages After Damage Caused by Military Operations

Oleh Tabarkevych[1] , Oleksandr Lapenko[1]([envelope]) , Svitlana Skrebneva[1] ,
and Oleksandr Nyzhnyk[2]

[1] National Aviation University, Kyiv, Ukraine
`my-partner@ukr.net`
[2] O.M. Beketov, Kharkiv National University of Urban Economy, Kharkiv, Ukraine

Abstract. An example of the restoration of a reinforced concrete pylon of a multi-storey residential building that was damaged as a result of military operations is presented. The photos of the pylon before and after reconstruction are presented, the drawings of the pylon after reconstruction with reinforcement are shown.

Keywords: Reconstruction · Reinforced concrete · Pylon · Metal clips

1 Introduction

Reconstruction of buildings and structures is a set of repair and construction works related to the re-arrangement of a building, structure or the entire facility in order to increase its capacity, comfort, etc. Reconstruction involves the dismantling of individual parts of structures and the construction of new ones. In other words, the reconstruction of a building includes the assessment of its condition and the implementation of a set of repair and construction works aimed at re-arranging or recreating individual structures or the entire structure in order to improve or change its functional purpose and extend its further operation. The reconstruction of a building or structure requires a range of activities, from planning to construction works. This procedure can be applied to industrial and commercial properties, as well as residential premises.

Reinforcing reinforced concrete structures is more labour-intensive than metal structures. This is due to the fact that reinforced concrete is a composite material in which steel reinforcement works in conjunction with concrete.

2 Aim and Objectives

The aim of the work is to ensure further reliable operation of a reinforced concrete pylon with a metal cage after its restoration as a result of military operations.

To achieve this goal, the following tasks were defined:

– detailed inspection and assessment of the technical condition of the reinforced concrete pylon;
– determination of the geometric parameters of the reinforced concrete pylon, calculation of the selection of the most optimal cross-section of the metal elements of the cage;
– development of a working drawing with selected cross-sections of metal elements for the cage;
– implementation of ready-made solutions for the restoration and reinforcement of the reinforced concrete pylon.

3   Presentation of the Main Material.

The procedure for restoring reinforced concrete structures includes several stages of work.

At the first stage, it is necessary to determine the extent of the damage, if the damage is not significant, i.e. the protective layer of concrete is damaged, or there are vertical or horizontal cracks on the pylon, it is possible to perform works on plastering the pylon along the wall in case of damage to the protective layer of concrete, and repairing cracks by injection. If the damage is destructive, it is necessary to consider restoring the concrete of the pylon and installing a metal casing. The casing can be metal or reinforced concrete. These cages reinforce the existing structure by taking compressive loads both directly and by restraining transverse deformations. Indirect reinforcement, such as with spiral reinforcement, only reduces the transverse deformation of the concrete. Due to their low compressive stiffness, such cage structures cannot directly support longitudinal forces. Whereas metal cages cover the entire cross-section of the structure, reinforced concrete cages can be installed on all four sides of the column cross-section, as well as on three, two or even one side. To enable the steel cages to be used, they are prestressed. The prestressing of the longitudinal corners of the cage is achieved by making the prefabricated elements of the spacers (two corners with cross bars welded to them) non-straight. In this prestressed state, all the cross bars are welded (Fig. 1).


Fig. 1. Pylon at the first stage of work. (Photo Oleh Tabarkevych).

The second stage of the reinforced concrete pylon restoration work includes the development of working drawings for the installation of formwork (if the damage is destructive and the pylon requires new concreting) and the installation of a metal casing. This also includes the calculation of the metal casing to select the most optimal cross-section of metal elements for the casing (Figs. 2, 3 and 4).

Fig. 2. Pylon in the formwork during the second stage of work. (Photo Oleh Tabarkevych).
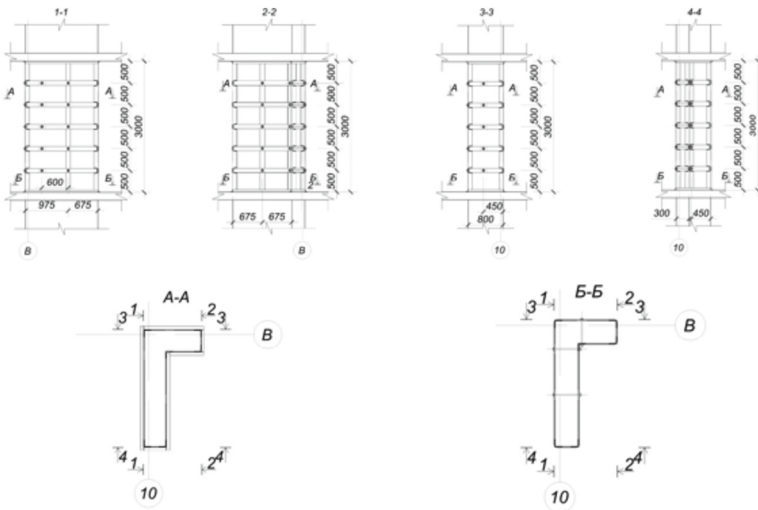
Fig. 3. Working drawings developed during the second stage of work

The third stage of the work is the implementation of the reinforced concrete pylon restoration, preparation of all elements of the metal cage, and determination of the concrete class for new concreting of the reinforced concrete pylon [10, 11].

Fig. 4. Oleh Tabarkevych. View of the pylon during the third stage of work

4 Conclusion

It has been established that residential buildings with reinforced concrete frame elements form the main three-dimensional compositional solutions of Ukrainian cities. Analysing such residential buildings, it was found that they need to be reconstructed as soon as possible. An analysis of foreign experience shows that reconstruction is the only appropriate method that can restore war-damaged and obsolete housing.

Reconstruction techniques are the main tool for improving the quality of housing. The idea of reconstructing typical residential buildings should be to create a unified perception of the building in the system: the street, the city district.

References

1. DSTU-N B V.1.2–18:2016. Guidelines for the inspection of buildings and structures to determine and assess their technical condition. Kyiv. SE "UkrNDNC" (2017)
2. DSTU B B.2.6.-210: 2016 "Assessment of the technical condition of steel building structures in operation"/Ministry of Regional Development of Ukraine, Kyiv p. 56 p. (2016)
3. DBN V.1.2–14–2009. System of ensuring the reliability and safety of construction facilities. General principles of ensuring the reliability and structural safety of buildings, structures, building structures and foundations / Ministry of Regional Development of Ukraine - Kyiv: Ukrarkhbudinform, p. 37 (2009)
4. DBN V.2.6–98: 2009. Concrete and reinforced concrete structures. Main provisions / Ministry of Regional Development of Ukraine. - Kyiv: Ukrarhbudinform, p. 71 (2011)
5. DSTU B.2.6–156: 2010. Concrete and reinforced concrete structures of heavy concrete. Design rules. Kyiv, Ministry of Regional Development of Ukraine (2010)
6. DBN B.2.6–162: 2010 Stone and reinforced stone structures. Main provisions. Ministry of Regional Development of Ukraine, Kyiv (2011)
7. DBN B.2.6–160:2010 - Steel and reinforced concrete structures. Basic provisions
8. DSTU B.1.2–3:2006 Deflections and displacements. Design requirements. Ministry of Construction of Ukraine. - K, p. 40 (2006)

9. Storozhenko, L.I., Yermolenko, D.A., Pents V.F.: Steel and reinforced concrete frames of one-storey buildings for universal use. - Poltava, pp. 221 - 225 (2018)

10. Lapenko, O.: Reinforced concrete structures with working reinforcement with fixed formwork. Poltava: ACMI (2009)

11. Lapenko, O., Palyvoda, O.: Study of joint work of shell and core of tube confined concrete elements with strengthened core. Trans Tech Publication Ltd, Switzerland **968**, 258–266 (2022)

A Complex Method for Purification of Radioactively Contaminated Waters the Object «Ukryttya» of the Chernobyl Nuclear Power Plant

Yuriy Zabulonov[1] , Tetyana Melnychenko[1(✉)] , Vadim Kadoshnikov[1] ,
Valerii Khan[2] , Oleksii Odintsov[2] , and Igor Peer[3]

[1] State Institution "The Institute of Environmental Geochemistry of National Academy of
Sciences of Ukraine", Kyiv, Ukraine
`tim--@ukr.net`
[2] Institute for Safety Problems of Nuclear Power Plants, NAS of Ukraine, Kyiv, Ukraine
[3] ALPHA ATOM LLC, Kyiv, Ukraine

Abstract. The paper considers the method of treatment of radioactively contaminated water of the "Ukryttya" facility of the Chernobyl nuclear power plant (after installation of a new safe confinement), formed mainly as a result of leakage of process solutions (dust suppressants) and trap water (after decontamination of surfaces). Taking into account heterogeneity, multiphase and multicomponent nature of radioactively contaminated water, an integrated method of its purification is proposed. At the pretreatment stage, a heterocoagulation process was applied and used to separate dispersions of micro- and nanoplastics. The use of nanocomposite based on magnetically sensitive thermally expanded graphite and smectites allows to reduce the activity of radiocesium and radiostrontium by 2–3 orders of magnitude. Application of the previously developed sorbent based on iron hydroxide nanoparticles, the surface of which is modified with nickel-potassium ferrocyanides, makes it possible to achieve the degree of purification from ^{137}Cs and ^{90}Sr – 99.99%.

Keywords: radioactively contaminated water · treatment · radiocesium · radiostrontium · sorption · complex sorbent

1 Introduction

The problem of decontamination of radioactively contaminated water generated at the "Ukryttya" facility of the Chernobyl Nuclear Power Plant (ChNPP) is still topical at present. The main method of liquid radioactive waste treatment is evaporation. The waters of the "Ukryttya" site contain a large amount of organic polymeric compounds in the dust suppressant solutions used at the site. The main component of the solutions used for dust suppression is siloxanacrylate binder with hydrophobising properties ($\approx$50% by mass); the rest is non-ionogenic surfactant OP-7, glycerin, oxalic, oleic and oxyethylenediphosphonic acids and ethyl alcohol [1].

Shortcomings of the technology of applying the composition containing siloxaneacrylate latexes resulted in the accumulation of radioactively contaminated water (RCW) containing emulsion of dust suppressors in the inner rooms of the "Ukryttya" facility. When these waters were fed to the evaporators of ChNPP special water treatment for processing, the heat exchangers of the evaporators began to fail, which became clogged with rubber-like deposits [2].

As a result of ageing and degradation of paint coatings, on the surface of which so-called condensation radiocaesium was sorbed as a result of the accident, micro- and nanoparticles (micro- and nanoplastics) are formed. During the deposition process, these particles may enter the trap water of the "Ukryttya" facility. Radionuclides in the dissolved state can sorb on the micro- and nanoplastic particles, significantly increasing the activity of the solid phase. The combination of surfactants, micro- and nanoplastics, siloxaneacrylate latexes in the presence of stabilisers leads to the formation of kinetically stable colloids or pseudocolloids containing significant amounts of radionuclides.

Earlier attempts were made to decontaminate radioactively contaminated waters of the "Ukryttya" object. The use of membrane methods (ultra- and nanofiltration using membranes based on aromatic polyamide with ultrathin selective polypiperazinamide layer) allows removing siloxanacrylate component, while additional purification of the solution from radionuclides is required [1].

In [2] the possibilities of dust suppressors removal from liquid wastes using different methods – oxidation, sorption and flocculation – were analysed. It is shown that the most effective extraction of dust suppressors and associated transuranic elements is provided by using cationic flocculants [2]. The action of coagulants is caused by the change of zeta potential and the formation of kinetically unstable dispersions. But application of this method does not allow to reduce significantly the total beta-activity of the filtered sample.

It is known to use reagent treatment of RWW with coagulant-flocculant of "Sisol" type. The use of "Sisol-2500" preparation allows to achieve significant extraction of polymeric compounds and alpha-emitting uranium radionuclide with a significant reduction in the share of secondary waste with less use of the added reagent [3].

The work [4] describes a method for purifying liquid radioactive waste from the "Ukryttya" object of the Chernobyl Nuclear Power Plant from organic substances and uranium using reagent treatment with lime milk, iron (III) chloride and polyacrylamide. After such treatment, the COD index decreases from 2100–2500 to 1000–1200 mgO_2/dm^3 (purification degree 42.9–60%), and the uranium concentration decreases from 16.1 to 9.5 mg/dm3 (purification degree 41.1%), which is insufficient. Titanium-iron coagulants can be a sufficiently effective coagulant for removal of organic substances, including siloxaneacrylate binder, uranium and transuranic elements (titanium-iron coagulant is a by-product of processing at production of titanium dioxide) [5]. But the use of coagulants for decontamination of radioactively contaminated water from the "Ukryttya" facility does not allow removing completely dose-determining radiocesium and radiostrontium.

The purpose of the work is to develop a method for purifying radioactively contaminated waters of the "Ukryttya" object of the Chernobyl Nuclear Power Plant, which

contain, in addition to water-soluble radionuclides, micro- and nanoparticles of plastics (residues of dust suppressant and paint coatings).

2   Research Results

The experimental studies used a sample of radioactively contaminated water taken from room 001/3 of the "Ukryttya" facility, where most of the water leaks through the reactor block are collected. Radionuclide composition of RCW to be treated: $^{137}Cs – 3.3 \cdot 10^6$, $^{90}Sr – 4.9 \cdot 10^5$, $^{154}Eu – 2.4 \cdot 10^2$, $^{241}Am – 2.2 \cdot 10^3$ Бк/дм^3.

The main sources of the formation of water flows and accumulations of radioactively contaminated water inside the "Ukryttya" object after the installation of the Arch (a new safe confinement) in the design position are condensate formed in the premises at the lower elevations of the "Ukryttya" object in the summer months, and dust suppression solutions supplied into the under-roof space during dust suppression sessions. Water flows enter rooms where fuel-containing masses (FCM) are localized. The interaction of water with structural materials and FCM leads to the formation of rare earth metals containing uranium, fission products and transuranium elements. As a result of leaks inside the "Ukryttya" object from the upper elevations to the lower ones in the rooms located below the $+ 12.5$ m elevation, constant accumulations of hazardous substances are observed [6].

The study of the composition of radioactively contaminated water of the "Ukryttya" object [4] showed that RCW is a heterogeneous, multiphase and multicomponent system. The activity of ^{137}Cs in the studied water samples is $2.3 \cdot 10^7 – 3.1 \cdot 10^8$ Bq/dm^3. The share of dissolved cesium isotope is equal to $81 – 86\%$ of the total content of this isotope. Activity of ^{137}Cs in the composition of suspended solid phase (coarse-dispersed and colloidal particles) varies from $8 \cdot 10^5$ to $1.4 \cdot 10^7$ Bq/dm^3. The share of solid phase with particle size larger than 0.1 microns in the total activity of ^{137}Cs in water is $0.6 – 3\%$. On colloidal particles with the size of $0.01 – 0.1$ microns $1.6 – 2.3\%$ of the total activity of ^{137}Cs in water is concentrated.

The activity of ^{90}Sr in water samples is $9.3 \cdot 10^4 – 9.5 \cdot 10^5$ Bq/dm^3. The share of dissolved strontium isotope in cationic form is equal to $21 – 92\%$ of the total activity of this isotope in water. Activity of ^{90}Sr in the composition of suspended solid phase varies from $8.5 \cdot 10^3$ to $7.3 \cdot 10^5$ Bq/dm^3 of water. The share of solid phase with particle size larger than 0.1 μm in the total activity of ^{90}Sr in water is $5.9 – 77\%$. On colloidal particles with the size of 0.01–0.1 microns there is $0.6 – 3.2\%$ of the total activity of ^{90}Sr in water [4].

Taking into account the fact that the RCW to be purified contains micro- and nanoparticles of polymers in the solid phase, we used the basic principles of separating dispersions of micro- and nanoplastics.

At the stage of pretreatment of purified RCW as a result of adsorption-coagulation processes, phase separation takes place. In the solid phase there are particles of $0.01 – 0.1$ microns in size and coagulated residues of destroyed colloid (micro- and nanoparticles of siloxanacrylates and paint coatings).

Sorption methods and methods using plasma chemical processes are effective for the elimination of micro- and nanoplastics (MNPl) from the environment.

The use of carbon-based composites and magnetic materials is known. The carbon-magnetite composite is used as an adsorbent to treat water containing MNPl. The microplastics are retained by the surface of the composite and can then be successfully removed using an external magnetic field [7].

For the same purpose, magnetically sensitive carbon nanotubes are used, which adsorbed efficiently on polyethylene, polyethylene terephthalate and polyamide, and all the composites formed were easily removed by magnetic separation. Probably, the adsorption process of MNPL is the result of electrostatic interaction of chemical bonds between microplastic and carbon [8].

A significant disadvantage of such composites, in which the magnetosensitive component is combined with a carbon matrix, is the difficulty of their preparation and the low affinity of the magnetosensitive component to carbon. To eliminate this disadvantage, we applied magnetosensitive nanosorbents based on thermally expanded graphite (TEG) used as a carbon matrix [9, 10]. Thermally expanded graphite is obtained by thermal shock of intercalated graphite. The high efficiency of TEG is due to its highly developed specific surface area as well as high activity of the nanocarbon structure. It is possible to use TEG for purification of natural and waste water from transition metals (copper, manganese, zinc) [11].

The disadvantage of TEG is its low density and high hydrophobicity, which can be partially eliminated by introducing a magnetically sensitive component based on iron particles and iron oxides. We have proposed a method for producing such a magnetically sensitive nanosorbent, which involves thermal expansion of oxidized graphite mixed with a magnetically sensitive component. In this case, a mixture of micro- and nanoparticles of metallic iron and ferrihydrites obtained by a plasma-chemical method is used as a magnetically sensitive component, which is mixed with oxidized graphite, and then heat treated using microwave irradiation [10]. The high specific surface area of the resulting sorbent is due to the complex surface relief of the TEG flakes. Simultaneously with the formation of TEG, partial penetration of iron particles of the magnetically sensitive component heated by microwave radiation into the TEG flakes occurs, which causes the formation of a strong metal-carbon bond, as a result of which the resulting magnetically sensitive TEG contains an increased amount of iron and oxides, which determines the magnetic properties and high sorption properties of in relation to transition metal ions (cobalt, manganese, copper, iron, nickel). Taking into account the complex composition of the RCW to be purified, in order to increase the hydrophilicity of the nanosorbent and ensure high sorption capacity with respect to cesium and strontium ions, highly dispersed smectites (bentonite clay with a montmorillonite content of at least 70%) are added to the resulting magnetically sensitive TEG while stirring in a certain ratio.

The obtained nanocomposite was used for preliminary purification of RCW as follows: 200 ml of RCW was introduced into the vessel, pH was corrected with sodium hydroxide solution (mass concentration 10%) to pH≈10, with intensive stirring the calculated amount of composite consisting of magnetically sensitive TEG [10] and bentonite clay of the brand was introduced P4T2К (DASH-BENT JOINT-STOCK COMPANY, Cherkasy region, Ukraine), the obtained suspension was stirred for 30 min at temperature 20 ± 2 °C, after that to it, for heterocoagulation, the calculated amount of positively

charged colloid of iron hydroxide (III) was added [12]. The mixture was stirred for another 30 min and filtered (blue ribbon filter).

The purification resulted in a solution characterized by the absence of opalescence and Tindal cone in the side illumination, which indicates the absence of colloidal dispersion particles. Gamma activity measurements showed that the activity of the solution for cesium-137 decreases by 2–3 orders of magnitude. We believe that the residual gamma-activity is due to the presence of cesium-137 in ionic form.

The solution obtained after preliminary purification was purified by the sorption method using a complex sorbent based on iron hydroxide nanoparticles, the surface of which was modified with nickel-potassium ferrocyanides, which we had previously developed [13]. The specified sorbent [13], intended for purification of technogenically contaminated and radioactive water from radionuclides and heavy metals, was used as follows: 50 – 100 ml of RCW pre-cleaned from micro- and nanoplastics was introduced into the container, the calculated amount of complex sorbent (taking into account the activity of purified water) was added with stirring, stirred for 1 h at a temperature of 20 ± 2 °C, after which, as a coagulant, bentonite clay of the brand was introduced P4T2К (DASH-BENT JOINT-STOCK COMPANY, Cherkasy region, Ukraine), the resulting suspension was stirred for 1 h at a temperature of 20 ± 2 °C. After completion of the sorption process, phase separation was carried out by filtration (blue ribbon filter).

Gamma activity measurements showed that the volumetric activity of cesium-137 decreased to $(220 \pm 15\%)$ Bq/dm^3. The volumetric activity of strontium-90, as a result of its radiochemical separation and beta-radiometric measurement, amounted to $(210 \pm 30\%)$ Bq/dm^3.

For deeper purification, purified water was treated with a complex sorbent again.

3 Conclusions

1. Analysis of information materials has shown that radioactively contaminated water of the Chernobyl NPP "Ukryttya" site is heterogeneous, multiphase and multicomponent.
2. Considering the composition of the RCW, we used a differentiated approach. At the pretreatment stage, a heterocoagulation process was applied, which was used to separate dispersions of micro- and nanoplastics with additional use of positively charged iron (III) hydroxide colloid with subsequent separation of solid and liquid phases.
3. Taking into account that a considerable amount of radionuclides is adsorbed on solid particles and colloids, the use of nanocomposite based on magnetically sensitive thermally expanded graphite and smectites allows reducing the activity of radiocesium and radiostrontium by 2 – 3 orders of magnitude.
4. Application of the previously developed sorbent based on iron hydroxide nanoparticles, the surface of which is modified with nickel-potassium ferrocyanides, allowed to achieve the purification degree from ^{137}Cs and ^{90}Sr - 99.99%. To increase the degree of purification, repeated treatment is necessary.

References

1. Rudenko, L.I., Gumenna, O.A., Dzhuzha, O.V.: Membrane methods of treatment of water, which contains polymericsubstances and compounds of uranium, strontium, and sodium. Reports Nat. Acad. Sci. Ukraine **6**, 134–138 (2010)

2. Avramenko, V.A., Bratskaya, S.Y., Egorin, A.M., Markovtseva, T.G., Ryabushkin, A.N., Harjula, R.: Nanosize latexes containing polyacrylic acid and their role in transport and immobilization of radionuclides at nuclear energy objects. Voprosy Radiatsionnoi Bezopasnosti **4**, 23–29 (2008)

3. Rudenko, L.I., et al.: Reagents purification of liquid radioactive waste from organic substances and uranium. Reports Nat. Acad. Sci. Ukraine **54**, 140–144 (2011)

4. Rudenko, L.I., Sklyar, V.Y., Khan, V.E.: Treatment of liquid radioactive waste from the shelter object to remove transuranic elements, Sr, and γ-Emitters. Radiokhimiya **46**(2), 184–187 (2004)

5. Rudenko, L.I., et al.: Purification of liquid radioactive waste from organic compounds with titanium-ferrous coagulants. Energy Technol. Resource Saving **4**, 59–64 (2013)

6. Odintsov, O.O., Khan, V.E.: Radioactive water in object «Ukryttya» after pulling down of «Arch» of nev safe confinement in project statute. Probl. Nucl. Power Plants Saf. Chornobyl 30, 67–77. https://doi.org/10.31717/1813-3584.18.30.8

7. Elmaci, G.: Microwave-assisted rapid synthesis of C@ Fe_3O_4 composite for removal of microplastics from drinking water. Adıyaman Univ. J. Sci. **10**(1), 207–217 (2020). https://doi.org/10.37094/adyujsci.739599

8. Tang, Y., Zhang, S., Su, Y., Wu, D., Zhao, Y., Xie, B.: Removal of microplastics from aqueous solutions by magnetic carbon nanotubes. Chem. Eng. J. **406**, 126804 (2021). https://doi.org/10.1016/j.cej.2020.126804

9. Zabulonov, Y.L.: Patent UA № 77123; IPC C02F 1/28 (2006.01) C02F 1/48 (2006.01) C02F 101/32 (2006.01). Method removal of non-polar organic liquids from the surface of natural reservoirs and from man-made polluted waters using a complex magnetically sensitive nanosorbent. №u202004413; Appl. 15.07.2021; Publ. 13.01.2021, Bull. № 2. https://sis.nipo.gov.ua/uk/search/detail/1472524

10. Zabulonov, Y.L.: Patent UA № 152970; IPC B01J 20/30 (2006.01) B01J 20/20 (2006.01) C02F 101/32 (2006.01) B82Y 30/00. A method for producing a magnetically sensitive nanosorbent. №u202203929; Appl. 20.10.2022; Publ. 03.05.2023, Bull. № 18. https://sis.nipo.gov.ua/uk/search/detail/1734965/

11. Berestneva, Y.V., Voitash, A.A., Raksha, E.V., Balkushkin, R.N., Mezhevova, A.S., Savoskin, M.V.: Assessment of the possibility of thermally expanded graphite application for polluted natural waters purification. Chem. Saf. Sci. **5**(1), 110–124 (2021). https://doi.org/10.25514/CHS.2021.1.19007

12. Zabulonov, Y.L., Kadoshnikov, V.M., Melnychenko, T.I., Zadvernyuk, H.P., Kuzenko, S.V., Lytvynenko, Y.V.: Geochemical behavior of ferric hydroxide nanodispersion un der the influence of weak magnetic fields. Mineralogicheskiy Zhurnal **43**(2), 74–79 (2021) . https://doi.org/10.15407/mineraljournal.43.02.074

13. Zabulonov, Y.L.: Patent UA № 152730; IPC (2023.01) G21F 9/06 (2006.01), B01J 20/00, B82B 3/00, B01J 23/70 (2006.01), B82Y 40/00. The Method of Obtaining a Nanodispersion of a Complex Sorbent for the Purification of Technogenically Polluted and Radioactive Waters. №u202203053; Appl. 22.08.2022; Publ. 05.04.2023, Bull. № 14. https://sis.nipo.gov.ua/uk/search/detail/1729765/

New Sorbents and Their Application for Deactivation of Liquid Radioactive Waste

Yuriy Zabulonov[1] 📧, Tetyana Melnychenko[1](✉) 📧, Vadim Kadoshnikov[1] 📧, Svitlana Kuzenko[1] 📧, Sergii Guzii[1] 📧, and Igor Peer[2] 📧

[1] State Institution "The Institute of Environmental Geochemistry of National Academy of Sciences of Ukraine", Kyiv, Ukraine
tim--@ukr.net

[2] ALPHA ATOM LLC, Kyiv, Ukraine

Abstract. The article deals with the methods of obtaining sorbents and the possibilities of their application for deactivation of liquid radioactive waste. A method for obtaining nanodispersion of nickel-potassium ferrocyanides is proposed. The mechanism of formation of nanoparticles and a diffuse layer on the surface of nickel-potassium ferrocyanides nanocrystals is considered. The increased sorption of cesium ($K_d > 100000$, ml/g), in addition to ion exchange, is associated with the inclusion of cesium ions in the structure of the surface layer of ferrocyanide nanocrystals, which is due to the presence of octahedral cavities in the crystal lattice of nickel-potassium ferrocyanides, which contain water molecules, The efficiency of the proposed sorbents based on iron oxide micro- and nanotubes and iron (III) hydroxide nanoparticles modified with nickel-potassium ferrocyanides, whose size is mainly 1–100 μm, is shown. To decontaminate liquid radioactive waste containing complementary substances of organic nature, plasma-chemical treatment is used, which results in the formation of a dispersion containing nanoparticles of metals and metal oxides that show increased affinity for strontium and transition metals. The integrated use of this dispersion in combination with montmorillonite allows for effective treatment of multicomponent liquid radioactive waste. To increase the strontium recovery rate while maintaining high efficiency of cesium and transition metals recovery, it is advisable to apply preliminary plasma chemical treatment followed by the use of sorbents based on ferrocyanide-modified iron (III) oxides/hydroxides. The choice of the deactivation algorithm depends on the composition of liquid radioactive waste to be treated.

Keywords: Liquid radioactive waste · Radionuclide · Cesium · Sorbent · Ferrocyanide · Iron (III) oxides/hydroxides

1 Introduction

The relevance of the issue of creating new sorbents is primarily due to the need to treat liquid radioactive waste (LRW) generated during the operation of NPPs and other nuclear industry enterprises, including in emergency situations [1]. At present, the main dose-determining radionuclides are cesium and strontium, which, due to their high solubility, enter ground and groundwater, contaminating the environment.

A well-known method of LRW treatment is sorption, which involves removal of radionuclides in the form of a solid phase as a result of adsorption, ion exchange, adhesion, etc. Sorption is carried out in special devices under dynamic or static conditions on bulk or alluvial filters, including ion exchange resins [2]. Spent sorbents contain absorbed radionuclides (^{137}Cs, ^{134}Cs, ^{60}Co and ^{90}Sr) and have high activity (about 100000 Bq/dm^3). Positive results can be obtained when working with LRW using inorganic sorbents. The known natural sorption materials are structural aluminosilicates such as smectites and highly dispersed hydromica (montmorillonite, baidelite, illite, chlorite, and framework natural and synthetic zeolites) [3].

In addition to radionuclides, the liquid radioactive waste to be processed contains significant amounts of complementary substances - inorganic substances, mainly in the form of alkali metal salts, borates, as well as organic substances, such as oxalates and citrates, surfactants and complexing agents that interfere with sorption processes. Given the multicomponent and multiphase composition of liquid radioactive waste, in particular NPP ladder water, the development of a universal sorbent is a challenge, especially for radiocesium removal.

Specific sorbents for radiocesium removal are transition metal ferrocyanides with general Formula (1):

$$A_xM_y\left[Fe(CN)_6\right]_z \cdot nH_2O \tag{1}$$

where A–K$^+$, Na$^+$, NH$_4$$^+$, M–Ni^{2+}, Co^{2+}, Cu^{2+}, Fe^{3+}, Zn^{2+}, etc., the main synthesis of which is the formation of insoluble metal ferrocyanides by the interaction of water-soluble alkali metal ferrocyanides with soluble transition metal salts [4]. Copper, nickel, and iron are of practical importance for the creation of sorbents. To enhance the selective sorption of cesium, ferrocyanides deposited on the surface of a solid carrier (polymer-inorganic, natural, and synthetic sorbents) are used [4, 5].

The use of metal oxide nanoparticles (TiO_2, V_2O_5, ZnO, MoO_3, MnO_2, Fe_2O_3) as adsorbents of heavy metals and radionuclides is of interest due to their greater efficiency compared to traditional materials due to their high surface area [6].

The main mechanisms of adsorption on metal oxide nanoparticles are mainly complexation, ion exchange, and electrostatic interaction. Nanotubes, in particular, iron oxide nanotubes, have higher adsorption properties compared to metal oxide nanoparticles.

In view of the above, the aim of our study is to develop new sorbents for the deactivation of radioactively contaminated water, including the ladder water of nuclear power plants.
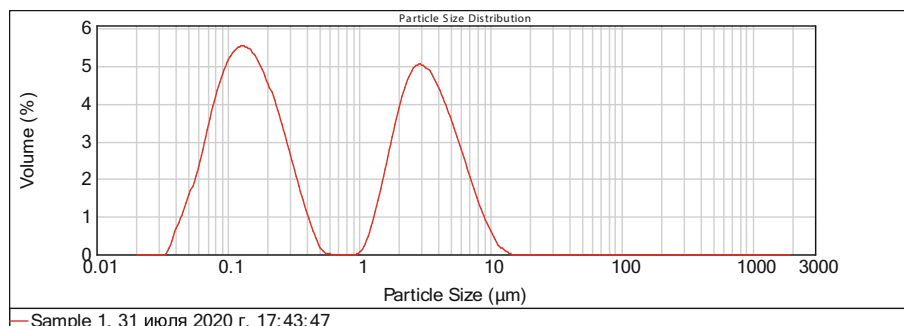
2 Research Results

In the experimental studies, we used the sorbents developed by us: a nanodispersion of nickel-potassium ferrocyanides [7], a nanocomposite based on ferrocyanide-modified iron oxide micro- and nanotubes [8], and a nanodispersion of a complex sorbent based on ferrocyanide-modified iron hydroxide nanoparticles [9].

The sorption of radiocesium by ferrocyanides depends significantly on the particle size of the sorbent. We have developed a method for obtaining a nanodispersion containing colloids of nickel ferrocyanide or nickel-potassium ferrocyanide and nanoscale

ferrocyanide crystals [7]. In the process of its synthesis, it is necessary to maintain conditions under which the rate of nucleation is higher than the growth of crystals. In addition, conditions are required to ensure chain breakage. Such conditions can be realised with a significant excess of nickel ions and a sufficiently high temperature, which reduces the likelihood of nanoparticle aggregates. The formation of nanoclusters plays a significant role in the studied processes [10]. The most important parameters responsible for this condensation of particles are the Van der Waals interaction and the submicroscopic potential. The mechanism of solid phase formation from aqueous solution is a submicroscopic extension of Ostwald's phenomenological theory [11]. According to Ostwald's rule, metastable layered crystals or other forms first appear in water, which then spontaneously transform into a more stable polymorph with a clear crystal structure. The surface of the formed nanocrystals contains fragments of the structures of smaller formations, which determines their high sorption properties.

The size and particle size distribution of the obtained nanodispersion were determined by the method of light scattering of monochromatic laser radiation (see Fig. 1). The measurements were performed on a Mastersizer 2000 laser sedimentograph with a HydroS liquid dispersion module (Malvern Instruments, UK).

The data clearly show that there are two distribution maxima for the dispersion. In our opinion, this is due to the fact that initially, with an excess of nickel ions, nickel ferrocyanide nanocrystals are formed, which, with the subsequent addition of a potassium ferrocyanide solution, form nickel-potassium ferrocyanide nanocrystals. The effective particle size is ≈ 30 and 90 nm.
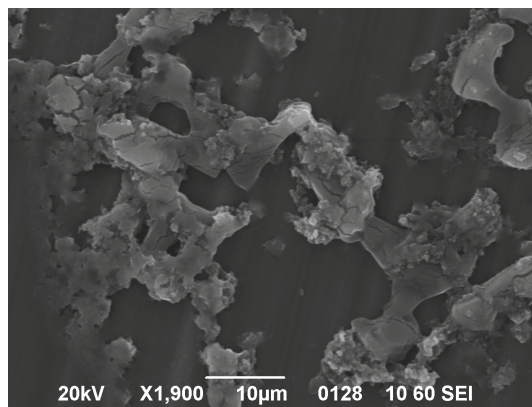

Fig. 1. Differential distribution curve of particles of nickel-potassium ferrocyanide nanodispersion (by volume)

Particles with a size of 90 nm are not formed by coagulation of small particles, but by nanocrystals growing during the synthesis process. The nanoparticles interact with each other through intermolecular forces and form irregularly shaped aggregates (see Fig. 2).

The outer surface of nickel-potassium ferrocyanide nanocrystals interacts with water and is partially hydrolysed to form negatively charged centres localised on the surface of the microcrystals and potassium ions that migrate into the aqueous medium. The

Fig. 2. SEM image of aggregates of nickel-potassium ferrocyanide nanoparticles

potassium ions released as a result of dissociation are partly located directly at the crystal surface and partly form a diffuse ionic atmosphere due to electrostatic interaction.

Using the general laws of formation of colloidal particles, we propose the following structure (2) of the resulting colloidal particle:

$$m\text{NiK}_2\big[\text{Fe(CN)}_6\big] * n\text{NiK}\big[\text{Fe(CN)}_6\big]^- * x\text{K}^+/(n - x) * \text{K}^+ \qquad (2)$$
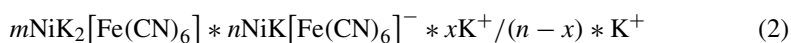
where m is the number of non-ionised ferrocyanide molecules in the near-surface layer of the nanoparticle, n is the number of ionised ferrocyanide molecules in the near-surface layer of the nanoparticle, x is the number of potassium ions directly located near the surface of the nanoparticle.

The study of cesium sorption from aqueous solution by nanodispersion of nickel-potassium ferrocyanides showed that the synthesised nanodispersion allows for the efficient removal of cesium ions from solution. It was found that the degree of cesium extraction by nanodispersion of nickel-potassium ferrocyanides was 95–99%, and the distribution coefficient K_d (ml/g) of cesium ions between the liquid and solid phases was more than 100000. In real conditions, it is necessary to take into account the presence of elements that can compete with cesium during adsorption. The results of the study are shown in Fig. 3.

The sorption of cesium, strontium, cobalt, and manganese ions from the solution by nickel-potassium ferrocyanide nanoparticles is mainly due to the ionic exchange of cations of the dispersion medium with ion exchange centres localised on the outer surface of the nanocrystal and is described by the Langmuir isotherm of the 2nd order. A similar mechanism is typical for the sorption of cesium and strontium by smectites [12].

The increased sorption of cesium ($K_d > 100000$, ml/g), in addition to ion exchange, is associated with the inclusion of cesium ions in the structure of the surface layer of ferrocyanide nanocrystals, which is due to the presence of octahedral cavities in the crystal lattice of nickel-potassium ferrocyanides, which contain water molecules capable of exchange with cations of the dispersion medium. The preferential sorption of cesium compared to other cations is due to the low electric charge density of the cesium ion
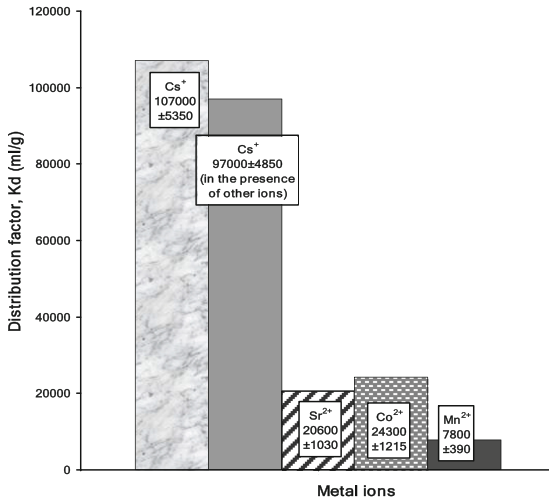
Fig. 3. Distribution coefficient K_d (ml/g) of cesium, strontium, cobalt, manganese ions

compared to other cations [10]. In addition, the low electric charge density of the ion promotes its migration through a diffuse layer of potassium ions localised on the surface of ferrocyanide nanoparticles.

To enhance the selective sorption of cesium, ferrocyanides deposited on the surface of a solid carrier (matrix) are used. We used iron oxide nano- and microtubes as a matrix, for which we applied the template method, which consists in the formation of nanostructures on the surface of the matrix. For this purpose, cotton fibre was treated with iron (III) hydroxide colloid [13], after which the impregnated fibre was subjected to heat treatment in a stepwise mode. By X-ray diffractometry, infrared spectroscopy, scanning electron microscopy, and light scattering of monochromatic laser radiation, it was found that the synthesized nanotubes consist of alpha- and gamma-modified iron oxides, as well as partially hydrated β-FeOOH. The nanotubes are presented in the form of fibre fragments of various shapes, 50–500 μm in size, with irregularly shaped cavities in them, 10–20 μm in cross-section (see Fig. 4).

The results of the study of the sorption properties of iron oxide micro- and nanotubes for cesium, strontium, cobalt, and manganese are shown in Fig. 5.

The obtained results show that the degree of cesium removal from the studied solution (a simulator of floor drain waters of nuclear power plants Ukraine) is extremely low, which is due to its chemical nature, the nature of the sorbate and the sorption mechanism, which is dominated by ion exchange. The high degree of removal of transition metals and strontium is due to the high affinity of these elements for the sorbent.

To improve the sorption of cesium, the surface of iron oxide micro- and nanotubes was modified with nano- and microcrystals of nickel-potassium ferrocyanides [8]. Figure 6 shows SEM images of iron oxide micro- and nanotubes modified with nickel-potassium ferrocyanides.
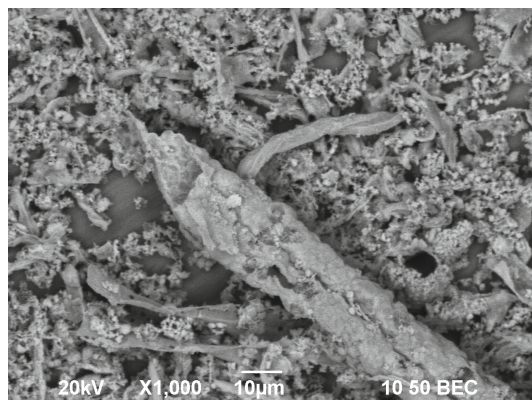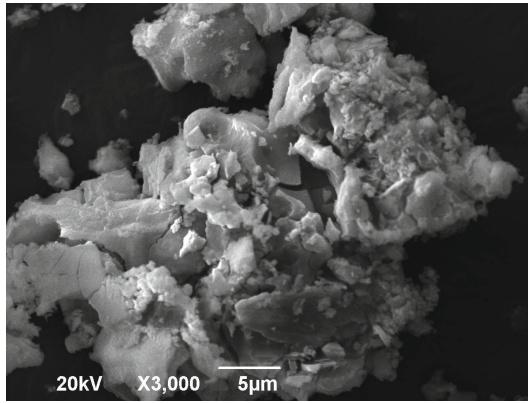
Fig. 4. SEM image of iron oxide nanotubes
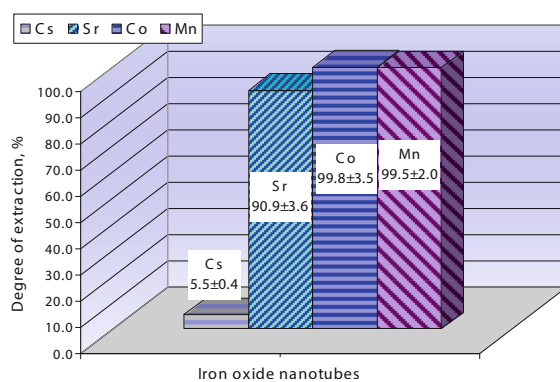
Fig. 5. The degree of extraction of imitation radionuclides by iron oxide nanotubes from the imitation solution

The SEM image shows both single small crystals, which may belong to iron oxides and nickel-potassium ferrocyanides, and agglomerates formed by micro- and nanotubes with ferrocyanide nanoparticles deposited on their surface.

The study of the sorption properties of ferrocyanide-modified iron oxide nanotubes showed that the modification significantly increased the sorption properties of iron oxide micro- and nanotubes for cesium ions (see Fig. 7).

The high degree of cesium extraction is explained by the specific mechanism of interaction of cesium ions with micro- and nanocrystals of nickel-potassium ferrocyanides. At the same time, a decrease in strontium recovery is observed compared to unmodified iron oxide nanotubes. A significant disadvantage of this method is the rather complicated technology of matrix preparation. The replacement of iron oxide nanotubes with iron (III) hydroxide nanoparticles, followed by their modification with transition metal ferrocyanides [9], allows to obtain a sorbent that is almost as good as a nanocomposite based

Fig. 6. SEM image of iron oxide micro- and nanotubes modified with nickel-potassium ferrocyanides
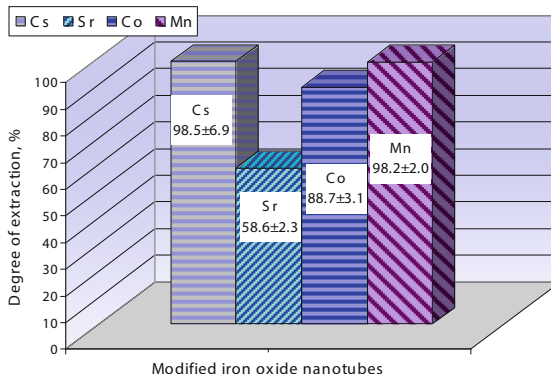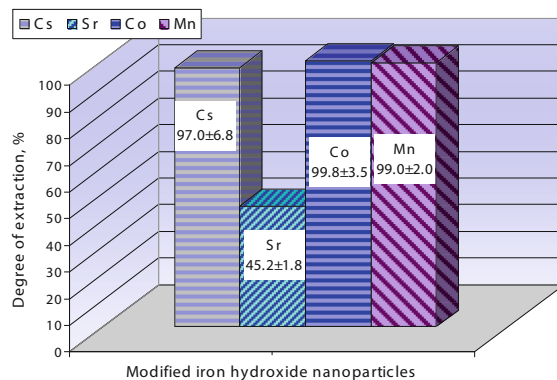

Fig. 7. The degree of extraction of imitation radionuclides by modified iron oxide nanotubes from the imitation solution

on iron oxide nanotubes modified with ferrocyanides in terms of cesium sorption properties (see Fig. 8). The degree of removal of transition metals (cobalt and manganese) is quite high and amounts to about 98–99%.

The degree of strontium extraction does not exceed 50% (see Fig. 8), which is most likely due to the peculiarities of sorption of strontium ions on amorphous iron hydroxide micelles. In addition, the low strontium recovery is probably due to the high content of transition metals in the solution under study, which compete with strontium and whose affinity for ferric hydroxide is much higher than that of strontium ions.

The disadvantage of all sorption methods is the negative impact of organic matter on sorption processes. An effective way to destroy organic matter in contaminated water is plasma treatment, which results in the formation of metal and metal oxide nanoparticles in a plasma reactor simultaneously with the destruction of organic matter. When the reactor is loaded with iron pellets, spherical nanoparticles of metallic iron, its oxides and ferrihydrites are formed. The SEM image (see Fig. 9) clearly shows aggregates

Fig. 8. The degree of extraction of imitation radionuclides by modified iron hydroxide nanoparticles from the imitation solution

consisting of diamagnetic material (iron oxides or hydroxides) in which spherical iron particles are unevenly distributed, which provides high magnetic properties of such aggregates.
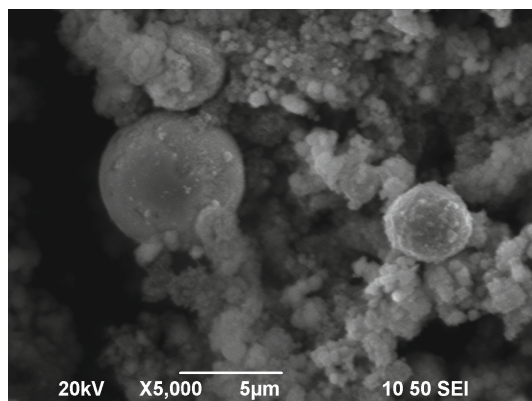
Fig. 9. SEM image of the dry residue of the solid phase of the dispersion (plasma chemical reactor loading – iron)

The ability of the formed nanoparticles to sorption heavy metal ions and radionuclides from the simulator solution is shown in Fig. 10.

The high sorption capacity of the particles of the solid phase of the aqueous dispersion is due to the presence of iron oxides and hydroxides in it, which is explained by the interaction of the surface of iron oxides with transition metal ions and strontium, which may lead to the formation of complex compounds. The initial stage of complexation is characterised by the formation of intermolecular hydrogen bonds. With increased interaction, Fe-H (ionic type), Fe-O, O-H bonds are formed. An increase in the degree of cesium removal from the liquid requiring purification can be achieved by using montmorillonite with increased affinity for cesium ions [12]. The introduction of bentonite
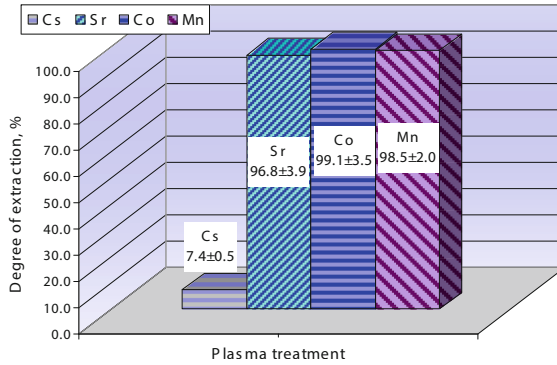
Fig. 10. The degree of imitation radionuclides extraction by nanoparticles of the dispersion obtained as a result of plasma-chemical treatment (loading – iron) of the imitation solution

clay (up to 2% by weight) [14] into the dispersion formed as a result of plasma chemical treatment leads to an increase in the degree of cesium extraction (see Fig. 11).
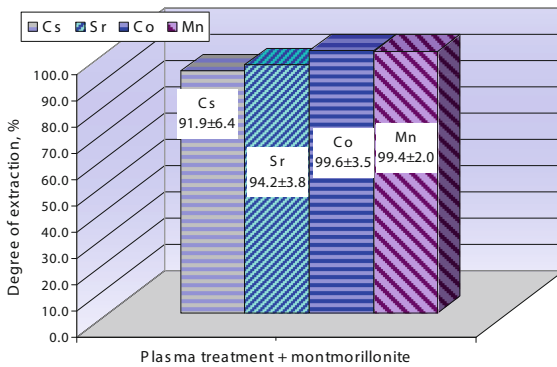
Fig. 11. The degree of imitation radionuclides extraction from the imitation solution as a result of plasma-chemical treatment (loading – iron) in combination with bentonite clay

3   Conclusions

The choice of sorbent, method of its application, sequence of decontamination stages is determined by the composition of liquid radioactive waste to be cleaned. To increase strontium recovery while maintaining a high recovery of cesium and transition metals, it is advisable to apply preliminary plasma chemical treatment followed by the use of sorbents based on nickel-potassium ferrocyanide-modified iron (III) oxides/hydroxides.

The efficiency of the radionuclide sorption process can be increased by the additional introduction of highly dispersed aluminosilicates (montmorillonite, illite, palygorskite) as sorbent-coagulants.

An alternative to the plasmochemical method of radioactive waste pretreatment for strontium and heavy metals extraction may be the sorption method, in particular, using iron (III) oxides/hydroxides.

Taking into account the sorption mechanisms of radionuclides and their chemical nature, as well as the multicomponent composition of the liquid to be cleaned, each specific case of liquid radioactive waste deactivation n requires a specific approach.

References

1. Ueda, S., Hasegawa, H., Ohtsuka, Y., Ochiai, S., Tani, T.: Ten-year radiocesium fluvial discharge patterns from watersheds contaminated by the Fukushima nuclear power plant accident. J. Environ. Radioact. **240**, 106759 (2021). https://doi.org/10.1016/j.jenvrad.2021.106759

2. Nosovskyy, A.V., Aleksyeyeva, Z.M., Borozenets', H.P., et al.: Radioactive Waste Management. Tekhnika, Kiev (2007)

3. Milyutin, V.V., Gelis, V.M., Leonov, N.B.: Study of the kinetics of sorption of cesium and sorption radionuclides by sorbents of different classes. Radiochemistry **40**, 418–420 (1998)

4. Rauwel, P., Rauwel, E.: Towards the extraction of radioactive cesium-137 from water via graphene/CNT and nanostructured Prussian blue hybrid nanocomposites: a review. Nanomaterials **9**(5), 682 (2019). https://doi.org/10.3390/nano9050682

5. Sharygin, L., Muromskij, A.: Inorganic sorbent for ion selective treatment of liquid radioactive waste. Radiokhimiya **46**(2), 171–175 (2004)

6. Akpomie, K.G., et al.: Adsorption mechanism and modeling of radionuclides and heavy metals onto ZnO nanoparticles: a review. Appl. Water Sci. **13**(1), 20 (2023). https://doi.org/10.1007/s13201-022-01827-9

7. Zabulonov, Yu.L., Kadoshnikov, V.M., Melnychenko, T.I., Shkapenko, V.V., Lytvynenko, Yu.V., Kuzenko, S.V.: Patent UA № 145466; MPC (2020.01) C02F 1/00, G21F 9/04 (2006.01), C02F 9/00, C02F 101/20 (2006.01). Method for Purification of Technogenically Contaminated Waters Containing Radionuclides and Heavy Metals in the Presence of Surfactants and Complexing Agents. № u202004414; Appl. 15.07.2020; Publ. 10.12.2022, Bull. № 23

8. Zabulonov, Yu.L., Kadoshnikov, V.M., Melnychenko, T.I., Puhach, O.V., Shkapenko, V.V., Kuzenko, S.V.: Patent UA №. 149345; MPC (2021.01 C02F 11/00, B82Y 40/00. The Method of the Nanocomposite Obtaining for the Treatment of Technogenically Polluted and Radioactive Waters. №u202102632; Appl. 20.05.2021; Publ. 10.11.2021, Bull. № 45

9. Zabulonov, Yu.L., et al.: Patent UA № 152730; MPC (2023.01) G21F 9/06 (2006.01), B01J 20/00, B82B 3/00, B01J 23/70 (2006.01), B82Y 40/00. The Method of Obtaining a Nanodispersion of a Complex Sorbent for the Purification of Technogenically Polluted and Radioactive Waters. №u202203053; Appl. 22.08.2022; Publ. 05.04.2023, Bull. № 14

10. Melnychenko, T., et al.: Nanodispersion of ferrocianides for purification of man-made contaminated water containing caesium. J. Environ. Radioact. **261**, 107135 (2023). https://doi.org/10.1016/j.jenvrad.2023.107135

11. Ostwald, W.: Studien über die Bildung und Umwandlung fester Körper. 1. Abhandlung: Übersättigung und Überkaltung. Z. Phys. Chem. **22**, 289–330 (1897)

12. Zabulonov, Y., Kadoshnikov, V., Zadvernyuk, H., Melnychenko, T., Molochko, V.: Effect of the surface hydration of clay minerals on the adsorption of cesium and strontium from dilute solutions. Adsorption **27**, 41–48 (2021). https://doi.org/10.1007/s10450-020-00263-y

13. Zabulonov, Y.L., Kadoshnikov, V.M., Melnychenko, T.I., Zadvernyuk, H.P., Kuzenko, S.V., Lytvynenko, Y.V.: Geochemical behavior of ferric hydroxide nanodispersion un der the influence of weak magnetic fields. Mineralogicheskiy Zhurnal **43**(2), 74–79 (2021). https://doi.org/10.15407/mineraljournal.43.02.074
14. Zabulonov, Yu.L., Kadoshnikov, V.M., Melnychenko, T.I., Nikolenko, V.O., Shkapenko, V.V., Puhach, O.V.: Patent UA № 150015; MPC (2021.01) C02F 1/00, G21F 9/04 (2006.01), C02F 9/00, C02F 101/20 (2006.01). A Complex Plasma-Chemical Method of Cleaning Technogencally Polluted Waters Containing Organic Substances, Radionuclides and Heavy Metals. №u202104379; Appl. 27.07.2021; Publ. 22.12.2021, Bull. № 51

Application of the Latest Design of Combined Adsorber-Settler Structure in the Purification (Deactivation) of Liquid Radioactive Wastes (LRW)

Sergiy Marisyk[1(✉)] , Yevhen Matselyuk[1] , Dmytro Charny[2], Yuriy Zabulonov[2] ,
Tetiana Nosenko[3] , Oleksandr Pugach[2] , and Mykhailo Rudoman[1]

[1] Institute of Water Problems and Reclamation NAAS, Kyiv 03022, Ukraine
`sergsi.marisik@ukr.net`
[2] State Institution Institute of Environmental Geochemistry NAS, Kyiv 03142, Ukraine
[3] Kyiv University named after Borys Grinchenko, Kyiv 04053, Ukraine

Abstract. In the conditions of modern progressive pollution by liquid radioactive wastes (LRW), and the ineffective purification of LRW using existing water treatment technologies, it is crucial to investigate and substantiate the application for retaining specific pollutants, particularly heavy metal ions and radionuclides, using sorption materials. One of the parameters affecting the efficiency of sorbents is their sedimentation rate. The sorbent's settling in the settlers occurs during the continuous movement of water at a low speed and uniform distribution throughout the volume of the purification structure from the inlet to the outlet. Experiments aimed at substantiating the constructive and technological parameters of a universal structure capable of working equally effectively with sorbents in different aggregate states. The process of sorbent sedimentation in water is characterized by the kinetics of sedimentation of sorbent flocculant conglomerates. These processes are reflected in the form of sedimentation kinetics graphs. The experiment used powdered bentonite and a solution of copper ferrocyanide, consisting of yellow blood salt and copper sulfate in a given ratio. A virtual full-scale spatial model of the illuminator-adsorber was used as the structure. During the research, the hydraulic size of bentonite powder clay was determined, the efficiency of different designs of the settler with ordinary and modernized thin-layer modules was established, and an increase in the sedimentation area was achieved. The use of virtual models of sedimentation of bentonite and zeolite powder clays and copper cyanoferrate allowed substantiating the optimal design of the illuminator-adsorber for stable and efficient sedimentation of the sorbent.

Keywords: Water purification structures · Water preparation · Bentonite · Illuminator-adsorber · Hydraulic size · Suspended particles · Sorbent · Liquid radioactive wastes

1 Introduction

Ukrainian and global problem of accumulating volumes of LRW:

- 486 million cubic meters of liquid radioactive wastes accumulated globally, and this number is only increasing;
- 22 thousand cubic meters of liquid radioactive wastes stored in the Chernobyl NPP repositories;
- 70% of Chernobyl NPP repositories are already filled;
- 450 operating reactors and NPPs continue to add thousands of cubic meters of liquid RAW to repositories annually, outpacing the rate of their utilization.

  Ways to solve the problem of minimizing the volumes of RAW:

- Extraction of radionuclides from RAW by transforming them from a soluble state to a fixed state in a solid phase, followed by their disposal.
- Returning the deactivated and purified water to its natural cycle on Earth.

  Challenges in this pathway:

- A wide variety of organic and inorganic compounds in the composition of RAW.

Besides the need for appropriate sorbents, there is a necessity to develop technological structures capable of ensuring the passage of adsorption and sedimentation processes during the purification of LRW with minimal involvement of additional energy, for example, only due to gravity.

The need for maximum compaction and dehydration of the spent sorbent.

In the context of modern progressive pollution with liquid radioactive wastes (LRW) and the ineffective purification of LRW using existing water treatment technologies, it is relevant to research the application for retaining ions of heavy metals and radionuclides, various sorption materials, and further development of appropriate technological structures where the processes of adsorption and sedimentation will occur.

Research results of the effectiveness of different sorbents are necessary for selecting the most efficient ones; their hydrodynamic characteristics will directly determine the structural solutions for the given structure. In modern conditions, it has become possible to establish the parameters of the technological structure through Computational Fluid Dynamics modeling by the Volume of Fluid – modeling the free flow of fluid by the free surface method. To reduce the model to an acceptable 3–5 million elements, it is necessary to conduct an accurate determination of the hydrodynamic characteristics of sorbent particles. Currently, there is no data on the hydrodynamic characteristics of the vast majority of sorbents in reference literature. This is especially true for colloidal conglomerates formed during the introduction of liquid reagents, the combination of which causes the formation of solid phases with undefined hydrodynamic properties. An example is one of the most effective sorbents - copper ferrocyanide ($Cu_2[Fe(CN)_6]$), which is formed from a mixture of two solutions: yellow blood salt ($K_4(Fe(CN)_6)$) and copper sulfate ($CuSO_4$) directly in the water being purified. The hydrodynamic characteristics of the promising combination of copper ferrocyanide with powdered bentonite clay are also unknown. The hydrodynamic characteristics of the most promising sorbents were determined for further development of the parameters of a universal adsorber-illuminator, capable of working effectively with both liquid reagents and solid fractions of sorbents, similar to powdered bentonites and zeolites.

Analysis of the Latest Research and Publications. The works [1–7] have investigated the impact of various sorbents on water treatment technologies and water quality in the removal of heavy metal ions. The studies [8–12] considered technologies based on the use of biological factors, and [13–16] focused on sorbents based on bentonite clays. In the research [3, 4], it is asserted that bentonites and zeolites are promising sorbents, primarily due to their availability and technological convenience.

2 Hydraulic Characteristics for the Sedimentation of Sorbents Bentonite, Zeolite, Copper Ferrocyanide, and Their Mixture

The process of sorbent sedimentation in water is characterized by the kinetics of settling of sorbent flake conglomerates. These processes are depicted in sedimentation kinetics graphs. In the study, bentonite clay powder with particle sizes of 0.1–0.072 mm and a solution of copper ferrocyanide ($(Cu_2[Fe(CN6)])$), consisting of yellow blood salt ($(K4(Fe(CN)6))$) and copper sulfate ($(CuSO4)$) in a proportional ratio of 1g yellow blood salt to 1.356g copper sulfate, were used. Mixing occurs in a measuring cup with the addition of distilled water not exceeding 50ml per 10g of dry mixture. The solution of copper ferrocyanide is prepared exclusively before use; otherwise, the effectiveness of the solution decreases.

The obtained data are compiled into tables, based on which the Graph of Dependencies of the Study (Figs. 1 and 2) are constructed, and calculations of hydraulic size [17, 18] are conducted.

As a result of the studies, a model of sorbent sedimentation was built, and their sedimentation speed was established (Figs. 1 and 2, Table 1).
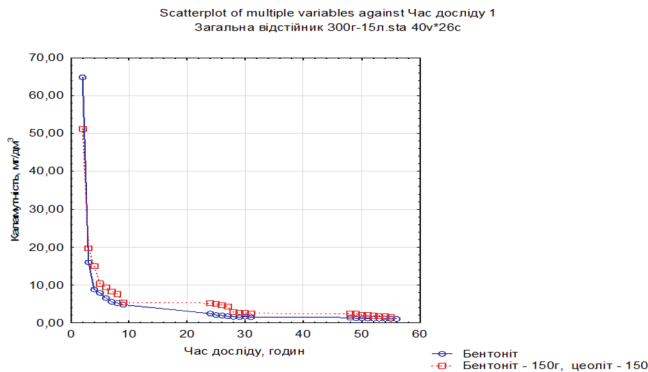
Fig. 1. Graph of dependencies of the hydraulic size of bentonite with an experiment duration of 56 h and a mixture of bentonite and zeolite with a duration of 54 h at a suspension temperature fluctuation of 14–16 °C.

The best result was obtained with a mixture of bentonite powder clay and copper ferrocyanide solution in a ratio of 2/0.5 g/dm^3 of dry matter - 99.8% of suspended particles settled and complete discoloration of the purified water from the remnants of copper ferrocyanide.
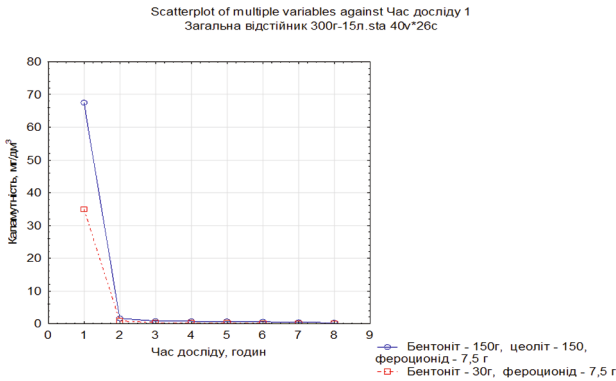
Fig. 2. Graph of dependencies of the hydraulic size of a mixture of bentonite and copper ferro-cyanide with an experiment duration of 2 h 20 min and a mixture of bentonite, zeolite, and copper ferrocyanide with a duration of 3 h 30 min at a suspension temperature of 8 °C.

Table 1. Sedimentation speed.

№	Name	Settling Time, t, hours	Hydraulic Size, U_0, mm/s	Proportionality Coefficient, n	Concentration of Suspended Substances, P, %
1	Bentonite	56	0.11	1.39	98.26
2	Bentonite + Zeolite	37	0.44	1.23	96.5
3	Bentonite + Zeolite + Copper Ferrocyanide	3.5	4.99	0.43	98.7
4	Bentonite + Copper Ferrocyanide	2.20	6.185	0.29	99.8

Calculation of Hydraulic Size [17, 18]:

$$U_0 = \frac{1000HK}{t_1(HK/h_1)^n} \tag{1}$$

where H – depth of the working part of the settler, m; K – coefficient of utilization of the settler's volume; t1 – duration of settling in the laboratory cylinder at the height of layer h1, during which the required effect of clarification is achieved; n – coefficient of proportionality, which depends on the agglomeration of suspended particles in the process of settling in different water layers (h1 > h2); it is calculated using the following formula:

$$n = \frac{\lg t_1 - \lg t_2}{\lg h_1 - \lg h_2} \tag{2}$$

where h1 and h2 – heights of settling layers, cm;

t1 and t2 – duration of settling in the respective layers, when the required effect is achieved, s.

The efficiency of suspension settling is calculated as the difference in values of the concentration of suspended substances in water before and after settling, namely:

$$P = \frac{\mu_{вих} - \mu_i}{\mu_{вих}} \cdot 100 \qquad (3)$$

where μBих - content of suspended substances in the original water; μi - content of suspended substances in the settled water, g/l, after the end of the settling period.

3 Modeling of Hydrodynamic Processes in Proposed Structures

As a result of simulation experiments conducted using the virtual machine in the Computational Fluid Dynamics Autodesk Simulation (CFD) environment, experiments were conducted to determine the hydrodynamic characteristics of the illuminator-adsorber based on modeling in a virtual environment (Fig. 3).

The presented scheme shows that the total height of the illuminator-adsorber with vertical flow is 6.22 m, the diameter of the illuminator is 3.5 m, and the central tube for suspension supply (hereafter: flocculation chamber) has a diameter of 0.5 m and a height of 3.8 m. The concentration of suspended particles is 7–12 kg/m^3. A structured grid containing 3,868,373 computational cells was used in the three-dimensional model.
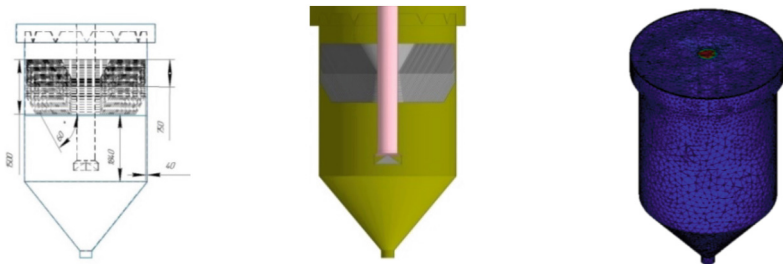
Fig. 3. General view of the illuminator-adsorber with a thin-layer module in cross-section and a sample of the computational virtual model based on the Finite Element Method (FEM).

To substantiate the model of sedimentation of bentonite and zeolite powdery clays and copper cyanoferrate, optimal suspension supply speeds of 0.014 m/s (14 mm/s) were determined. The results of the modeling in the form of flow velocity diagrams are presented in Fig. 4.

The analysis of modeling results showed (Fig. 4a) that in the classic model of the continuous-action illuminator at a fluid flow speed of 0.014 m/s at the entrance to the flocculation chamber with an equipped diffuser-reflector at the exit, there are zones of turbulent flow that hinder the normal formation of sorbent flocculant conglomerates and their sedimentation in the central section of the illuminator. The flow of LRW and sorbent, due to excessive turbulence, is unevenly distributed throughout the volume of
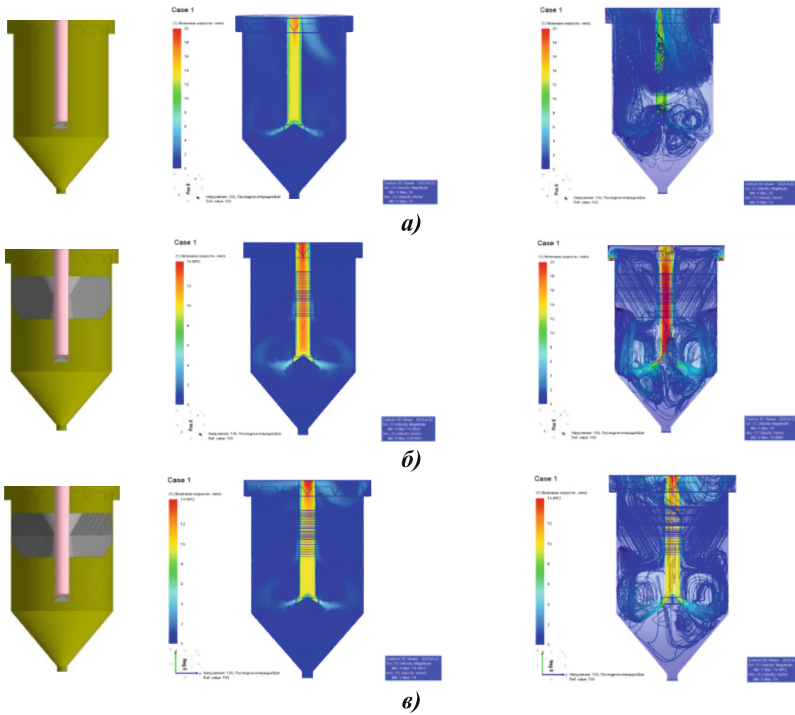
Fig. 4. Tracing of vectors and distribution of flow fields of sorbent solution and liquid radioactive wastes with a fluid supply speed of 0.014 m/s in the continuous-action illuminator-adsorber: a) model of the classic illuminator with a diffuser reflector; б) model of the illuminator-adsorber with a reflector and a thin-layer module; в) model of the illuminator-adsorber with a reflector and a modernized thin-layer module.

the settler, creating stagnation zones that hinder the sorption process, leading to the suction of spent sorbent into the outlet channel, and preventing the compaction of spent sorbent in the lower part of the structure designated for RAW removal.

In the model of the illuminator-adsorber with a regular and modernized thin-layer module (Fig. 4б, В), the sorbent solution is evenly distributed throughout the volume of the illuminator-absorber through the diffuser reflector and the thin-layer module, with a clear distribution into zones: creation of flow turbulence, laminar streamlining of the flow, and discharge of purified water.

Turbulence in the turbulent zone is achieved due to the diffuser reflector: stable, uniform swirls are formed, maintaining constant circulation of flocculant particles, increasing the contact time of the sorbent with polluted water, and accelerating the settling of spent sorbent. In the laminar flow leveling zone, the thin-layer module acts as a final water purification step from suspended sorbent particles by damping turbulent flows and increasing their settling area, preventing the suction of spent sorbent into the outlet channel. The difference between the regular and modernized thin-layer modules is that the modernized thin-layer module has an increased settling area by one and a half times

compared to the regular thin-layer module, achieved by introducing additional plates to half the height of the regular thin-layer module.

Thus, the use of virtual models of sedimentation of bentonite and zeolite powdery clays and copper cyanoferrate allowed substantiating the optimal design of the illuminator-adsorber for stable and efficient sedimentation of the sorbent in the illuminator-adsorber with a modernized thin-layer module (Fig. 4B) and an inlet speed for this design of the settler v = 0.014 m/s.

The virtual experiment is described using a mixture model. The mixture model is a simplified model with two liquids that can simulate two-phase flow or particle flow, solve the continuity equation of the mixed phase, momentum energy equation, and volume fraction equation of the second phase, and achieve relative algebraic velocity. Since the mixture model is simple, the calculations are relatively small, and the results are more reliable, it is widely used. Below is the continuity equation of the mixture model:

$$\frac{\partial}{\partial t}(\rho_k) + \nabla \cdot (\rho_m \bar{v}_m) = \dot{m} \tag{4}$$

$$\bar{v}_m = \frac{\sum_{k=1}^{n} \alpha_k \rho_k \bar{v}_k}{\rho_m} \tag{5}$$

$$\rho_m = \sum_{k=1}^{n} \alpha_k \rho_k \tag{6}$$

In Formulas (4)–(6): ρ_m – density of the mixed phase; ρ_k – density of the k-phase; α_k – volume fraction of the final phase k; $\bar{v}_m$ – average mixing speed; $\bar{v}_k$ – average speed of k phase quality; – $\dot{m}$ through quality relative to the user-defined source quality.

The improved RNG (Renormalization Group Model) with two k-ε equations adds two factors: rotation of the average flow and flow turbulence for computation, better addressing situations of high variability and greater bending of flow lines. In this paper, the authors use a turbulence model for modeling the flow scheme in settlers. The turbulent kinetic energy k and the dissipation rate ε of the turbulent kinetic energy transfer equation are:

$$u_i \frac{\partial k}{\partial t_i} = \frac{\partial}{\partial x_i}\left[\left(\mu + \frac{\mu_t}{\sigma_k}\right)\frac{\partial}{\partial x_i}\right] + P_k - \varepsilon \tag{7}$$

$$u_i \frac{\partial k}{\partial t_i} = \frac{\partial}{\partial x_i}\left[\left(\mu + \frac{\mu_t}{\sigma_k}\right)\frac{\partial}{\partial x_i}\right] + C_{\varepsilon 1}\frac{\varepsilon}{k}P_k - C_{\varepsilon 2}\frac{\varepsilon^2}{k} \tag{8}$$

In the formula: μ – viscosity; μt – turbulent viscosity coefficient;
$P_k = \mu_t\left[\frac{\partial u_i}{\partial x_j}\left(\frac{\partial u_i}{\partial x_j} + \frac{\partial u_i}{\partial x_j}\right)\right]$ is the generated elements of turbulent energy;
$\sigma_k = 0.7179; \sigma_\varepsilon = 0.7179; C_{\varepsilon 1} = 1.42 - \frac{\eta(1-\eta/\eta_0)}{1+\beta\eta^3}; \eta = \frac{Sk}{\varepsilon};$
$S = \left(S_{ij}, S_{ij}\right)^{1/2}; \eta_0 = 4.38; \beta = 0.012 - 0.015; C_{\varepsilon 2} = 1.68.$

4   Conclusions

The classic vertical settler provides only primary sedimentation of formed colloidal conglomerates.

The well-known thin-layer module slightly improves the sedimentation process of the sorbent.

The proposed construction, thanks to the specific distribution of hydraulic flow vectors in the water-sorbent suspension, allows one structure to provide the appropriate contact time of the sorbent in the form of a layer of suspended sediment with gradual enlargement of sorbent flake conglomerates forming a sediment that gradually thickens and compacts. Thus, we managed to combine an "adsorber" and a "settler" in one structure.

This allows considering this construction of the structure as universal, combining the processes of adsorption and sedimentation, which, in turn, allows conducting a complete cycle of LRW purification with a reduction in the number of involved technological structures.

References

1. Bulut, G., Yenial, Ü., Emiroğlu, E., Sirkeci, A.A.: Arsenic removal from aqueous solution using pyrite [Text engl]. J. Clean. Prod. **84**, 526–532 (2014)
2. Gao, S., Wang, Q., Nie, J., et al.: Arsenate(v) removal from aqueous system by using modified incinerated sewage sludge ash (ISSA) as a novel adsorbent [Text engl]. Chemosphere **270**, 129–423 (2021)
3. Huo, J., Yu, G., Wang, J.: Magnetic zeolitic imidazolate frameworks composite as an efficient adsorbent for arsenic removal from aqueous solution [Text engl]. J. Hazard. Mater. **412**, 125–298 (2021)
4. Khalil, A., Hashaikeh, R., Hilal, N.: 3D printed zeolite-y for removing heavy metals from water [Text engl]. J. Water Process Eng. **42**, 102–187 (2021)
5. Li, Y., Qi, X., Li, G., Wang, H.: Double-pathway arsenic removal and immobilization from high arsenic-bearing wastewater by using nature pyrite as in situ Fe and S donor [Text engl]. Chem. Eng. J. **410**, 128–303 (2021)
6. Muedi, K.L., Brink, H.G., Masindi, V., Maree, J.P.: Effective removal of arsenate from wastewater using aluminium enriched ferric oxide-hydroxide recovered from authentic acid mine drainage[Text engl]. J. Hazard. Mater. **414**, 125–491 (2021)
7. Rha, S., Waste Jo, H.Y.: Foundry dust (wfd) as a reactive material for removing As(iii) and Cr(vi) from aqueous solutions [Text engl]. J. Hazard. Mater. **412**, 125–290 (2021)
8. Chen, W.-H., Hoang, A.T., Nižetić, S., et al.: Biomass-derived biochar: from production to application in removing heavy metal-contaminated water [Text engl]. Process. Saf. Environ. Prot. **160**, 704–733 (2022)
9. Rilstone, V., Vignale, L., Craddock, J., et al.: The role of antibiotics and heavy metals on the development, promotion, and dissemination of antimicrobial resistance in drinking water biofilms [Text engl]. Chemosphere **282**, 13–1048 (2021)
10. Shamim, M.A., et al.: Metal organic frameworks (MOFs) as a cutting-edge tool for the selective detection and rapid removal of heavy metal ions from water: recent progress [Text engl]. J. Environ. Chem. Eng. **10**, 106–991 (2022)
11. Shen, C., Wu, S., Meng, Q.: Construction of portable drinking water device using an agricultural biomass-derived material of polyethylenimine-grafted-corncob [Text engl]. Food Control **130**, 108–375 (2021)
12. Zhang, Y., Zheng, H., Zhang, P., et al.: Facile method to achieve dopamine polymerization in MOFs pore structure for efficient and selective removal of trace lead (II) ions from drinking water [Text engl]. J. Hazard. Mater. **408**, 124–917 (2021)

13. Bac, B.H., Nguyen, H., Thao, N.T.T., et al.: Performance evaluation of nanotubular hal-loysites from weathered pegmatites in removing heavy metals from water through novel artificial intelligence-based models and human-based optimization algorithm, [Text engl]. Chemosphere **282**, 13–1012 (2021)
14. Laghlimi, C.A.: New sensor based on graphite carbon paste modified by an organic molecule for efficient determination of heavy metals in drinking water [Text engl]. Chem. Data Collect. **31**, 100–595 (2021)
15. Trus, I.M., Gomelya, M.D., Makarenko, I.M.: The study of the particular aspects of water purification from the heavy metal ions using the method of nanofiltration. [Text engl]. Naukovyi Visnyk Natsionalnoho Hirnychoho Universytetu. **4**, 117–123 (2020)
16. Karbork, M., Muhammed, B.A., Tumer, M., Urus, S.: Organosilane functionalized graphene oxide hybrid material efficient adsorbent for heavy metal ions in drinking water. Phosphorus Sulfur Silicon Relat. Element. **2**, 20–22 (2021)
17. Royiv, H.A.: Ochysni sporudy hazonaftoperekachuval'ni stantsiy ta naftobaz [Text engl]. Nadra, Moskva (1981)
18. Den'hub, V.I.: Alhorytm nablyzhenykh rozrakhunkiv hidravlichnoi krupnosti zernystykh zavysiv hidrotransportu [Text engl]. Naukovyi visnyk budivnytstva, vol. 3 (2016). http://www.vestnik-construction.com.ua/images/pdf/3_85_2016/stroitel_3_85_2016_171_173.pdf
19. Anistratenko, V.O., Fedorov, V.H.: Matematychne planuvannya eksperymentiv v APK [Text engl]. Navch. posibnyk. Kyyiv: Vyshcha shkola. **375** (1993)

On the Creation of a Modern System for Handling Liquid Radioactive Waste at Nuclear Power Plants in Ukraine. Conditioning of Liquid Radioactive Waste

O. B. Andronov and Valentyn Bezmylov[(✉)] [ID]

Institute for Safety Problems of Nuclear Power Plants, 36-a, Kirova Str., Chornobyl 07270, Ukraine
v.bezmylov@ispnpp.kiev.ua

Abstract. The paper discusses approaches to creating a technological system for incorporating liquid radioactive waste (LRW) into a solid matrix to produce a final product that meets disposal requirements. The prompt resolution of this issue will alleviate the problem of LRW accumulation at operating nuclear power plants in Ukraine [1], complete the cycle of handling liquid waste, and focus the industry's potential on searching for and implementing a modern complex for handling both liquid waste and radioactively contaminated waters in general.

Keywords: Cementation · Inclusion in a polymetallic matrix · Flexible technology · Analysis of foreign experience · Adopted decisions

1 Introduction

The conditioning of LRW must be considered in the context of a strategy to minimize radioactive waste (RAW) with increasing safety requirements. This, in turn, necessitates the updating of regulatory frameworks. For example, for reliable and efficient handling of operational RAW at nuclear power plants and to meet the safety requirements of the International Atomic Energy Agency (IAEA) in the field of RAW management in Ukraine, it is necessary to develop and approve criteria for accepting RAW at nuclear power plants for long-term storage/disposal [2]. It should be noted that currently, there are no formally documented requirements for hardened LRW in Ukraine. Therefore, to assess the quality indicators of compounds, it is necessary to use the standard adopted in Russia (GOST 51883-2002).

A fundamental issue in the technology of conditioning by cementation is the development of binders (creating a compound recipe). The Research Institute of Binding Materials of the Kyiv National University of Construction and Architecture (RIIBM) is successfully working on this problem.

2 Foreign and Domestic Practice of LRW Conditioning

According to available foreign and domestic sources, when choosing a hardening method, most specialists today prefer cementation and vitrification (in general - inclusion in an inorganic matrix), primarily due to safety and economic considerations. It should also be noted that abroad, work has been carried out for over 30 years on the application of gypsum [3]. There is information that for cementation of boron-containing concentrate, 1 kg of sand, 0.8 kg of cement, and 0.07 kg of gypsum are added to it at pH 6.5–7 for every 1 kg of boric acid (the mixture hardens in 28 days, and the leachability for Cs137 is 2×10^{-3} g/(cm^2 day)).

Adding sodium silicate (liquid glass) to binders (gypsum, cement) improves almost all main indicators: strength, degree of filling, compatibility with the main components of waste, leachability.

To increase the degree of filling and reduce leachability, the practice of "dry" cementation has been introduced, where the water-to-cement ratio is reduced from 0.7 (usual) to 0.35–0.4 (the associated deterioration in the flowability of the cement paste is irrelevant when forming the solid product in transport containers). For a long time in global practice, reinforcing additives (zeolites; vermiculite; clays; silicon dioxide; diatoms for binding excess water; organic derivatives; formaldehyde to prevent the proliferation of bacteria causing gas formation) have been used to change the physicochemical properties of cements and improve their compatibility with waste.

Trends in hardening methods abroad can be seen from the brief overview provided below.

Conditioning of LRW occurs by mixing them with cement (cement solution), bitumen, or polymer (polystyrenes, formaldehyde resin, polyesters, epoxies, polyethylene) followed by hardening of the resulting mass. Various options for changing the compositions of the inorganic matrix and cements by adding various clays, polymeric materials, etc., have been proposed. The technological cycle includes the extraction of radionuclides from liquid waste with the localization of toxic concentrates in a minimal volume. Significant attention is paid to the removal of ballast (non-radioactive) salts, which in turn reduces material costs for cementation.

Comparison of Different Methods of Solidifying Medium-Level (MLW) and Low-Level (LLW) Waste: A comparison of different methods of solidifying medium-level (MLW) or low-level (LLW) waste shows that all three types of matrices (bitumen, cement, polymers) are monolithic without any free water remnants. Cement and polymers are stronger substances, with their strength determined at 300–600 and 2000 kg/cm^2, respectively. Polymers and bitumen are fire hazards (polymers are combustible and partially decompose in fire, bitumen melts and ignites, hence their widespread future use is doubtful) [3].

Choice of Equipment: Both stationary and mobile conditioning plants can be used at nuclear power plant sites. Previously, stationary plants were constructed at each site of foreign nuclear power plants. In some countries, the use of mobile plants for conditioning both LLW and MLW is becoming widespread. In the UK, BNFL Environmental Services has been operating the country's first mobile plant for solidifying MLW (Transportable ILW Solidification Plant - TILWSP) since 2003 [4]. TILWSP is designed to process

sludges and spent ion-exchange resins. The plant includes operations not only for processing wet MLW but also for their subsequent packaging in standard containers. Wet MLW are placed in 3 m^3 drums, where they are dehydrated and cemented. After checking the quality of the hardened mass, waste is poured with cement solution and the drum is sealed. Using remote equipment, the drum with conditioned MLW is placed in shielded transport packaging and transported to a special site for MLW storage.

In France, conditioning of technological wastes and very low-level ion-exchange resins is carried out in steel drums. All other types of wastes are conditioned in reinforced concrete containers, which have an internal steel lining.

At nuclear power plant sites with PWR-900 and some with PWR-1300, there are stationary facilities for encapsulating filters and cementing sludges and concentrates from evaporation in reinforced concrete containers. Mobile plants are used for conditioning such wastes at other nuclear power plants due to their cost-effectiveness and simpler mode of operation.

Cementing of LLW and MLW in the coming decades will likely remain in many countries the simplest, cheapest, and sufficiently safe method of conditioning. The main advantages of cementation are: low-temperature process; well-proven technology; the cemented product is non-combustible and has good thermal stability, chemically and biochemically stable; all forms of waste can be included in the cement matrix. Cementation can achieve reliable effective immobilization of waste, reducing its loading in cement, but this increases the volume of final products. Moreover, using this method, the salts contained in the waste interfere with the main processes of cement hydration, leading to deterioration of the cemented product quality over time.

The company NUKEM GmbH (Germany) has been offering cementation plants with various mixing methods for many years. Among them, the most widespread in the company's deliveries since the mid-1990s is the highly efficient mixing method in the drum (High Performance In-Drum Mixer - HPIDM [5]). Examples of the company's product deliveries include:

Ukraine, Khmelnytskyi NPP (HNPP) - cementation plant with an inclined mixer for the Waste Processing Center;
China, Qinshan NPP, Institute of Atomic Energy, Jiangsu Nuclear Corporation, CIAE - cementation plant in a 200-L drum;
Slovak Republic, Jaslovské Bohunice NPP - cementation plant with an inclined mixer for the Waste Processing Center;
Russia, Balakovo NPP - cementation plant with an inclined mixer for the Waste Processing Center.

The HPIDM method is applicable in both stationary and mobile installations (DEWA., MOWA). Depending on the radiation level, contact and non-contact control of the plant is possible. In mobile DEWA plants, the cementation process is carried out directly in waste containers; cement is loaded in advance. There are no special requirements for waste; it can contain up to 25% boric acid and up to 35% dry material. The MOWA system has features and advantages of a compact plant, as the waste is transported and stored in 20-foot containers that meet ISO standards. The system has high waste throughput (possible use of drums of various sizes (100–400 l)) and various protections.

The MOWA plant can process concentrates, pulp, granulated resins with high specific activity. Technical data of MOWA: length 5700 mm, width 2220 mm, height 2180 mm; weight 22,000 kg. Throughput: pulp/concentrate - up to 10 m^3 per shift; resin - up to 2 m^3 per shift [5].

Improvement in Cement Matrix Composition: Research is being conducted to improve the composition of the cement matrix, including for the purpose of reducing the leaching of Cs137 and decreasing hydrogen generation due to the corrosion of aluminum contained in the cement. It has been established that the addition of lithium nitrate to cement reduces hydrogen formation by approximately tenfold, and the addition of zeolite (clinoptilolite) reduces the leaching rate of Cs137 by tenfold.

Advancements in Vitrification Technology: Although the vitrification process was initially developed for processing high-level waste (HLW), it is now used for conditioning LLW and MLW. Vitrification of LLW has the advantage in terms of waste minimization and is suitable for all LLW generated at nuclear power plants.

In the USA, operational and planned new industrial facilities for vitrification of LLW, as well as mixed waste, are in place. The feasibility of vitrifying mixed LLW, consisting of granulated activated carbon contaminated with chemical and radioactive elements, has been demonstrated. The throughput of the industrial facility launched by ATG in 2001 in Hanford is 158.5 kg/h.

AMEC Nuclear (UK) has developed the GeoMelt technology, which is considered one of the most effective solutions for stabilizing LLW before removal [6]. The GeoMelt process (vitrification directly in the container) results in the immobilization of radioactive contaminants and heavy metals and the destruction of other toxic pollutants, forming a strong glass-like product. The feasibility of this technology was confirmed by hot trials on an experimental scale. GeoMelt technology was chosen for vitrifying LLW in Hanford after processing and vitrifying all HLW and some LLW stored in 177 underground tanks in Hanford.

The Hanford Vitrification Plant, under construction in Hanford for vitrifying LLW (Hanford Vitrification Plant), is part of the Waste Treatment and Immobilization Plant (WTP), also known as the "VitPlant." The complex is intended for processing LRW stored in Hanford's underground tanks. The complex includes four sections - for preliminary waste processing, for vitrifying LLW and HLW, and an analytical laboratory. The total area of the complex will be 26.3 ha. The VitPlant complex is to be constructed by 2016 and operational by 2019. The total cost is estimated at $12.2 billion [7].

However, the vitrification process, using expensive melting equipment with complex gas venting systems, leads to the formation of secondary waste. Due to these drawbacks, research continues to identify new binding materials (matrices) for immobilizing LLW/MLW. In the USA, a low-temperature method for stabilizing salt-containing waste using phosphate ceramics is being developed. In this process, magnesium oxide reacts with potassium phosphate and waste salts, resulting in a dense monolith with low porosity, primarily consisting of magnesium and potassium phosphates.

In South Korea, the Ulchin Vitrification Facility (UVF) for vitrifying LLW/MLW in a cold crucible melter (CCM) was commissioned at the Ulchin NPP in 2007 [4]. LLW/MLW generated at Ulchin-1 and -II NPPs (four units) contain 26% liquid concentrates, 18% spent ion-exchange resins, 4% spent filters, and more than half mixed

heterogeneous waste. A technology representing a single-stage combustion and vitrification process for LLW/MLW was used. Combining a melting furnace with a cold crucible and a plasma torch melter (PTM), it is possible to separately vitrify combustible waste and melt non-combustible waste. The capacities of the CCM and PTM melters at the facility are 300 kW and 500 kW, respectively [8].

In 2013, a technology for conditioning LRW developed at the Jaslovské Bohunice NPP (Slovakia), based on incorporating waste into the SIAL geopolymer matrix, was presented in Ukraine [9]. However, tests of the technology at the Chornobyl NPP did not provide sufficient grounds for its industrial implementation at Ukrainian NPPs. Further testing is planned.

A positive domestic contribution to solving the problem of conditioning LRW is the research conducted at the Khmelnytskyi NPP on the study of stages of solid compound formation during the curing of real cubic residue (CR) and salt melt (SM), and the analysis of the properties of the resulting solid compounds. The research showed that with the help of polymetallic sorbents, it is possible to obtain a solid product suitable for subsequent long-term storage and disposal. The work was not completed (data as of 2004).

3 Cementation

Developing specialized compound recipes that allow for the cementation of salt-saturated solutions to produce a product that meets regulatory requirements is the basis of the cementation technology. In the past, the salt saturation limit for cementation according to SPORO-85 was restricted to 200 g/l, as higher concentrations significantly worsened the quality indicators of the cement stone. Currently, technologies for cementing solutions with high salt content have been successfully tested (from 750 g/l at the Chornobyl NPP to 950 g/l at the Rostov NPP).

The compound recipe must ensure the necessary quality indicators of the cement stone for a storage period of 300 years. In Ukraine, there are still no formally documented requirements for cured LRW, which forces developers to rely on standards adopted in the Russian Federation [10]:

Leaching rate (for Cs), g/cm^2 day - not more than 10^{-3};
Mechanical strength (compressive strength limit), MPa (kg/cm^2) - at least 4.9 (50);
Frost resistance (at –40… + 40 °C), cycles - at least 30 (*);
Immersion resistance to prolonged submersion in water, days - 90 (*);
Radiation resistance at a dose, Gy - 106().
() - reduction in compressive strength limit after testing not more than 25%.

Let's take a closer look at two quality indicators of the final product of conditioning: durability and leaching rate. Regarding the durability of the final product in terms of maintaining its strength properties, direct studies of artificial stone based on any of the known hydrational hardening binders, including alkaline binding systems, confirming their durability for at least 300 years, have not been conducted. The reason is that, for example, Portland cement has been known for less than 200 years (E. Chiliev, 1822; D. Aspdin, 1824), and alkaline binding systems for less than 60 years (V.D. Glukhovsky, 1957).

The durability of materials is determined by the interaction and mutual influence of different factors, the main ones being: operating conditions; features of structural solutions of constructions; leaching; internal corrosion; compatibility of materials in the composition; resistance to alternating freezing and thawing, abrasion and wear; the influence of the condition of the structure on its durability, etc.

However, there are a number of indirect indicators and signs that suggest that stone based on alkaline binding systems can provide the required operational characteristics for 300 and more years.

Currently, the science of cement is focused on ancient structures made from artificial mixtures, which included soda and potash as components. In the last century, an attempt was made to decipher the reasons for the exceptional durability of ancient concrete, and the mineralogical composition of the cement stone of several ancient structures preserved under the long-term influence of various aggressive factors was studied [11–13]:

Roman aqueduct (Caesarea) - groundwater, flowing water;
Roman wharf - fresh flowing water;
Harbor walls (Caesarea) - Mediterranean seawater;
Roman baths - hot water from mineral springs.
In the structure of ancient concretes, artificial neoformations were found, analogous to natural zeolites of the type $Na_2O(K_2O)$ Al_2O_3. (2–4) SiO_2 $2H_2O$.

At the same time, numerous cases of rapid destruction of Portland cement concrete (after 30…50 years of operation), used for the restoration of ancient Roman structures, are known, while ancient concretes operating in similar climatic conditions continue to be used for more than 2000 years (Table 1).

Table 1. Chemical composition of ancient lime-pozzolanic cements.

Name of territory	Mass share of oxides,%				
	SiO_2	Al_2O_3	$K_2O + Na_2O$	$CaO + MgO$	CO_2
Ancient Greece (350 years BC)					
Syria (Tel-Ramad, 70 years BC)	18,0	4,30	1,44	45,9	13,1
Egypt (Pyramid of Khufu)	24,6	4,92	1,55	41,8	25,9
Ancient Rome (169…140 years BC)	3,10	0,50	0,20	52,6	41,4

The format of the article does not allow for a detailed description of alkaline binding systems. It should be noted that a significant contribution to the implementation of the technology for cementing liquid radioactive waste (LRW) has been made by the work of Ukrainian scientists. For instance, the Research Institute of Binding Materials, in the framework of developing the D-2 package for the LRW Processing Plant strategy and considering the requirements [10, 14], conducted several studies to determine: the radioactive properties of the final product with real LRW; the influence of alkaline cements from various manufacturers on the recipes for solution mixes and the characteristics of the final product; the influence of kaolin on the solution mix recipe and properties of the final product; durability (analytical assessment) of the final product in terms of

maintaining strength properties; compliance of the final product's characteristics with the requirements stated in the criteria for acceptance in specially equipped near-surface storage of solid radioactive waste (NSSRW), as well as in technical specifications.

The reliability of radionuclide binding is ensured by the fact that many radionuclides (primarily alkaline and alkaline earth types such as cesium, strontium, sodium, potassium) are chemically capable of entering the structure of zeolite-like neoformations and are firmly fixed in them. Other non-alkaline radionuclides can be reliably physically bound by the zeolites of slag-alkaline cement stone, which have sorption properties [11].

Evidence of the high efficiency of using alkaline cements as a binding material for immobilizing LRW can be seen in the fact that such natural zeolites as analcime, chabazite, sodalite, natrolite, clinoptilolite, mordenite, etc., which also occur in the formation of the stone structure on alkaline cements, are capable of cation exchange of sodium and potassium for cesium, and calcium for strontium. These data confirm the increased reliability of radionuclide localization in the matrix of artificial stone based on alkaline cements, and the high sorption properties of zeolite-like neoformations synthesized in alkaline cement stone serve as an additional factor of reliability for radionuclide binding. It should be noted that regardless of the directionality and scale of the technological process of using alkaline cements, the formation of properties of artificial stone will be accompanied by the synthesis of the above-mentioned structural formations, ensuring high density of the stone and stability of structural compounds under leaching conditions.

In the research, products from domestic manufacturers were used as binding materials: cement LCEM I-400 according to DSTU B V.2.7-187:2009 produced by CP "Ekosplav", and as additives - plasticizer "Poliplast SP-3" according to TU 5870-006-58042865-05, kaolin from LLC "Prosyansky GOK" grade KR-2 according to GOST 19608-84, and Portland cement PC I-500 (DSTU B V.2.7-46-96) by LLC "Volyn-Cement" (Zdolbunov). To determine the influence of the qualitative characteristics of the cement component on the characteristics of solution mixes and the characteristics of the cured final product, cements LCEM I-400 according to DSTU B V.2.7-187:2009 from other manufacturers were additionally used, namely slag cement by CP "Golden Technologies Company" and cement produced by LLC "Promcement". As materials included in the composition of slag-alkaline cements, granulated blast furnace slags from the Zaporizhzhia metallurgical combine (ground product producer CP "Golden Technologies Company"), Mariupol metallurgical combine named after Ilyich, and Kryvyi Rih combine "Arcelor Mittal Kryvyi Rih" were considered.

4   On the Choice of Technology for Operating Nuclear Power Plants in Ukraine

As noted in the work [1], for the prompt solution of the problem of conditioning LRW at Ukraine's nuclear power plants, experts from the Scientific and Technical Center of NAEK Energoatom chose cementation. The technology of cementation has been mastered in the Russian Federation at the Rostov NPP (VVER) where a curing installation (UI) is in operation, and in Ukraine at the Chornobyl NPP LRW Processing Plant (RBMK).

The developer of the comprehensive technology of cementation for the Rostov NPP is the Open Joint Stock Company "Sverdlovsk Research Institute of Chemical Engineering" (OJSC SVNIKhM) [15]. The UI has been in pilot-industrial operation since 2005 and currently performs operations for cementing only cubic residues (CR). During the implementation of the project, the personnel identified several shortcomings in the project, which were eliminated during the commissioning and testing phase. It was also necessary to work out the mixture recipe to bring the processing product in line with the requirements of the current nuclear power guideline in Russia, RD 95 10497-93 ("Guidelines for the Quality of Compounds Formed During Cementation"). VNIINM, SVNIKhM, ZAO NPO "Energochimproject", and NPO "Radon" participated in the development of the compound recipe. The matrix is a cement-clay mixture (a mix of bentonite and Portland cement brand M500 (PC 1-500) of Russian manufacturers in a ratio of 1:9). The cement compound recipe: CR concentrate – 38%; PC + bentonite – 59%; NaOH solution (46%) – 3%. Since 2011, after the modernization of the installation, they switched from barrel to container storage of cured waste (containers NZK-150-1.5P), which simplified and reduced the cost of the technological process.

The technological process is structured as follows: concentration of CR; preparation of the cement mix with technological additives (CMTA); mixing of concentrated CR (CCR) with CMTA; packaging of the cement compound in NZK container; transportation of containers to the sedimentation tank; transportation of containers after sedimentation to the TRW storage of the special-purpose building (TRW SPB).

The installation consists of four main technological units: reception, preparation and dosing of LRW; reception, preparation and dosing of cement; mixing; packaging with a transport system.

The decision to use the experience of the Rostov NPP in Ukraine is complicated by the absence of a document confirming that the final product meets all the requirements of GOST 51883-2002 and there is no cost calculation for conditioning and storage of the final product.

The Chornobyl NPP LRW Processing Plant (ZPLRW) is Ukraine's first experience in solving the problem of creating technology for the final stage of handling liquid waste. The cementation technology for ZPLRW was created by a domestic developer - NIIVM. The technology uses the following materials and reagents: cements LCEM 1-400 and PC-500, plasticizer SP-3, special-purpose additives (calcium nitrate), thinning additives (Pozzolith 400 N), additives (PPFeNi), NAOH, HNO3.

The functions of ZPLRW include: extraction of waste from storage tanks by pumping and mixing; transportation of extracted waste to reception tanks with partial use of existing pipelines; preliminary processing of waste to bring their characteristics in line with the requirements of subsequent stages of the technological process; volume reduction: centrifuging of resins and perlites (to adjust the moisture content of the waste) and further evaporation of CR; processing and cementation of LRW; packaging of the final product in barrels; retention of barrels with the final product; packaging of barrels in transport packaging sets (TPS) in groups of four barrels; removal of filled TPS.

The plant is designed to process 2500 m^3/year of waste stored in 14 tanks, with an operational life of 10 years. It should also be noted that the permission for the acceptance of RAW from ZPLRW to the NSSRW is temporary, as are the acceptance criteria. Out

of 22 sections of the storage, only two are permitted for reception (storage volume 71280 m^3).

The technology of ZPLRW is oriented towards conditioning complex composition waste. The specifics of LRW are due to both the waste of the Chornobyl NPP and the inflows from the Shelter object (the waste contains transuranic elements, a large amount of sulfates, phosphates, oxalates, as well as petroleum products, synthetic surfactants, film-forming materials, and organic substances) [16].

Unlike VVER NPPs, LRW from RBMK NPPs does not contain boric acid, and heterogeneous waste contains perlites, which have high abrasive properties. The presence of abrasives negatively affects the resource of the moving elements of the mixer (noted by the plant personnel).

From a technical point of view, the processes of cementation at the UI of the Rostov NPP and at the ZPLRW of Chornobyl NPP are fundamentally identical.

5 Comparative Assessment

Let's focus on issues important for deciding on the choice of cementation technology and the LRW handling production system for Ukrainian NPPs.

The Chornobyl NPP ZPLRW and the UI of the Rostov NPP are production systems with different levels and scales of implementation, different technical and strategic tasks (with the same tactical task).

Overall, the technology of ZPLRW is on the scale of a plant, and the technology of the Rostov NPP is on the scale of a workshop.

Regardless of the large volume of waste accumulated at the Chornobyl NPP and the volume of their inflows in the process of liquidating the object and transforming the NPP zone into an environmentally clean system, it has a finite size. According to the developer's assessment, this is 13,481.5 m^3 of CR, 4,059.7 m^3 of ion-exchange resin pulp, and 2,272.18 m^3 of filter perlite pulp. These wastes are stored in LRW and LRWTO. SP is absent. ZPLRW performs, practically, a one-time task.

On operating facilities, LRW is generated and arrives continuously, and therefore the life of the LRW conditioning system should be no less than the life cycle of the station. Based on this, it is important to assess the productivity of the technology, based on the dynamics of LRW accumulation (on the principle of reasonable sufficiency).

At ZPLRW, the finished product is sent for disposal outside the NPP within the boundaries of the Chornobyl exclusion zone. At the Rostov NPP, long-term storage is carried out at the station's industrial site.

At the Chornobyl NPP LRW Processing Plant (ZPLRW), the drum packaging principle of the processed product is implemented, with subsequent use of Transport Packaging Sets (TPS) as returnable, reusable packaging. At the Rostov NPP, a container packaging principle is laid down, in which containers (NZK) are not returned.

The Chornobyl NPP ZPLRW, whose creation stretched over 15 years, does not yet have sufficient operational statistics, which are available at the Rostov NPP.

The economic aspect is of great importance. At ZPLRW, its specialists performed an "Economic calculation of operational costs for processing LRW for one year, taking into account technological means, electricity, and labor fund, including disposal in the

Near-Surface Waste Disposal Facility (NSSWDF), as well as the calculation of the cost of processing 1 m^3 of LRW for one year" (by L.A. Gladneva). Based on the calculation at 2012 prices:

Cost of disposal (according to the letter of the State Specialized Enterprise "Centralized LRW Management Company" № 105/1509 dated 28.12.2011) at the first stage of the "Vector" complex (NSSWDF) - 10,300 UAH/m^3;
Cost of processing 1 m^3 of CR - 73,973.2 UAH/m^3;
Cost of processing 1 m^3 of ion-exchange resins - 139,846.8 UAH/m^3;
When co-disposing homogeneous and heterogeneous waste in a cement matrix, the average price is 68,000 UAH/m^3. Note that cementation of LRW (ion-exchange resins) in Slovakia costs 32,567 euros/m^3, and disposal – 112,000 euros/m^3 (data from 2013, including the prices for disposal in the National RAW Repository).

With the design capacity of ZPLRW of 632.1 m^3 of CR per year (2100 m^3 of final product), their conditioning and storage per year will cost 46,758,870.98 UAH. The same for heterogeneous waste (ion-exchange resins) with the plant's design productivity of 322.1 m^3 per year (2102 m^3 of final product) will cost 45,044,654.22 UAH.

The Rostov NPP does not provide such calculations.

6 Conclusion

As noted, the priority direction for the prompt solution of the problem of conditioning LRW by the Scientific and Technical Center of NAEK Energoatom has been chosen to be cementation [1]. In terms of creating a modern system for handling LRW at operating NPPs in Ukraine, a number of requirements are presented for the cementation system:
Implementation level taking into account the reduction of cementation scale as the complex for handling LRW is introduced and technological processes are automated. The levels of implementation can be: the level of a technological line, the level of a site, the level of a workshop, and the level of a plant. It is necessary to seek an optimal way of solving the problem, possibly at a lower level.

1. Strategic flexibility. This means that the equipment should provide work with other matrix materials (for example, geopolymers).
2. Tactical flexibility, allowing various options of technological processes to be tested during pilot-industrial operation.
3. Adaptability to the skill level of the facility's staff.
4. Mobility of some technical means, their unification in terms of the prospective task of creating a flexible mobile technology.
5. Maximum use of standardized equipment.

Cementation is a real way to solve the problem of LRW of domestic NPPs today. At the same time, it is necessary to continue searching for more efficient matrix materials. The high cost of conditioning and disposal should stimulate work to reduce the volume of waste. The task of the next stage is the deep processing of CR [9].

References

1. Andronov, O.B.: Of creation of up-to-date system for treatment of liquid radioactive wastes at Ukrainian NPPs. Statement of problem. In: Problemy bezpeky atomnyh electrostantsiy i Chornobylya (Problems of Nuclear Power Plants' Safety and of Chornobyl), no. 24, p. 32 (2015)
2. Analysis of RAW Management During Operation of NPPs of SE NNGC «Energoatom». Report (2011)
3. Nikiforov, A.S., Kulichenko, V.V., Zhikharev, M.I.: Sterilization of Liquid Radioactive Wastes (1985)
4. First mobile intermediate-level waste solidification plant. Nucl. Engng. Intern. **48**(589), 12 (2003)
5. Cementation of Radioactive Waste. NUKEM Technologies GmbH (2007)
6. Nucl. Waste News. **24**(6), 54 (2004). www.haaretz.com. Accessed 28 June 2004
7. Radwaste Solutions. **17**(5), 10 (2010). Hanford Press Releases. http://www.hanford-vitplant.com/28.07. Accessed 16 Sept 2010
8. Jo, H.-J., et al.: Commercialization Project of Ulchin
9. Materials of Session of Council of Deputies to Chief Engineers of SE NPPs, to Whose Competence EPY RAW Management Issues Pertain. Accessed 18 Dec 2013
10. GOST 51883-2002. Waste radioactive cemented. General technical requirements
11. Final Report for Contract C-1/9/071, «D-2» Work Package. Determination of end product formulae for LRWTP. Accessed 12 Dec 2011
12. Malinowski, R., Slatkine, A., Ben Yair, M.: Durability of roman mortars and concretes for hydraulic structures at Caesarea and Tiberias. In: International Symposium on Durability of Concrete, Prague, pp. 1–14 (1961)
13. Malinowski, R.: Betontechnische Problemlösung bei antiken Wasserbauten, vol. 64, pp. 7–12. Leichtweiss-Institut. – Mitteilungeng, Braunschweig (1979)
14. Criteria for acceptance of radioactive waste for burial in specially equipped surface repository for solid radwaste (SESRBSRW). First stage of SESRBSRW operation. In: Reception of RAW from PMRAW and PMSRW of ChNPP for Burial in Two Symmetric Departments of SESRBSRW, 5th edn, 36p (2009)
15. Opened Joint Stock Society. «Sverdlov research & development institute for chemical machine building». Cementing plant
16. Program of Radwaste Management at «Shelter Object»

Author Index